4D PRINTING OF HYGROSCOPIC WOOD BASED ACTUATORS FOR CLIMATE RESPONSIVE SKIN

A THESIS SUBMITTED TO
THE GRADUATE SCHOOL OF NATURAL AND APPLIED SCIENCES
OF
MIDDLE EAST TECHNICAL UNIVERSITY

BY

MEHMET OĞUZ NAS

IN PARTIAL FULFILLMENT OF THE REQUIREMENTS
FOR
THE DEGREE OF MASTER OF SCIENCE
IN
BUILDING SCIENCE IN ARCHITECTURE

JULY 2023

Approval of the thesis:

4D PRINTING OF HYGROSCOPIC WOOD BASED ACTUATORS FOR CLIMATE RESPONSIVE SKIN

submitted by **MEHMET OĞUZ NAS** in partial fulfillment of the requirements for the degree of **Master of Science** i**n Building Science in Architecture, Middle East Technical University** by,

Prof. Dr. Halil Kalıpçılar
Dean, Graduate School of **Natural and Applied Sciences** _____

Prof. Dr. Fatma Cânâ Bilsel
Head of the Department, **Architecture** _____

Prof. Dr. Arzu Gönenç Sorguç
Supervisor, **Architecture, METU** _____

Examining Committee Members:

Assoc. Prof. Dr. Mehmet Koray Pekeriçli
Architecture, METU _____

Prof. Dr. Arzu Gönenç Sorguç
Architecture, METU _____

Assist. Prof. Dr. Işıl Ruhi Sipahioğlu
Architecture, TOBB ETU _____

Date: 26.07.2023

I hereby declare that all information in this document has been obtained and presented in accordance with academic rules and ethical conduct. I also declare that, as required by these rules and conduct, I have fully cited and referenced all material and results that are not original to this work.

Name Last name : Mehmet Oğuz Nas

Signature :

ABSTRACT

4D PRINTING OF HYGROSCOPIC WOOD BASED ACTUATORS FOR CLIMATE RESPONSIVE SKIN

Nas, Mehmet Oğuz
Master of Science, Building Science in Architecture
Supervisor : Prof. Dr. Arzu Gönenç Sorguç

July 2023, 115 pages

Adaptive building systems are designed to enhance user comfort while decreasing energy consumption. However, sensing the environment and generating relevant motion requires complex systems. The cost of the installation, maintenance, and energy consumption of these traditional systems obstruct their widespread adoption. A more efficient solution can be found in nature by utilizing the inherent properties of materials. Recent research inspired by pinecones revealed that wood bilayers with different swelling and shrinking ratios can passively shape change in response to environmental humidity. The morphing direction is dictated by fiber orientation, which can be controlled by extrusion-based 3D printers. While hygroscopic wood actuators hold significant promise as climate-responsive building skins, challenges persist in motion predictability, response speed, and scalability. Consequently, this research investigates mesostructural and macrostructural design space for controlled, scalable motion. A systematic study on design and fabrication parameters was conducted in a controlled environment to observe actuation dynamics. Using the collected data, a model was developed to control and predict shape changes in macrostructural design explorations. Two implementations are proposed: the first harnesses combined actuators for motion amplification, while the latter employs bistability to regulate actuation speed. Experiments at scales of ½ and 1:1, using

wood-based filament and wood veneer actuators, validate that coupled actuators significantly enhance actuation speed. Moreover, it is demonstrated that the triggering humidity level of the shapeshifts can be tuned thanks to the prestressed bistable structures. This is promising in terms of adaptivity to various climatic conditions and providing higher energy efficiency in buildings.

Keywords: 4D Printing, Climate-Responsive Skin, Shape-Changing Materials, Hygroscopic Wood Bilayer, Pre-stressed Bistability

ÖZ

İKLİM-DUYARLI CEPHE İÇİN HİGROSKOPİK AHŞAP BAZLI AKTÜATÖRLERİN 4 BOYUTLU BASKISI

Nas, Mehmet Oğuz
Yüksek Lisans, Yapı Bilimleri, Mimarlık
Tez Yöneticisi: Prof. Dr. Arzu Gönenç Sorguç

Temmuz 2023, 115 sayfa

Adaptif bina sistemleri, enerji tüketimini azaltırken kullanıcı konforunu artırmak amacıyla tasarlanmıştır. Ancak, çevreyi algılamak ve ilgili hareketi oluşturmak karmaşık sistemler gerektirir. Bu geleneksel sistemlerin kurulum, bakım ve enerji tüketim maliyetleri yaygın olarak benimsenmelerini engellemektedir. Daha verimli bir çözüm, doğada, malzemelerin yapısında bulunan özelliklerden yararlanılarak bulunabilir. Çam kozalaklarından ilham alan son araştırmalar, farklı şişme ve büzülme oranlarına sahip ahşap çift katmanların, çevresel nem değişikliğinde pasif olarak şekil değiştirebildiğini ortaya çıkardı. Bükülme yönünü, ekstrüzyon tabanlı 3B yazıcılar tarafından kontrol edilebilen lif doğrultusu belirler. Higroskopik ahşap aktüatörlerin iklime duyarlı cephelerde kullanılması umut vaat ederken, hareket öngörülebilirliği, tepki hızı ve ölçeklenebilirlik konusundaki zorluklar devam ediyor. Bu nedenle bu araştırma kontrollü, ölçeklenebilir hareket için mezoyapısal ve makroyapısal tasarım alanını araştırmaktadır. Aktivasyon dinamiklerini gözlemlemek için kontrollü bir ortamda tasarım ve imalat parametreleri üzerine sistematik bir çalışma yapılmıştır. Toplanan veriler kullanılarak, makroyapısal tasarım keşiflerinde şekil değişikliklerini kontrol etmek ve tahmin etmek için bir model geliştirilmiştir. İki uygulama önerilmiştir: ilki hareket amplifikasyonu için

birleştirilmiş aktüatörleri kullanırken, ikincisi aktivasyon hızını kontrol etmek için bistabiliteyi kullanır. Ahşap bazlı filament ve ahşap kaplama aktüatörleri kullanan ½ ve 1:1 ölçeklerinde yapılan deneyler, çoklu aktüatörlerin çalıştırma hızını önemli ölçüde artırdığını doğrulamıştır. Bunun yanında, öngerilmeli bistabil yapılar sayesinde şekil değiştirmeyi tetikleyen nem seviyesinin ayarlanabileceği gösterilmiştir. Bu, çeşitli iklim koşullarına uyum sağlaması ve binalarda daha yüksek enerji verimliliği sağlaması açısından umut vericidir.

Anahtar Kelimeler: 4B Baskı, İklim Duyarlı Cephe, Şekil Değiştiren Malzemeler, Higroskopik Ahşap Çift Katmanlı, Öngerilmeli Bistabilite

To my beloved mother

ACKNOWLEDGMENTS

I would like to sincerely express my deepest gratitude to Prof. Dr. Arzu Gönenç Sorguç, my supervisor, for her invaluable support and guidance throughout my thesis. I consider it a great honor to have had the opportunity to work alongside her, and I am truly grateful for her patience and understanding.

I also want to thank my jury members, Assoc. Prof. Dr. Mehmet Koray Pekeriçli and Assist. Prof. Dr. Işıl Ruhi Sipahioğlu for sharing their valuable critics to develop my thesis.

I am grateful to METU Design Factory for supporting this research. I deeply appreciate the insightful, sophisticated comments provided by Dr. Müge Kruşa Yemişcioğlu and the technical assistance from Anıl Koç.

I am forever grateful to my best friend, Kürşat Avan, who unwaveringly supported me over the years. Having an engineering genius by my side enriched the quality of this thesis. My heartfelt gratitude goes to dearest Ceren Kara, who has been with me, providing invaluable emotional support throughout this journey.

I consider myself incredibly fortunate to have a friend like Aslı Zeynep Doğan, whose remarkable support encompasses both emotional encouragement and knowledge has been a game-changer for me. İlkim Canlı, with her expertise that shines as brightly as daylight, and Reyhan Nazlıaydın, for standing by me throughout this entire process.

Lastly, I would like to thank my parents, Rukiye Nas and Seyfullah Nas, for their loving and constant support, as well as my brother Emre Nas, whose helping hand was always there when I needed it.

This thesis is supported by the Scientific and Technological Research Council of Turkey under the TUBITAK 2210-C National MSc Scholarship Program in the Priority Fields in Science and Technology.

TABLE OF CONTENTS

LIST OF TABLES

TABLES

LIST OF FIGURES

FIGURES

LIST OF ABBREVIATIONS

ABBREVIATIONS	
3D	Three-Dimensional
4D	Four-Dimensional
DIW	Direct Ink Writing
FDM	Fused Deposition Modeling
SLA	Stereolithography
SME	Shape Memory Effect
SMA	Shape Memory Alloy
SMP	Shape Memory Polymer
SMM	Shape Memory Material
LCE	Liquid Crystal Elastomer
HWA	Hygroscopic Wood Actuator
PLA	Poly Lactic Acid
TPU	Thermoplastic Polyurethane
ABS	Acrylonitrile Butadiene Styrene
Tg	Glass Transition Temperature
RL	Restriction Layer
AL	Active Layer

CHAPTER 1

INTRODUCTION

Buildings account for approximately one-third of global energy consumption (IEA, 2019), primarily attributed to heating, cooling, ventilation, hot water, lighting, and electrical equipment (Ramesh et al., 2010). Building envelopes have a significant influence on energy efficiency and reducing energy consumption (Méndez Echenagucia et al., 2015). Similiar to natural skin, building envelopes are a barrier between the external and internal environment, regulating energy transfer. However, its challenge lies in continuously adapting to changing outdoor conditions and occupant preferences.

Since the primary functions of the building envelope are to provide occupants with a comfortable indoor environment and minimize the need for operational energy, any additional energy consumption to cope with these changes can compromise the effectiveness of the building skin. Therefore, it is essential to design building envelopes that can adapt to changing conditions with minimal energy input.

The advent of 3D printing revolutionized manufacturing, enabling the consideration and modification of not only the external geometries of objects but also their internal structures. This complexity offered by 3D printing technology allows for infinite customization of 3D objects at no additional cost. By leveraging the advancement in manufacturing technologies and drawing inspiration from nature, it becomes possible to embed responsiveness into materials.

An example of passive shape-changing in nature is observed in mature pine cones, which disperse seeds through passive shape changes even after the cells have died. This mechanism is attributed to the bilayer structure of the seed-bearing pine cone

scales, where differences in cell type, dimensions, and hygroscopic expansion coefficients cause mechanical stress and induce bending motion (Dawson et al., 1997).

The passive shape-changing behavior of wood-based bilayers holds promise for climate-responsive building skins. Wood exhibits this behavior without requiring any additional energy and responds to daily variations in humidity, which are directly correlated with daylight (Menges & Reichert, 2012). In addition to these, wood possesses superior features when compared to other shape-changing materials, making it well-suited for climate-responsive skin applications. As a commonly used material in the construction industry, wood waste can be recycled through 3D printing, offering extensive customization and design possibilities. Thanks to its cost-effectiveness and ease of manufacturing, the widespread adoption of wood for shape-changing architectural skin applications possible and promising for enhancing the sustainability of buildings.

1.1 Problem Statement

The International Energy Agency (IEA, 2019) reported that the building and construction sector is responsible for 36% of global energy consumption and 39% of energy-related carbon dioxide emissions. Operating energy constitutes the largest portion, accounting for 80% to 90% of a building's lifecycle energy consumption (Ramesh et al., 2010). Therefore, finding ways to reduce energy use in buildings is crucial. One significant factor influencing energy efficiency is the building envelopes, making it a critical parameter for reducing the reliance on active systems (Méndez Echenagucia et al., 2015).

While adaptive building envelopes have shown a potential to improve a building's internal environment and performance characteristics (Loonen et al., 2013), traditional systems relying on sensors and motors face challenges when it comes to sensing the environment, processing data, and generating relevant motion at a

building scale (Menges & Reichert, 2012). The complexity and maintenance costs associated with these systems compromise their effectiveness (Holstov et al., 2017).

To overcome these challenges, there is a growing interest in responsive materials that can change shape in response to environmental stimuli without requiring additional energy input (López et al., 2017). Wood, with its swelling and shrinking characteristic in response to environmental humidity, holds promise for the development of climate-responsive building skins (Holstov et al., 2015; Zuluaga & Menges, 2015).

In terms of sustainability and design freedom, extrusion-based 3D printing of wood-based materials outperforms the traditional approach of bilayering wood veneers. By utilizing wood flour derived from waste products and local production, 3D printing reduces both the environmental impact and cost (Mazzanti et al., 2016, 2019). Furthermore, the filament production process and shear-induced stress during printing align the wood fibers, enabling greater design space and more predictable motion through designed print-paths (Le Duigou et al., 2016a; Zuluaga & Menges, 2015).

However, 4D printing of wood by FDM is restricted to wood-based filaments available in the market (Gauss et al., 2021). These materials lack robustness, display delamination of bilayers (Correa et al., 2020), and are responsive to water immersion rather than environmental humidity (Tahouni et al., 2020). Even though customized filaments can enhance responsiveness (Tahouni et al., 2022), small nozzle diameters of FDM printers limit the printable wood content of the filaments (Kariz et al., 2018). This results in a slow and limited shape change in response to environmental humidity (Correa et al., 2015).

In addition to response speed, the existing literature highlights several challenges in utilizing hygroscopic wood actuators for climate-responsive building skins, including the predictability of motion and scalability. Hence, this research investigates the design space at both mesostructural and macrostructural levels for controlled, scaleable motion. To this end, a series of experiments will be conducted

in a controlled environment to observe the actuation dynamics. The experiments will explore design parameters including thickness, porosity, bilayer ratio, layer orientation, and 3D printing parameters such as layer thickness and printing order. Collected data will be utilized to construct a model that can predict the actuation and find the configuration for the required motion. Implementations of this model will be developed and fabricated. The coupling of actuators and pre-stressed bistability will be tested for amplified and controlled motion. Experiments will be carried out at larger scales to test the scaleability of the implementations.

Two implementations of this model are proposed. While the first design makes use of combined actuators for motion amplification, the latter employs pre-stressed bistability to control the timing of motion. Both designs were tested at scales of ½ and 1 to 1, using a wood-based filament and wood veneer as actuators, respectively. The results demonstrate that the use of multiple-joined actuators significantly increases the actuation speed. Moreover, it is shown that the humidity level required to trigger the shape-shifts can be tuned thanks to the pre-stressed bistable structures. This is promising in terms of adaptability to diverse climates and enhancement of energy efficiency in buildings.

This study aims to contribute to the growing body of literature on wood-based hygroscopic climate responsive building skin applications. Employing available 3D printing filaments and wood veneers, configurations at both meso and macroscale will be investigated to understand the relative weight of the design and fabrication parameters. The results of the experiments and collected data will provide insight into developing prototypes that can overcome state-of-the-art challenges, including motion control, motion amplification, and scalability.

1.2 Aim and Objectives of the Research

This thesis aims to provide an exploration of the design and fabrication parameters to overcome the state-of-the-art challenges of wood-based hygroscopic climate responsive building skin applications. The objectives of the thesis can be listed as:

- To explore the influence of design and fabrication parameters on the actuation behavior
- To find the configuration that can fulfill the requirements of climate responsive skin
- To develop climate responsive skin prototypes that can adapt to various climates

To achieve the objectives, these research questions will be answered:

- How do the thickness, bilayer ratio, restriction layer porosity, 3D printing path rotation, and 3D printing layer height affect the response speed and bending angle of the shape change?
- What is the best configuration of design and fabrication parameters for the climate responsive building skin applications?
- How the coupling of wood based actuators can be implemented to enhance response speed?
- How the pre-stressed bistability can be integrated into wood based actuators to enhance motion control?
- How is the actuation behavior altered by different wood based actuators and at different scales?

CHAPTER 2

LITERATURE REVIEW

This chapter presents the literature review based on the problem statement of this study. Firstly, the definition of building envelopes and their significance on the energy efficiency of buildings are provided. The drawbacks of static envelopes and the significance of adaptive envelopes are explained. Then, traditional adaptive envelops are compared with responsive skins that utilize shape-changing materials. The recent studies on wood-based responsive skins are reviewed.

Secondly, an overview of the concept of 4D printing technology is provided. The state-of-the-art material and fabrication technologies to develop shape-changing structures are examined. Among the shape-changing materials, wood-based materials are found promising for the creation of climate-responsive skin. Therefore, a literature survey on fabrication technologies focused on the techniques that utilize wood-based materials.

Lastly, smart structures and motion mechanisms in the literature are reviewed. Examples are studied in terms of how motion control is achieved with various shape-changing materials. Studies at bath macro and mesoscale were provided. Particularly the works on designated print-paths and motion amplification strategies are studied, which are related to challenges faced on wood-based responsive skins. Bistable structures are closely studied since they provide well-defined controlled motion. A particular focus was given to bistable structures and origami since the integration of these structures into shape-changing materials is promising for amplification and control of the motion.

2.1 Building Envelope

According to the International Energy Agency (IEA), in 2019, the building and construction sector accounts for 36% of global energy consumption and 39% of energy and process-related carbon dioxide (CO2) emissions. Operating energy is the largest contributor, ranging from 80% to 90%, while embodied energy accounts for 10-20% of a building's lifecycle energy consumption (Ramesh et al., 2010). The term "operating energy" refers to the energy consumed in buildings during their operational phases, such as heating, cooling, ventilation, hot water, lighting, and other electrical equipment. It can be described in terms of either end-use or primary energy (Sartori & Hestnes, 2007). It is commonly acknowledged that enhancing the use of natural heating, cooling, and lighting, with less reliance on powered systems, is one of the most efficient methods to minimize building operating energy (Tzikopoulos et al., 2005). Passive design principles, such as natural lighting and ventilation schemes, activated thermal mass, and the use of a well-insulated exterior, ensures that reliance on active systems is minimized (Sadineni et al., 2011). Building envelopes or shells have a significant influence on the energy efficiency of buildings, making them a critical parameter in reducing the use of active systems.(Méndez Echenagucia et al., 2015). Foundation, walls, roof, shading devices, and every component that separates the indoor and outdoor conditions are all parts of building envelopes (Sadineni et al., 2011). They serve as a filter that regulates the energy transfer from outside environmental conditions to the occupant’s desired conditions inside (Berköz & Yílmaz, 1987; Oral & Yilmaz, 2003).

Fulfilling the desired indoor conditions is a challenging task and significantly affects the welfare of the building’s users since a recent study demonstrated that in Europe, people spend 90% of their time indoors (EC, 2003). Many studies have been conducted on building envelopes to enhance energy efficiency and user comfort. In the last thirty years, broad and consistent application of these studies resulted in a huge reduction of operational energy. By enabling the use of clean energy sources, more sustainable structures are constructed (Perino & Serra, 2015). However,

environmental conditions alter throughout the year and even in a day as well as user requirements for indoor conditions (Loonen et al., 2013). Therefore, even structures with superior passive design need powered systems to mitigate the impacts of the changing climatic conditions (Sartori & Hestnes, 2007). For example, while buildings that are designed by utilizing the passive design principles reduce energy consumption for space heating, they frequently raise cooling loads to a large level, resulting in overheating of the interior. Another example is that optimized building envelops are designed for a specific energy demand, with a custom importance to heating, cooling, lighting, and electric energy (Perino & Serra, 2015). Traditional building shells are static and unable to adapt to any change in these demands or variations to environmental conditions throughout the year (Loonen et al., 2013). Generic architectural components that are designed to fulfill a wide range of situations and are not able to alter their attributes or functions are restrictive and unsatisfactory. Therefore, the notion of the building envelope must shift from insulation to adaptation (Perino & Serra, 2015).

2.1.1 Adaptive Envelope

The terminologies used in adaptive building envelope research are wide. The most frequent terms for shading devices that interact with their surroundings are performative, adaptive, and responsive (Barozzi et al., 2016). While Turrin et al. (2012) described performative envelopes as a regulative component between outside conditions and occupant comfort to achieve designed performance, adaptive envelopes are defined as components that can alter their shape or features to adapt to changing external conditions (Loonen et al., 2013; Turrin et al., 2012). Nicholas Negroponte (1973) described responsive components as when the environment is the one that triggers the change. Similiar to this definition, Velikov and Thün (2012) defined responsive as reactive and showing a response to an environmental stimulus rather than controlling them.

Instead of an envelope or shell, building skin or architectural skin reflect the biologically inspired concept, adaptivity, and change of the living systems (Velikov & Thün, 2012). The term architectural skin also separates the structural function with the envelope, and as with the human skin, it means that it serves as an organic, functional barrier between the outside and inside (Del Grosso & Basso, 2010).

Many adaptive building skins have been developed by both industry and academia. For meaningful evaluation, the characterization of the adaptive skins' parameters is necessary. The purpose of the skins varies according to their focused performance, such as thermal comfort, acoustic performance, visual performance, or multi-purpose. The external environmental factors, such as light, heat, air, or water, can be collected, rejected, or regulated. Sensing the triggering stimuli condition and changing the form and/or function can be the intrinsic property of the material or can be extrinsic. The spatial scale of the skins can be the opening of a small window or as large as a whole building, and strongly related parameter with the response speed. Response speed requirements of the adaptive building envelope highly depend on the controlled external factor and its speed of variation. For example, solar radiation control may require a response in the time range of a day, while seasonal change could be adequate for visual performance (Aelenei et al., 2016; Kuru et al., 2019).

To overcome the challenges associated with static ones, adaptable building envelopes were designed to react to changing external circumstances in order to reduce building operational energy consumption while ensuring thermal comfort to building occupants (Loonen et al., 2013). Although adaptive envelops improve a building's internal environment and performance characteristics (Loonen et al., 2013), the complex task of sensing the environment, processing data, and generating relevant motion at the building scale poses a significant challenge for traditional systems that rely on sensors and motors (Menges & Reichert, 2012). They are mostly energy-reliant (Loonen et al., 2013), which is a significant disadvantage for a system attempting to reduce operational energy. These systems are burdened by complexity and maintenance costs that compromise their effectiveness and the circularity of the building (Holstov et al., 2017).

2.1.2 Climate Responsive Skin

Due to the discussed drawbacks of traditional adaptive envelops, responsive materials that change shape in response to environmental stimuli without requiring additional energy input hold considerable promise for climate-responsive skins (López et al., 2017). Addington and Schodek (2005) defined smart materials as immediate and predictable self-actuating materials in response to a variety of environmental states.

Adaptive envelopes that incorporate smart materials are called responsive 'skin' due to the immediate, self-actuating response similar to the behavior observed in nature. Unlike 'intelligent' envelops, responsive skin does not process any information thorough computation or automation but response to external stimuli executed in real-time by the intrinsic properties of the smart material. In other words, smart materials employed in responsive skins eliminates the need for additional energy source, environmental sensor, information processors, and motion actuators (Addington & Schodek, 2005; Velikov & Thün, 2012).

There is a growing interest in literature to employ smart materials in responsive skin. The studies on climate-responsive skin applications can be classified as the controlled stimuli, employed smart material, the design strategy for integration of smart material (actuator, skin, amplifier, etc.) as well as the used fabrication technique (bilayer, 4D print, etc.) (Vazquez, Randall, et al., 2019). The following section of the literature review is conducted to explore these strategies and examine the advantages and limitations of the responsive skins that aim to provide daylight control.

2.2 4D Printing

3D printing is a manufacturing process to achieve the desired form by adding material layer by layer. The technology was invented in the 1980s, and since then, it has found applications in many industries, such as automotive, biomedical, and

aerospace, due to its high design freedom and customization capabilities (Ngo et al., 2018).

However, traditional 3D-printed objects are static and fail to adapt to changing environmental conditions (Melly et al., 2020). To address this limitation, the term '4D printing' was first introduced by Skylar Tibbits at the 2013 TED Talk. Tibbits defined the term as 3D-printed objects which can respond to certain stimuli to change their shape or functionality (Tibbits, 2014). Since the emergence of the term, it has taken great attention from academia, and its definition has evolved over time. One study described 4D printing as 'the shape, property, and functionality of a 3D printed structure could evolve with time when exposed to a predetermined stimulus, such as heat, water, light, pH, etc.' (Kuang et al., 2019).

Compared to traditional 3D printing, 4D printing technology offers several advantages. By strategically adjusting materials in three-dimensional space, it becomes possible to create smart materials that can self-assemble, self-repair, and exhibit multiple functions (Momeni et al., 2017). These capabilities allow the deployment of the structures and optimize the use of material, thus, leading to cost reductions in material consumption and transportation (Tibbits et al., 2013). For instance, flat manufactured objects capable of self-assembly by the free environmental energy in the application area provide flat packing and significantly decrease the volume during transportation (Tibbits, 2014). Another benefit of self-assembly is the elimination of the need for support during 3D printing. The 3D printing of complex structures requires support in most 3D printing technologies. By 4D printing, flat objects can later be activated to form complex structures, eliminating the need for support, and leading to material and time savings (Y. Zhou et al., 2015).

Adaptable structures are crucial for environments with changing needs, necessitating the incorporation of sensors and motors for shape change. 4D printing could be a more efficient alternative to active environments. 4D printed structures can be programmed to sense environmental changes and change their shape without relying

on external electromechanical sensors or actuators (Tibbits et al., 2014). An example of an active environment where 4D printing finds application is in the biomedical field, where 4D printed tissues can react to complex changing needs (Muehlenfeld & Roberts, 2018).

In an article by Kuang et al. (2019), the authors stated that there are two ways of constructing 4D-printed objects. The first is the utilization of stimulus-responsive materials in 3D printing, such as Shape Memory Polymers (SMP) and Shape Memory Alloys (SMA). SMPs are the most common stimulus-responsive materials, thanks to their unmatched properties. Various environmental conditions can activate them; they are easy to process and have high recoverable strains (Melly et al., 2020).

The second method involves multi-material 3D printing, where the different characteristics of materials, such as thermal expansion coefficient or swelling ratio, create localized eigenstrain within the object, resulting in targeted shape-shifting (Kuang et al., 2019).

According to a review paper, multi-material 4D printing consists of five main components. Firstly, a multi-material 3D printer is required since 4D printing relies on the distinct physical or chemical characteristics (thermal expansion coefficient, swelling ratio, etc.) of combined printed materials. The second component is the stimulus that triggers the 4D-printed object's response. Different application fields have varying environmental changes, and the stimulus needs to be chosen accordingly. Additionally, different materials respond to specific stimuli, making stimulus selection dependent on the materials used. Smart materials are the third component that can be branched into subcategories according to their response to stimuli, shape memory, multi-functionality, and self-adaptability. The fourth component is the interaction mechanism, also called programming. While some of the 4D printed objects can be triggered directly upon printing, some of them need an additional programming step to be able to activate. The final component is mathematical modeling, which plays a crucial role in manufacturing 4D-printed objects capable of transitioning between desired states, involving the understanding

of the relationship between design, material structure, and stimulus properties (Momeni et al., 2017).

2.2.1 Shape Changing Materials

Smart materials are defined as materials that can be programmed and precisely manipulated by desired external stimuli (Ahmad, 1988). A stimulus can cause a variety of changes in smart materials' properties, including electrical, chemical, optical, thermal, magnetic, and mechanical (Figure 2.1). However, this study only focuses on shape-changing materials, in which the stimuli cause a physical change in the material and resulting a deformation (Vazquez, Randall, et al., 2019).

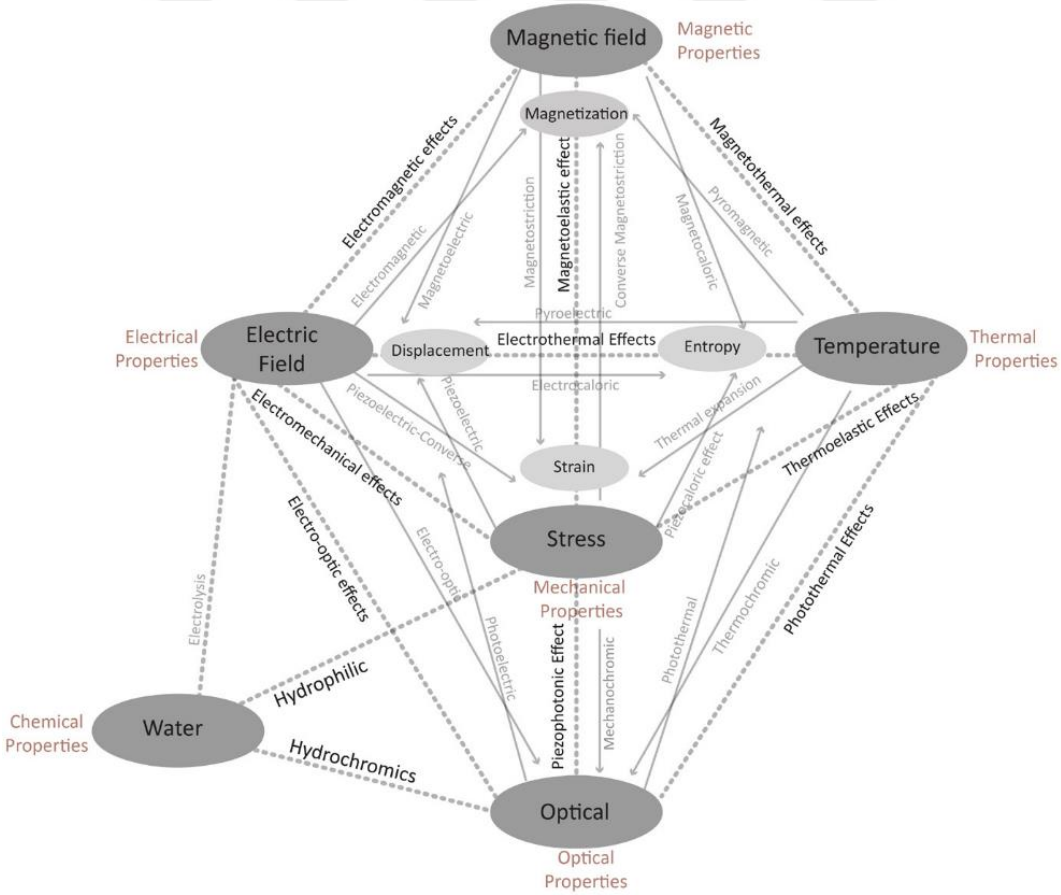

Figure 2.1. Illustration of smart materials' behavior (Vazquez, Randall, et al., 2019)

Shape-changing materials enable the construction of multi-functional, multi-state structures. The ability to change shape in response to defined stimuli attracted researchers in design-related fields because of the promising aspects for the creation of responsive structures (Correa et al., 2015). Design-oriented studies explore the integration of shape-changing materials into building skin to enhance building performance. Eliminating the need for additional energy input and utilizing environmental energy holds significant promise for the sustainability of the buildings, yet requires leveraging recent innovations in computational design and fabrication (Vazquez, Randall, et al., 2019).

This review on the shape-changing smart materials is particularly focused on the integration of these materials to climate responsive skins. Therefore, one of the most reported materials utilized for responsive skin research, such as SMA, SMP, and wood are studied. Additionally, hydrogels and LCEs are examined for their promising features to integrate climate responsive skins. An overview of these shape-changing materials is provided. Then, materials are evaluated based on the requirements of climate responsive skin. The considered features of the shape-changing smart materials are determined as follows: fabrication difficulty and cost, triggering stimuli, reversibility (One-way or Two-way), generated shape change, robustness, durability for the long-term, and sustainability of the material.

SMP (Shape Memory Polymer) and SMA (Shape Memory Alloy) are classified under materials that demonstrate Shape Memory Effect (SME). SME is a crucial aspect of 4D printing. It is defined as the material's capability to memorize the original shape and recover that shape from a trained temporary shape when triggered by stimuli (Pei, Loh, 2018). Materials that exhibit the SME effect can be evaluated with two parameters. First is the shape recovery ratio (SRR), the ratio of recovery to the original shape, which is measured between 0-100%. For example, the complete recovery of the object is calculated as 100%. The letter is the fixity ratio which is

defined as the capability of conserving the actuated shape when the stimuli are removed (Rastogi, Kandasubramanian, 2019).

2.2.1.1 Shape Memory Alloys (SMA)

Among the Shape Memory Materials (SMM), SMA's are the most widely applied and studied material because of their superior properties such as durability, fatigue resistance (Mohd Jani et al., 2014), biocompatibility, high corrosion, and electrical resistance (Hartl & Lagoudas, 2007; Huang et al., 2010) as well as the shape memory effect. SMA's are shape-changing materials that can recover their original form above a certain temperature (An et al., 2012). Unlike the complex traditional actuators, SMA's are lightweight, simple, and generate great force per unit (Cho et al., 2009).

On the other hand, low levels of design freedom in shape recovery, challenging and expensive manufacturing processes, and difficulties in precise prediction of the motion are primary restrictions of SMAs for the applications (Yi & Kim, 2021). When compared to the SMPs, SMAs display much greater recovery stress. However, the maximum strain of SMAs is between 4-8%, while SMPs are up to 50-100% (D. I et al., 2018; J. H. Lee et al., 2019).

According to the triggering stimuli, SMA's can be classified into two categories thermo-responsive and magneto-responsive (Fiorito et al., 2016). For the climate-responsive applications, thermo-responsive SMA's are used to utilize solar radiation. SMA's commercial availability in the markets mostly as wires and springs (Fiorito et al., 2016), led to it being mainly used as linear, spring-shaped actuators to dynamically move the facade elements (Vazquez, Randall, et al., 2019). Additionally, SMA's in the market mostly exhibit one-way shape memory; the ones having two-shape memory require a difficult and expensive manufacturing process and generate a lower force of recovery (Elahinia, 2016; A. Y. Lee et al., 2017; Xia et al., 2021).

2.2.1.2 Shape Memory Polymers (SMP)

SMPs are polymeric materials that require additional programming steps to actuate upon external stimuli such as heat or light. When heated above Tg for amorphous polymer (glass transition temperature) or Tm for semicrystalline polymer (melting temperature), they become rubber-like materials and are easy to deform. The deformation made above these temperatures is called programming. After the object cooled down below Tg or Tm, a permanent but stable shape is achieved. Then, the object is programmed and ready for actuation when heating is applied above the Tg or Tm (Kuang et al., 2019). This actuation method is achieved thanks to the entropic elasticity of SMP (Yu et al., 2016).

Research studies on SMP materials are fastly growing because it offers superior properties to other SME materials. While SMPs exhibit high deformation recovery and flexibility, relatively lower energy is required in the programming step. Furthermore, SMP can be triggered by various stimuli, which significantly increases potential application fields. In addition, biocompatibility, low cost, and available feedstock made it favorable among the other SME materials (W. G. Yang et al., 2014).

On the other hand, one of the main concerns for SMPs in 4D printing applications is that it requires reprogramming after each shape recovery which is not preferable where two-way actuation is needed. Moreover, low actuation energy and slow recovery time limit the wide-range application (Mehrpouya et al., 2021). Another concern is the durability of SMPs over time since the material is deformed in each cycle depending on the polymer used (Memarian et al., 2019).

As reported previously, SMPs can be triggered by diverse stimuli. Apart from heat as a triggering stimulus, photoresponsive SMP objects are printed using 3D-printed carbon black–reinforced polyurethane (PU). According to the research, direct exposure to sunlight is used to trigger actuation (H. Yang et al., 2017).

Remote actuation is also possible for single SMP structures by employing Magno-active materials such as Fe3O4. The material nanoparticles are heated when exposed to a magnetic field; therefore, SMP structures that consist of these particles can be remotely actuated (Wei et al., 2017).

Photoresponsive SMP objects also achieve sequential shape-shifting. Employing different colors of ink in the object by DIW printer, different parts of the object absorbed the light according to the wavelength of the colors. Thus, SMP objects with different levels of light absorption enabled sequential shape-shifting (Jeong et al., 2020).

2.2.1.3 Liquid Crystal Elastomers (LCE)

Liquid Crystalline Elastomers (LCEs) are a combination of the self-organization and anisotropic behavior of liquid crystals and the elastic property of rubber (Herbert et al., 2021). Decades ago, it was predicted that polymeric materials with liquid crystallinity would be able to be triggered by external stimuli and expand and contract as much as muscle fibers (de Gennes, 1997). Recent findings show that LCEs exhibit up to 400% strain depending on the variables such as degree of cross-linking and mesogen connectivity. Moreover, LCEs display soft elasticity, which is defined as nonlinear deformation to mechanical load (Herbert et al., 2021).

Deployable, lightweight, and self-folding structures are created by employing SMP materials. However, SMPs exhibit One Way Shape Memory Effect (OWSME), which means their actuation is not reversible when the triggering stimuli are removed. On the other hand, LCEs display the Two Way Shape Memory Effect (TWSME), so their actuation is reversible (Wang et al., 2020).

LCEs are cross-linked polymer networks, and order disruption of these networks enabling the stimuli response (Herbert et al., 2021). The orientation change of liquid crystalline mesogens -from nematic (ordered) to disordered (isotropic)- causes the

actuation of LCEs. Therefore, it is possible to tune the deformation by controlling the mesogen direction (Ohm et al., 2012).

Several methods are reported for the alignment of mesogens. Mechanical alignment is one of the methods by which mesogens are aligned by stretching; however, it is hard to pattern orientation. Surface alignment is another strategy that offers complex orientation patterns but is limited to thin-film samples and difficult to fabricate. The magnetic field-assisted alignment method also has constraints since it requires excessive magnetic or electric fields (Wang et al., 2020).

Reported drawbacks and difficulties of these alignment methods limited the wide-range application of LCEs. On the other hand, recently developed rheological alignment of mesogens by 3D printing offers a more straightforward process. During 3D printing by DIW printer, the deposition of ink to the build plate by moving the nozzle creates both shear and extensional stresses, which force the alignment of mesogens along the printing path. Other extrusion-based printing technologies, such as FDM and electrohydrodynamic jet, are also possible, but DIW is the optimal technology to manufacture aligned LCEs. Thick and high-force LCE structures can be manufactured by DIW, although the pattern resolution is relatively poor because of the rheological limitations (Herbert et al., 2021).

According to an article, it is possible to create LCE structures with tunable properties in one single print. Authors developed functionally graded LCE by changing the printing parameters and stated that actuation strain, actuation stress, and mechanical stiffness of structure can be controlled (Wang et al., 2020).

According to research, ink consisting of LCE and photo-initiators heated to Tni (nematic-isotropic phase transition temperature) is printed by a DIW printer. Printed ink on the build plate is cross-linked by UV light immediately so that mesogens do not have time to go back to the polydomain (unaligned) state. However, the authors report that printed ink creates two different structures: shell and core. This is due to the ambient temperature that immediately cools down the shell of the printed ink, increases the viscosity, and fixes the mesogens in an aligned state. However, the core

structure of printed ink cools sown slowly; therefore, they are able to go back to the polydomain state (Figure 2.2) (Wang et al., 2020).

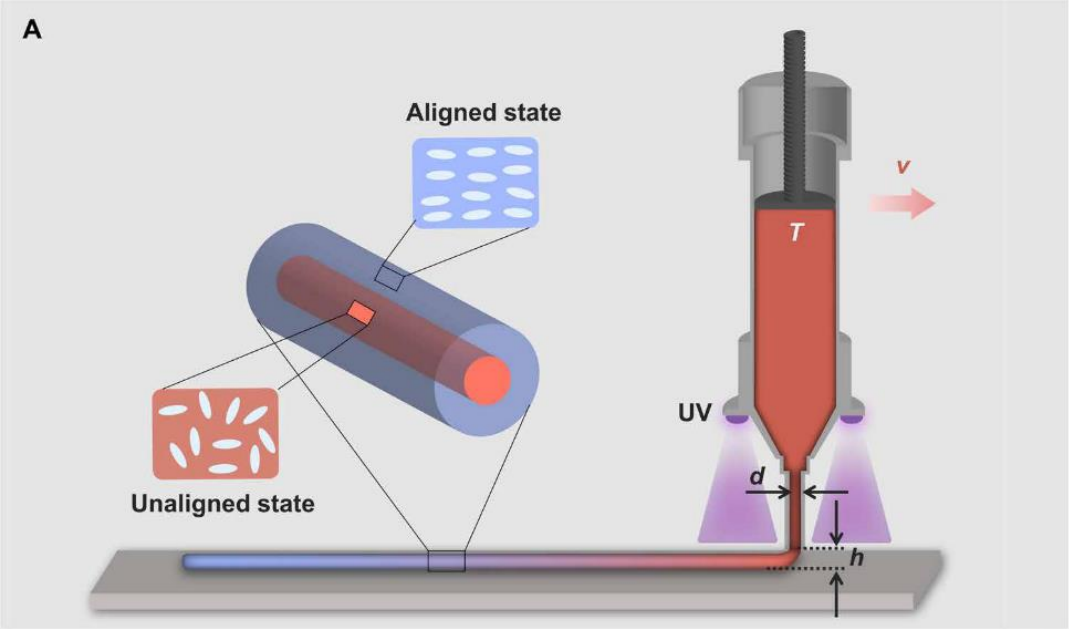

Figure 2.2. Illustration alignment of mesogens during the Direct Ink Writing of LCE (Wang et al., 2020)

These findings show that only the shell structure has the aligned mesogens, and thus actuation behavior is limited to the shell structure's behavior. This discovery has paved the way to create functionally graded LCE since the ratio of shell structure to core structure can be controlled by the printing parameters. Increasing the nozzle diameter or height between the nozzle and the build plate lowers the velocity of printed ink, thus decreasing the mesogen alignment. Changing the printing temperature is a more-straight forward solution because it does not affect the printing quality. Lowering the temperature increases the velocity of ink and creates a higher ratio of aligned mesogens (Wang et al., 2020).

To conclude, printing LCE ink by DIW printers enables control of the magnitude and direction of actuation behavior, thus offering high design space for designers (Wang et al., 2020).

2.2.1.4 Hydrogels

Hydrogels are extremely hydrophilic polymeric with high water-absorption capacity. Their size remarkably enlarges by swelling when immersed in water or exposed to humidity. They can be actuated with a wide-range of actuation methods, such as osmotic (pH, Humidity, Ionic, Thermal, Optical), pneumatic, magnetic, or acoustic actuation.

Hydrogels exhibit large and reversible deformation by swelling and de-swelling behavior. Their actuation is high-speed at the beginning, but complete actuation takes so much time due to the logarithmic trend of osmotic pressure (Stoychev et al., 2012).

However, in order to generate controllable and practical actuation, heterogeneity is required in hydrogel structures. Heterogenous hydrogel structures can be created either by the structure's design or employing dopants that alter the electrical or chemical properties of the structure (Zhang & Khademhosseini, 2017).

The most common method for actuating hydrogels is osmotic pressure changes such as ph and humidity. Actuation by an electrical or magnetic field is also possible by introducing nanoparticles in hydrogel composite (Sun et al., 2021). Moreover, the actuation of hydrogels can be graded by employing hydrogels whose water-absorbing capacity changes with temperature. Functionally graded multilayer hydrogel structures with different volume expansion properties are reported in the literature (Odent et al., 2019).

Another research demonstrated that light-actuated hydrogel structures by photoresponsive hydrogel composites with light-absorbing nanoparticles. The light absorbed by these nanoparticles transformed to heat to generate actuation. Actuation

by light enables more precise and local actuation compared to heating (Zheng et al., 2020).

Manufacturing of hydrogel structures is possible by direct 3D printing of hydrogel or 3D printing of the mold and casting. Among these methods, 3D printing offers higher design space since the microstructure and mesostructure of the object can be designed. Inkjet printing is used to direct the printing of hydrogel actuators, but due to the nature of this technology, printed hydrogel needs to have low viscosity (Zolfagharian et al., 2017). This causes low structural integrity, and reinforcing materials are introduced to tackle this challenge (Jakab et al., 2010).

Laser-based 3D printing of hydrogel structures is advantageous in many ways. Excellent resolution of these printing technologies enables the creation of highly complex structures. Furthermore, anisotropic swelling behavior can be encoded by controlling different printing parameters. For example, crosslinking density can be tuned by controlling the magnitude of the laser system (Odent et al., 2019). On the other hand, high cost and small build volume are negative aspects of this printing technology (Sun et al., 2021).

Extrusion-based printing technologies offer control of actuation direction with designed micro and mesostructure of the object by well-defined printing paths. However, the low viscosity of hydrogel inks causes weak buildability properties, which creates difficulties in extrusion-based printing technologies (Sun et al., 2021). To tackle this, thermoreversible support structures are introduced, and hydrogel material is embedded into them. After the printing, the object is heated, and liquified support structures are easily removed (Hinton et al., 2015).

2.2.1.5 Wood

Wood has been a common, traditional material in the construction industry for years. However, the differential dimensional change of the wood in response to humidity has been seen as a deficiency for a long time. Inspired by pinecones seed disposal,

recent developments in material and fabrication technology demonstrated that the swelling and shrinking properties of wood can be utilized to develop responsive structures. The difference in the swelling ratio of bilayered materials results in a bending motion when the ambient humidity is changed (Burgert & Fratzl, 2009; Dawson et al., 1997).

The direction of shape change can be predicted since the expansion and contraction of wood occur perpendicular to the fiber direction (Menges & Reichert, 2015; Vailati et al., 2018). This is due to the cellulosic structure of wood, and it wants to remain at equilibrium with the environmental humidity, and moisture diffusion occurs in the case of an imbalance (Skaar, 1988). While the dimensional change by swelling can occur up to ten percent perpendicular to Microfibrillar orientation, almost no change can be observed in fiber direction (Dinwoodie, 2000). This clear anisotropic shape change allows to control the motion.

Moreover, the bending curvature of the wood bilayers can be calculated by the Timoshenko Theory, which was originally developed for the temperature change of bi-metals (Correa et al., 2015; Rüggeberg & Burgert, 2015; Timoshenko, 1925). The magnitude of the generated shape change is directly related to the total thickness of the bilayer, in particular, the wood-based active layer. When exposed to outdoor conditions, it is proven that wood bilayers can preserve their functionality with slight loss (Holstov et al., 2017; Reichert et al., 2015).

Wood-based bilayers outperform synthetic hygroscopic smart materials not only in terms of the actuation range but also in terms of generated actuation force and strength (D. M. Wood et al., 2016). For instance, in ancient Egypt, hygroscopic swelling of wood was utilized to split granite stones (Tarkow & Turner, 2005). This remarkable force generated by the changes in relative humidity occurs between 25-100% (D. M. Wood et al., 2016).

The studied five materials, SMAs, SMPs, LCEs, hydrogels, and wood, are evaluated based on the identified eight features for climate responsive skin applications (Table 2.1). The first feature is the reversibility of the motion. This is one of the key

parameters, and most of the smart materials are not even considered for the application since they are not capable of reversible motion. Among the examined five materials, only SMP requires a programming step which is a significant challenge for applications.

The second feature is how applicable is the triggering stimuli of materials. SMA, SMP, and LCE are triggered by high temperatures, which are not in the range of daily variations. Therefore applications employing these materials require additional energy input to the system, which compromises their effectiveness. On the other hand, hydrogels and wood-based bilayers are triggered by the relative humidity, which significantly changes throughout the day.

Table 2.1 Evaluation of Materials Based on Identified Features for the Climate Responsive Skin Applications

	SMA	*SMP*	*LCE*	*Hydrogel*	*Wood*
Reversible Motion	+	-	+	+	+
Triggered by the natural, daily variations of stimuli	-	-	-	+	+
High Response Speed	+	+	+	-	-
High Actuation Force	+	-	+	-	+
High Design Space	-	+	+	+	+
Robust	+	-	-	-	+
Durable in long-term	+	+	+	-	-
Inexpensive	-	+	-	+	+
Sustainable	-	-	-	-	+

The third is the high response speed. The materials are evaluated based on being capable of opening and closing in the time range of a day. Some SMAs, SMPs, and LCEs are able to shape change in a matter of seconds. However, hydrogels and

wood-based materials are slow since they rely on vapor diffusion from the environment, and diffusion speed slows down as it gets closer to equilibrium.

The fourth feature is the actuation force. SMAs springs generate great actuation force and are used as actuators for many responsive skin applications. LCEs are also able to generate high force and promising applications as actuators. Depending on the thickness, hygroscopic expansion of wood could generate a high force of actuation. For the state-of-the-art, SMPs, and hydrogels are not able to provide a force that can actuate elements apart from themselves, so they are required to be directly employed as skin.

Apart from SMA's, which are mostly used as linear actuators in the form of wires and springs, evaluated shape-changing materials can be programmed by the internal structure to perform desired actuation. On the other hand, SMA's are much more robust when compared to these materials. Robust, responsive mechanisms can also be created by wood, depending on the thickness. However, responsive wood mechanisms are not durable when exposed to outdoor conditions for a long period of time. Wood-based composites at different ratios can ensure higher durability in the long term. Additionally, in terms of material cost and sustainability, employing wood-based materials for responsive skin applications outperforms the other evaluated materials.

To conclude, wood-based hygroscopic bilayers have a significant feature that makes them well-suited to the application of climate responsive skins, and due to the discussed merits, this study focused on wood-based materials for the application of climate responsive skins.

2.2.2 Fabrication Methods for Hygroscopic Wood-Based Actuators

The fabrication of hygroscopic, wood-based responsive structures is based on Timoshenko's beam theory on bi-metals. By employing this bilayer principle, the dimensional change of the materials can transform into a bending motion. In the case

of wood bilayers, the dimensional change is induced by humidity variations and the swelling behavior of wood. The methods used to fabricate these structures in literature can be classified by how the wood-based material is employed. The wood-based filament printed by FDM printers (Cheng et al., 2021; Tahouni et al., 2021; Tomec et al., 2021; Vazquez & Gursoy, 2020), wood ink printed by DIW technology (Kam et al., 2019) and glued wood layers (El-Dabaa et al., 2020; Grönquist et al., 2020; Vailati et al., 2017; D. Wood et al., 2018) are reported as hygroscopic, wood-based active materials. The reported fabrication methods significantly affect the actuation behavior, including response speed and generated shape change, as well as the scaleability and sustainability of the actuators. This section focuses on these methods and the pros and cons of the construction of climate responsive skin.

2.2.2.1 Wood Layers

Apart from the study by Krapež Tomec et al. (2022), which directly printed PLA on wood layers, most studies employing wood layers as an active material use adhesives to glue the restrictive layers. Different species of wood layers, in the form of wood veneers or thicker layers, are used. The employed wood species can be determined according to the application requirements. The difference between swelling ratios, mechanical properties, and workability of the species can play a role in the selection process (D. Wood et al., 2018). Most studies employ beech (Vailati et al., 2017) or maple (E. Chen et al., 2022) because of their high swelling and shrinking characteristics. For the restriction layer, wood species with low hygroscopic expansion or other materials can be employed.

The orientation of the wood fibers determines the hygroscopic expansion, thus, bending the bilayer. According to the cut of the wood layer, twisting, bending, or both twisting and bending are possible with this technique (Erb et al., 2013). However, the fiber orientations are limited to sections of wood cut, therefore offering a restricted design space compared to 3D printing with customized print paths.

Unlike 3D printed wood layers, the humidity range of actuation can be determined for cut wood layers at the time of gluing with a restriction layer. The wood layers are conditioned to specified humidity and then glued with water-resistant, elastic adhesive (Rüggeberg & Burgert, 2015) to restriction layer to alter the humidity range of motion. It is important to control the bilayering humidity to predict the motion. Therefore some studies condition the active wood layers in a humidity chamber for a long time (up to 72 hours) (Pelliccia et al., 2020) or keep the glued wood layers in a plastic bag (Vailati et al., 2017) to maintain the humidity level.

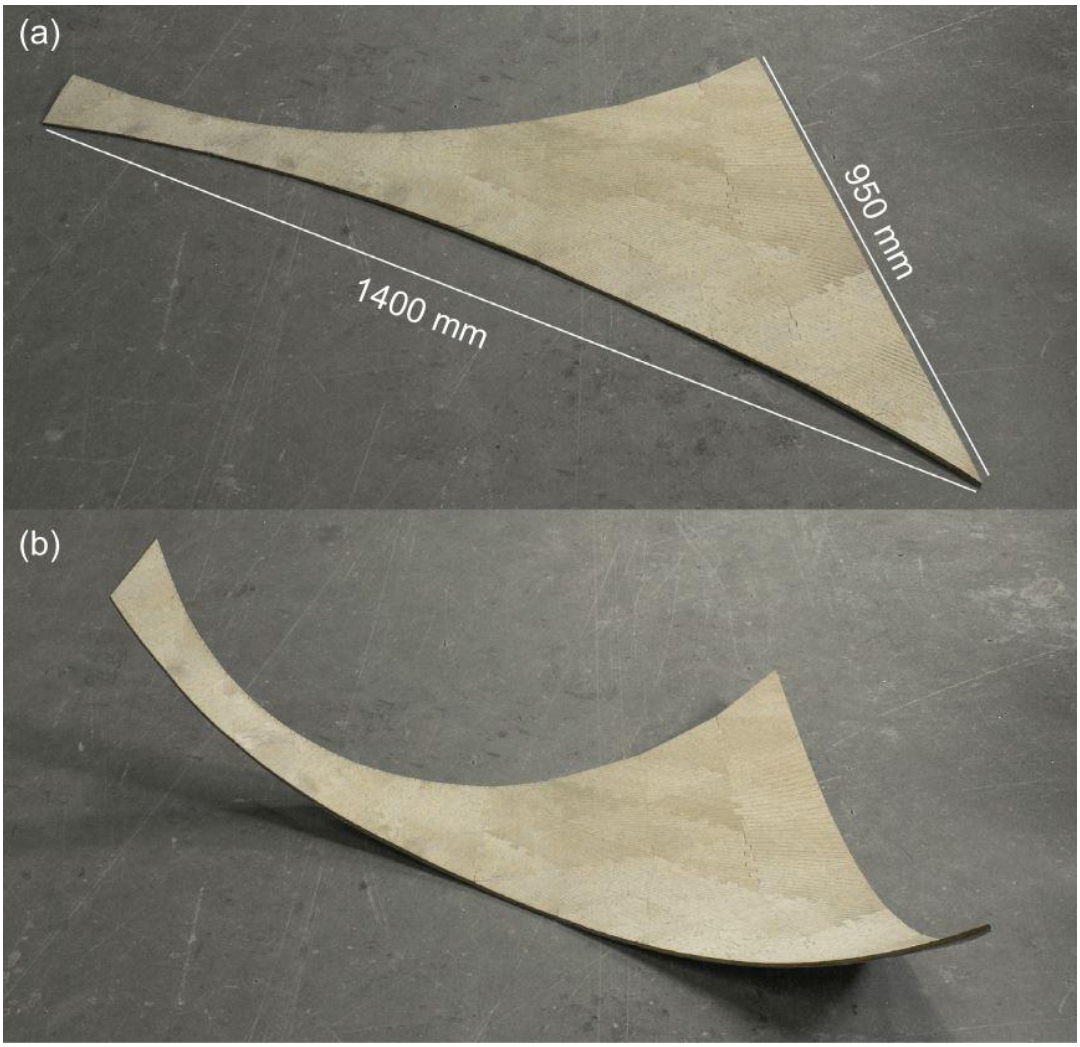

Figure 2.3. Hygroscopic actuation of maple-spruce bilayers joined together with finger joints in different fiber directions to create gaussian curvature (D. Wood et al., 2018)

Up to the author's knowledge, all the studies upscaled the wood-based hygroscopic change (Grönquist et al., 2019; Nan et al., 2020; Rüggeberg & Burgert, 2015; D. M. Wood et al., 2016) use this method (Figure 2.3) for the state of the art. The primary reason is that large-scale applications require a greater thickness of hygroscopic actuators, which slows down the response speed. This method employs 100% wood for actuators. Therefore, high response speed can be achieved even with thicker actuators. Unlike the extrusion-based 3D printing methods,

which degrades the material, mechanically stronger wood bilayers are created with this method since the natural structure of the wood is preserved. Joints such as mechanical (Vailati et al., 2018) and traditional wood finger joints (Nan et al., 2020; D. Wood et al., 2018) are used for large-scale applications.

2.2.2.2 Fused Deposition Modeling (FDM)

FDM utilizes thermoplastic polymers and composites in the form of solid filaments, heated to a semi-liquid state and deposited through a moveable nozzle on a build plate. Deposition of the filament is processed layer by layer to form the 3D object (Ngo et al., 2018).

It is the most common 3D printing technology because of the simplicity of FDM printers. They are relatively low-cost, accessible, and easy to use. Depending on the printer, a high speed of printing is also possible. Moreover, complete functional parts can be printed. On the other hand, it has the lowest resolution among the other 3D printing techniques, which limits their application that requires precise manufacturing. Printed parts have weak mechanical properties, anisotropy in the z-direction, and step structure on the surface (González-Henríquez et al., 2019).

Various process parameters affect the mechanical property of the printed object as well as dimensional accuracy and printing time, such as layer thickness, layer width, printing speed, and printing temperature of the nozzle and build plate.

Utilized materials for FDM printers mostly have relatively lower melting temperatures with higher Tg to solidify fast enough after the deposition. The most common materials are PLA (Polylactic Acid), ABS (acrylonitrile butadiene styrene), and PC (Polycarbonate) as they transform semi-liquid after deposition, but the available range of materials fastly growing. Apart from the commercially available materials, custom materials can be made with minor complications allowing infinite options of composites for different applications (Peng et al., 2019).

It should be noted that heating thermoplastic material to a specific temperature and depositing it through the small opening of the nozzle is a process that affects the

mechanical properties of the material. Therefore, the raw material characteristics of these materials may not be the same when they are printed (L. Novakova-Marcincinova and J. Novak-Marcincin, 2012).

FDM is highly adapted for 4D printing since it can directly print thermal responsive SMP. Another advantage of this technique is that it is possible to construct multi-material objects at once by multiple nozzles, which significantly increases the options for 4D printing applications.

In terms of sustainability and design freedom, extrusion-based 3D printing of wood-based materials outperforms the traditional approach of bilayering wood veneers. By utilizing wood flour derived from waste products and local production, 3D printing reduces both the environmental impact and cost (Mazzanti et al., 2016, 2019). Furthermore, the filament production process and shear-induced stress during printing align the wood fibers, enabling greater design space and more predictable motion through designed print-paths (Le Duigou et al., 2020; Zuluaga & Menges, 2015).

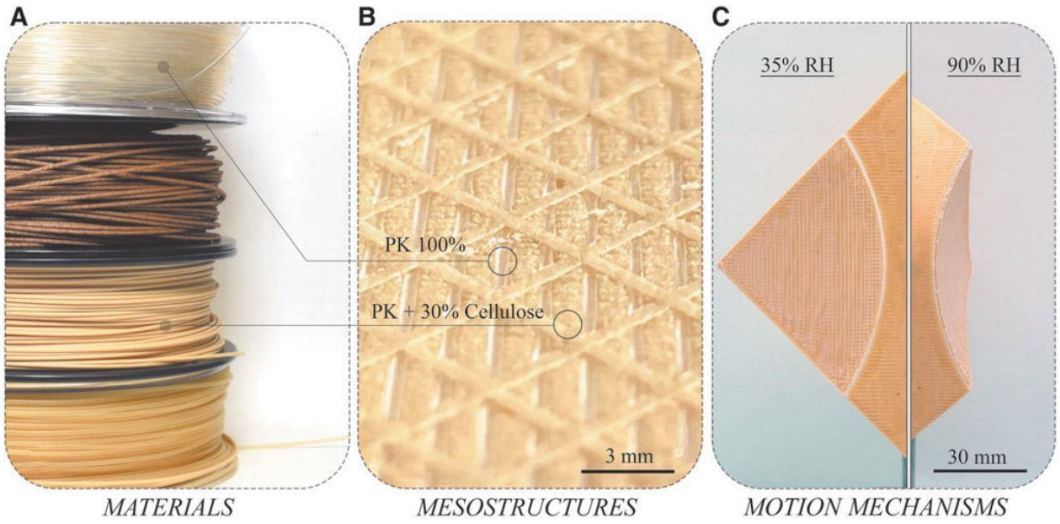

Figure 2.4. Custom FDM filaments with biobased matrix polymers and cellulose powder 4D printed for hygroscopic actuation (Tahouni et al., 2022)

However, 4D printing of wood by FDM is restricted to wood-based filaments available in the market (Gauss et al., 2021). These materials lack robustness, display delamination of bilayers (Correa et al., 2020), and are responsive to water immersion rather than environmental humidity (Tahouni et al., 2020). Even though customized filaments can enhance responsiveness (Figure 2.4) (Tahouni et al., 2022), small nozzle diameters of FDM printers limit the printable wood content of the filaments (Kariz et al., 2018). This results in a slow and limited shape change in response to environmental humidity (Correa et al., 2015). For that reason, several methods are employed for higher response speed and greater shape change, such as origami (Tahouni et al., 2020) and biomimicry (Poppinga et al., 2020).

Another limitation of FDM technology is that filament moisture should be reduced as much as possible to prevent possible shortcomings in mechanical properties (Wichniarek et al., 2021). Unlike the bilayering method, this dictates the active material's humidity level at the printed state. Therefore, the RH range for actuation can not be tuned for different climatic conditions.

2.2.2.3 Direct Ink Writing (DIW)

Similar to FDM, DIW (also called Robocasting) technology utilizes material extrusion to build plate by a moveable nozzle. However, visco-elastic materials (printing ink) are used in DIW, which are in a semi-liquid state or paste-form; therefore, it requires no heating at the nozzle in most prints. Materials are extruded through a dispenser either mechanically or pneumatically (Shafranek et al., 2019). Since most prints require no heat in DIW, the material is not degraded as FDM; thus, it is common for biomedical applications. (Rafiee et al., 2020).

To ensure adequate material flow through the nozzle without high printing pressure, printing ink requires low-viscosity under stress, also called printability. Another requirement is the buildability of the ink, which is defined as the capability of retaining the shape right after printing. These requirements led to the use of

thickening or thinning additives. If the rheological properties of the composite are met for DIW, there are endless possibilities for material combination. Some examples of printed objects show high flexibility and self-healing capability (Muehlenfeld and Roberts, 2019).

Employing SMP in the ink composites is possible to create 4D printed structures. Printable hydrogel inks with significant swelling behavior are reported in the literature (Cheng et al., 2019).

Constructing 4D printed objects with active and passive regions requires multi-material printers. However, most DIW printers have a single printhead, and printers with multiple printheads are slow because it takes significant time to switch between nozzles. To this end, a multi-material DIW printer with a single nozzle is designed, which allows continuous prints (Liu et al., 2016).

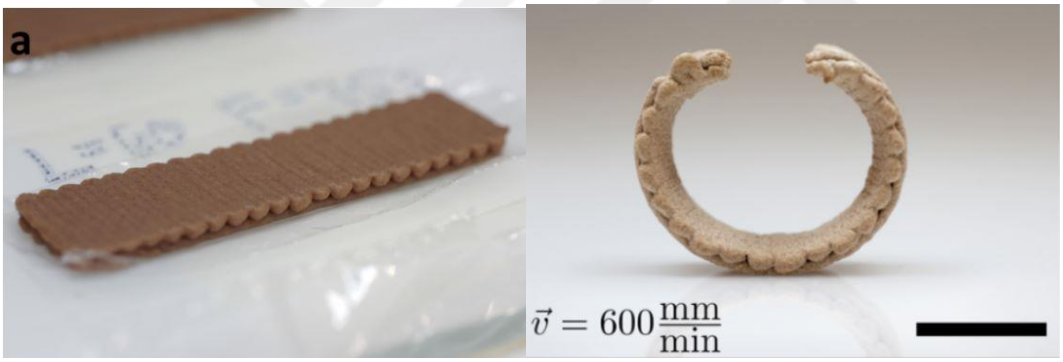

Figure 2.5. Direct Ink Writing of wood ink composed of 100% wood-based material, wood flour, and natural binders (Kam et al., 2022)

Since the DIW technique offers greater material customization (Deng & Lin, 2022), it enables mixtures with higher wood content and cost-efficient manufacturing (Rosenthal et al., 2018). Recent research has reported significant shape changes in 4D-printed wood using the DIW technique, which can be manipulated by adjusting the printing speed (Figure 2.5) (Kam et al., 2022). The combination of the DIW technique and advanced material compositions shows

promise for their enhanced responsiveness and needs to be investigated further for architectural implementations.

2.3 Smart Structures and Motion Mechanisms

The shape-changing materials and their potential applications for climate responsive skins are studied in the previous chapters. Wood-based materials are selected for further research because of the discussed merits. Fabrication technologies for wood-based materials are reviewed. Although slow response speed, motion control, and scalability are the main challenges faced in literature, wood-based motion mechanisms are promising to overcome these challenges. The great design space offered by extrusion-based 3D printers and customizability allows the creation of motion mechanisms that can amplify the response speed or enhance the motion control. This chapter presents the studies at both meso and macroscale motion mechanisms that aim to control and amplify the motion.

2.3.1 Material Programming

Natural fibers' anisotropy and sensitivity to moisture are the main reasons they are used for 4D printing (Tomec et al., 2021). In the creation of hygroscopically actuated objects, the anisotropic swelling of natural fibers has been employed to achieve the actuation (Le Duigou et al., 2020). This morphing behavior in response to humidity levels is called hygromorphing. Hygromorphic shape changes are reversible, and objects can shift between various equilibrium states and turn back to their initial shapes. The magnitude and direction of the motion, however, are programmed in the mesostructure of the material (J. Zhou & Sheiko, 2016). Expansion occurs perpendicular to fiber orientation. Therefore, the motion can be predicted. Moreover, by manipulating the fiber orientation, designated motions can be generated. Using 3D printing technology, customized wood grain patterns can be designed to accurately regulate the direction of morphing, as opposed to altering the natural

wood grain. That is because fibers are oriented along the 3D printing filaments during production (Le Duigou et al., 2016). Moreover, thanks to the nature of FDM technology, fibers are aligned along the print-path by the shear-induced between the nozzle and heatbed (Zuluaga & Menges, 2015). This alignment effect was also studied in the research on LCEs. It is stated that mesogens are aligned due to the shear stress during printing. Therefore, lowering the layer height or using nozzles with smaller width result in greater alignment of mesogens or fibers.

Furthermore, wood, in conjunction with various materials, unique wood composites displaying new macro-level characteristics can be fabricated thanks to multi-material 3D printing. These composites make use of the wood's inherent swelling and shrinkage ability and enlarge its design space. (Zuluaga & Menges, 2015).

In order to control and predict the motion of hygromorphing bilayer strips, mathematical models are developed, as well as physical experiments with various material and printing parameters. A study on 4D printed bilayer structures with unequal effective layer widths used Timoshenko's beam theory which describes the behavior of thick beams. The authors used Timoshenko's model to predict the curvature and deflection of 4D-printed bilayer structures with different numbers of active and passive layers. The computed figures and overall trends were close to the physical experiments. However, on the samples with different effective layer widths (porous structures), Timoshenko's model had to be modified to match with experiment figures. Authors state that created models can be used to predict the hygromorphing structures curvatures (Figure 2.6) (Krüger et al., 2021).

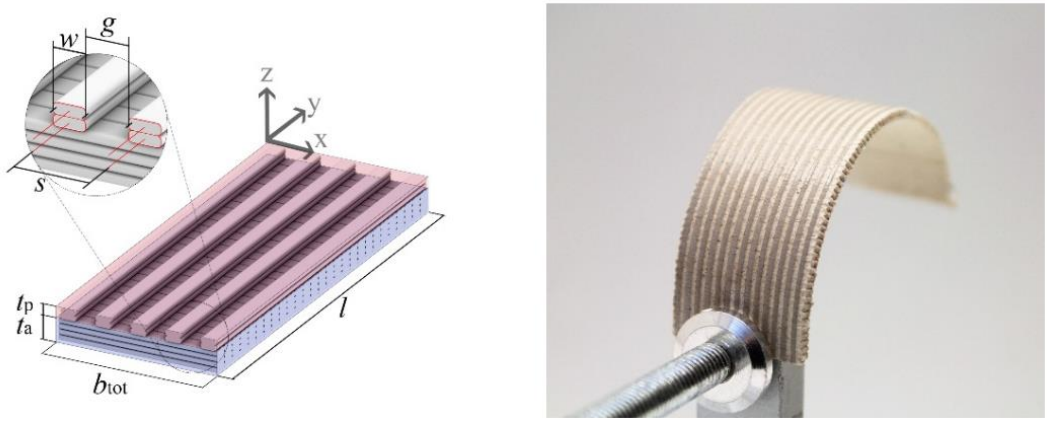

Figure 2.6. Mesostructure of 4D-printed hygroscopic bilayer showing the aspect ratio, layer thickness, bilayer ratio, line width, and line gaps (left), dry state of the bilayer (right) (Krüger et al., 2021)

Research on 4D printing of HWAs mainly focused on physical experiments, altering the design and 3D printing parameters to accurately predict and control the hygromorphing. One example is the study by Vazquez and Gursoy et al. (2019); the study presents a systematical approach to designing and creating architectural responsive skins. Firstly both PLA and Wood/PLA are printed with various tool-paths in different aspect ratios to understand their response to temperature and humidity (Figure 2.7). Then, six triangular bilayer samples are created. The sizes, bilayer ratios (3 Active / 1 Constraint Layer), and printing parameters such as layer height, bed temperature, and nozzle temperature were kept constant. Print paths of active and constraint layers are designed perpendicularly in all samples but in different orientations. Three samples' constraint layers were printed with a gap of 1 mm, while the other three were printed with 1.5mm. When exposed to humidity, more porous structures displayed greater bending motion, and the direction of the hygromorphing is strongly related to the print path orientation. The knowledge is then transferred to create architectural skin prototypes. After six and a half hours in a humid environment, a significant shape change is observed in the prototype.

However, shape change was not completely reversible in the dry environment. Moreover, the authors reported collisions during the shape change. Therefore, it is pointed out that simulation tools should be developed to control and predict the motion (Vazquez, Gursoy, et al., 2019).

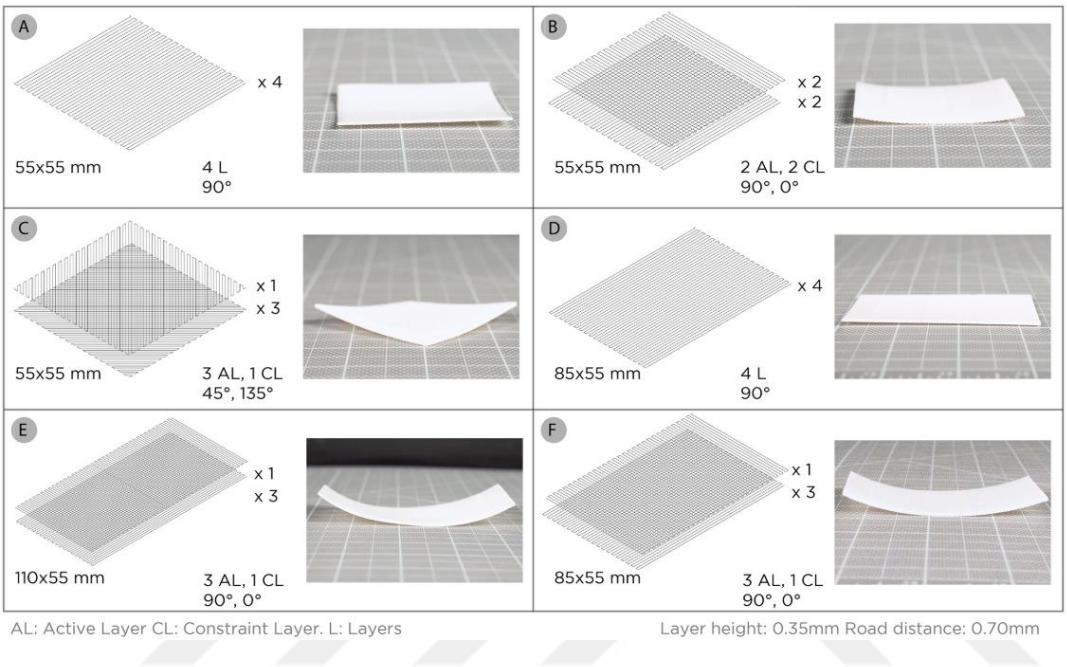

Figure 2.7. Mesostructured samples with various aspect ratios, print-path rotation, and bilayer ratios 4D-printed and immersed in water for hygroscopic actuation (Vazquez, Gursoy, et al., 2019)

2.3.2 Bistable Structures

Bistable structures are defined as structures with two mechanically stable shapes. There is a potential energy barrier between these two states and any impact above this energy barrier results in snap-through action from one state to another. The transition between the states is reversible and can be made multiple times. Unlike linear mechanical systems with one equilibrium state, bistable structures have two equilibrium states where no external energy is required to maintain the shape. Unless there is an impact with a magnitude above the critical level, the form of the structure is protected (Cao et al., 2021).

When impact above the energy barrier is applied, snap-through action is triggered, input energy is amplified, and a large magnitude of movement is created. Impact with any magnitude above the barrier results in the same stable state, therefore enabling very simple but precise, reliable motion (Jeong et al., 2019).

Bistable structures are preferable where high energy output is required with low energy input. They are used in various application fields, such as energy absorbers, energy harvesters, robotics, and actuators (Cao et al., 2021).

When compared with other actuators, bistable actuators are lightweight and have simple designs with ease of assembly. Significant merits such as large displacement capacity and very fast transition between states made it favorable among the other actuators. These structures can be created by either topological design or introducing of smart materials (Cao et al., 2021).

2.3.2.1 3D Printing of Bistable Structures

Due to the nature of technology, 3D printing enables the manufacturing of highly customized, complex bistable structures. Using single or multi-material printers, bistable structures can be created in one single print or by assembling many prints. By controlling the printing parameters, potential energy diagrams of these structures can be tuned.

According to research that utilizes this concept, twisting and rotational bistable structures with tunable properties are created. The authors state that understanding energy diagrams of bistable structures is essential to creating reconfigurable structures. Two valleys in the energy diagram correspond to stable states, and the hill corresponds to the energy barrier.

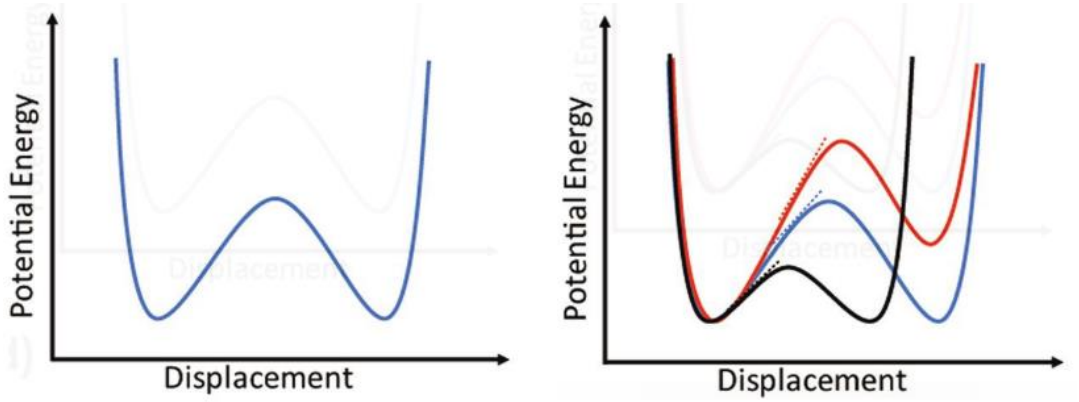

Figure 2.8. Schematic Potential Energy / Displacement diagram of a symmetrical (left) and asymmetrical (right) bistable structure (Jeong et al., 2019)

As can be seen in Figure 2.8, the hill's height is the threshold energy, while the slope is the required force to generate transition action. In the symmetric diagrams, the energy required for the transition from state A to state B and B to A is the same. On the other hand, in the asymmetric diagrams, one state may have more potential energy than another, which means the difference between valley and hill is smaller, and the transition is easier (Jeong et al., 2019).

The authors reported controllable readjustment of the twisting bistable structure. It is stated that changing the material with lower elasticity or an increase in the thickness of the beam results in a higher energy barrier. Moreover, a rotational bistable structure with two different joints is examined. While the structure with a ball joint showed symmetrical behavior, the structure with a fixed joint performed asymmetrically since the deformed stable state had higher potential energy than the original shape (Jeong et al., 2019).

Similarly, another research is conducted on bistable structures with tunable properties. According to the authors, the main aim of the study is to design and manufacture bistable unit actuators that have predictable and adjustable energy barriers and achieve maximum stroke-to-length ratio. The design consists of a pin connected to the bracket by two trusses on both sides (Figure 2.9). Thanks to the

multi-material printer, rigid-plastic material is used for printing, while the joint of trusses is printed with flexible material to ensure durability after many cycles of actuation. The flat shape of the structure simplified both printing and transportation and facilitated deployability (T. Chen et al., 2017).

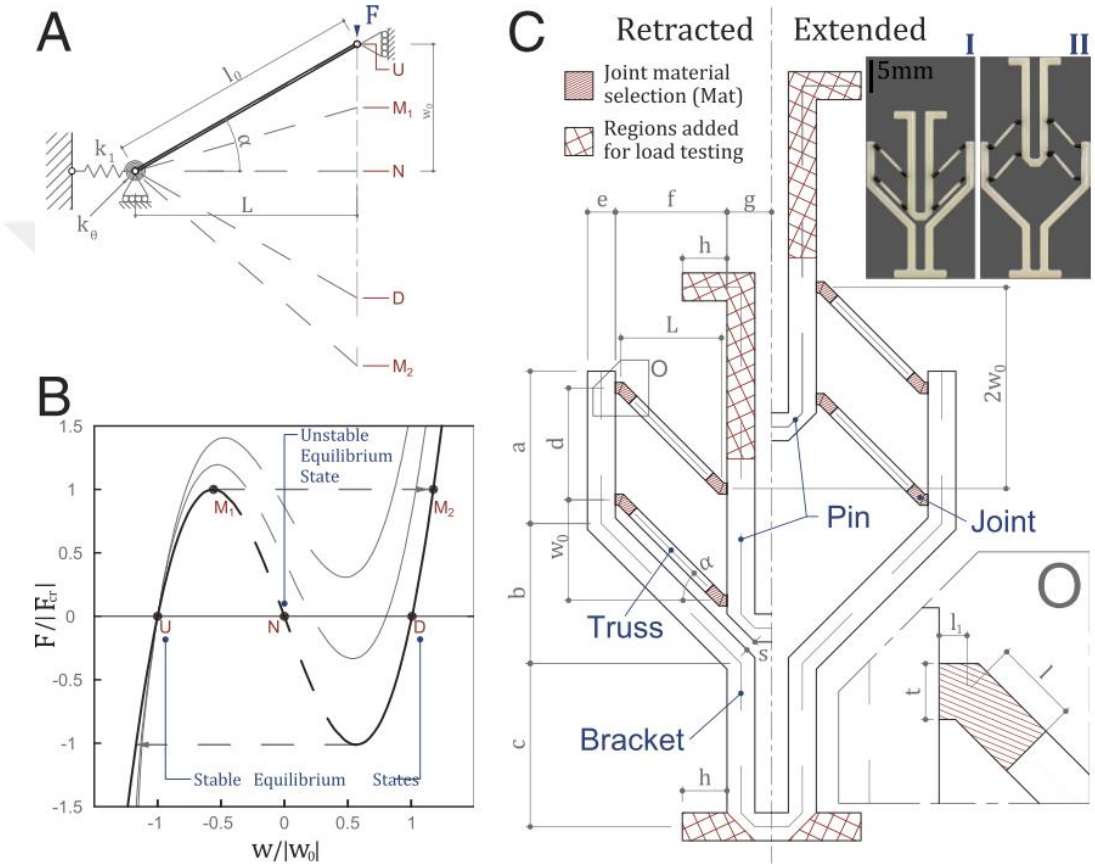

Figure 2.9. (A) Beam variables of Von Mises Truss, (B) Potential Energy / Displacement diagram of the bistable structure, (C) Retracted and extended states of the bistable structure (T. Chen et al., 2017)

The authors declare that with a truss angle of 45°, rotation in the joints is 90° which results in a 100% stroke-to-length ratio. However, it is possible to control this ratio

by changing the truss angle. Another tunable property is the energy barrier of bistable structures. An increase in the stiffness of joint material results in a higher energy threshold, while growth in joint length lowers the barrier. These adjustments make it possible to achieve an actuation force from 0.5N to 5N (Chen et al., 2017).

Multi-stable structures are reported in the article by combining unit actuators. The number of possible, stable states increases drastically after adding each actuator. When serially connected, the required activation force stays the same while the total length of the stroke increases. On the other hand, activation force increases in parallel connection while the total length of the stroke does not change (Chen et al., 2017).

The initial design of the unit actuator is reversed to create both positive and negative actuators, which remarkably increases the design space. Different combinations are presented by the authors, with each design having a load-bearing capacity. However, combined 3D structures require actuation force in multiple directions, creating difficulty in complete actuation (Chen et al., 2017).

On top of this research, a recently published article demonstrated the potential of these units through a computational implementation (Figure 2.10). Four of the unit actuators are combined to create bistable units. Initially, these units are 3D printed in flat configuration but are able to form 3D mountain or valley structures when actuated (T. Chen & Shea, 2021).

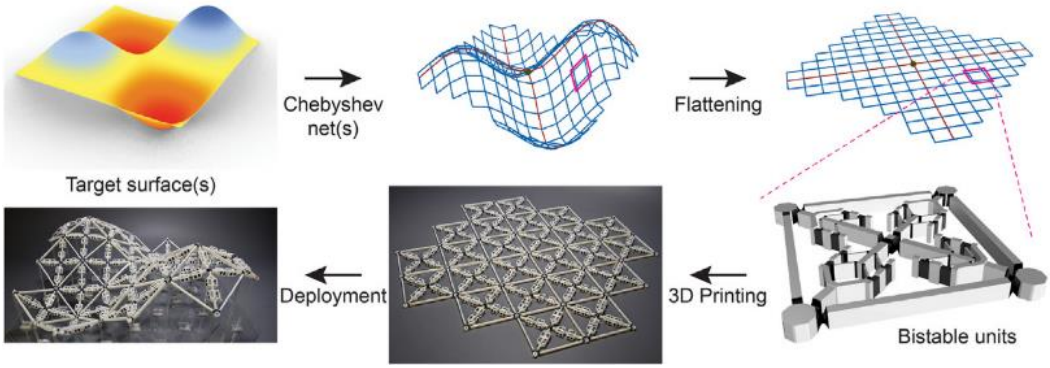

Figure 2.10. Achieving targeted surface by the activation of multiple deployed bistable units (T. Chen & Shea, 2021)

Meshing targeted 3D surface with double curvature, arrangement of the bistable units are computationally designed. As a result, a deployable bistable structure that can form any 3D surface is manufactured. Achieved 3D surface can maintain its shape against any impact lower than the actuation force of unit actuators (Chen and Shea 2021).

2.3.2.2 Smart Material Actuated Bistable Structures

As mentioned previously, the most common methods to achieve bistability are through design topology or by introducing smart materials. Two papers focusing on 3D printing of bistable structures are reported in the previous section. The attachment of smart materials to these structures enables bistable actuation in response to external stimuli.

Bistable unit actuators designed by (Chen et al., 2017) were further developed in another study by employing smart materials. Actuation of combined bistable units is a difficult task since different directional actuation is required for each unit. Smart material actuators are an optimal choice as an energy source because they are relatively simple, versatile, and highly customizable. SMPs are preferred over hydrogels since hydrogels have lower actuation force and lower load-bearing capacity. SMPs are used due to their high actuation strain, while imprecise programming step creates no difficulty thanks to bistability (T. Chen & Shea, 2018).

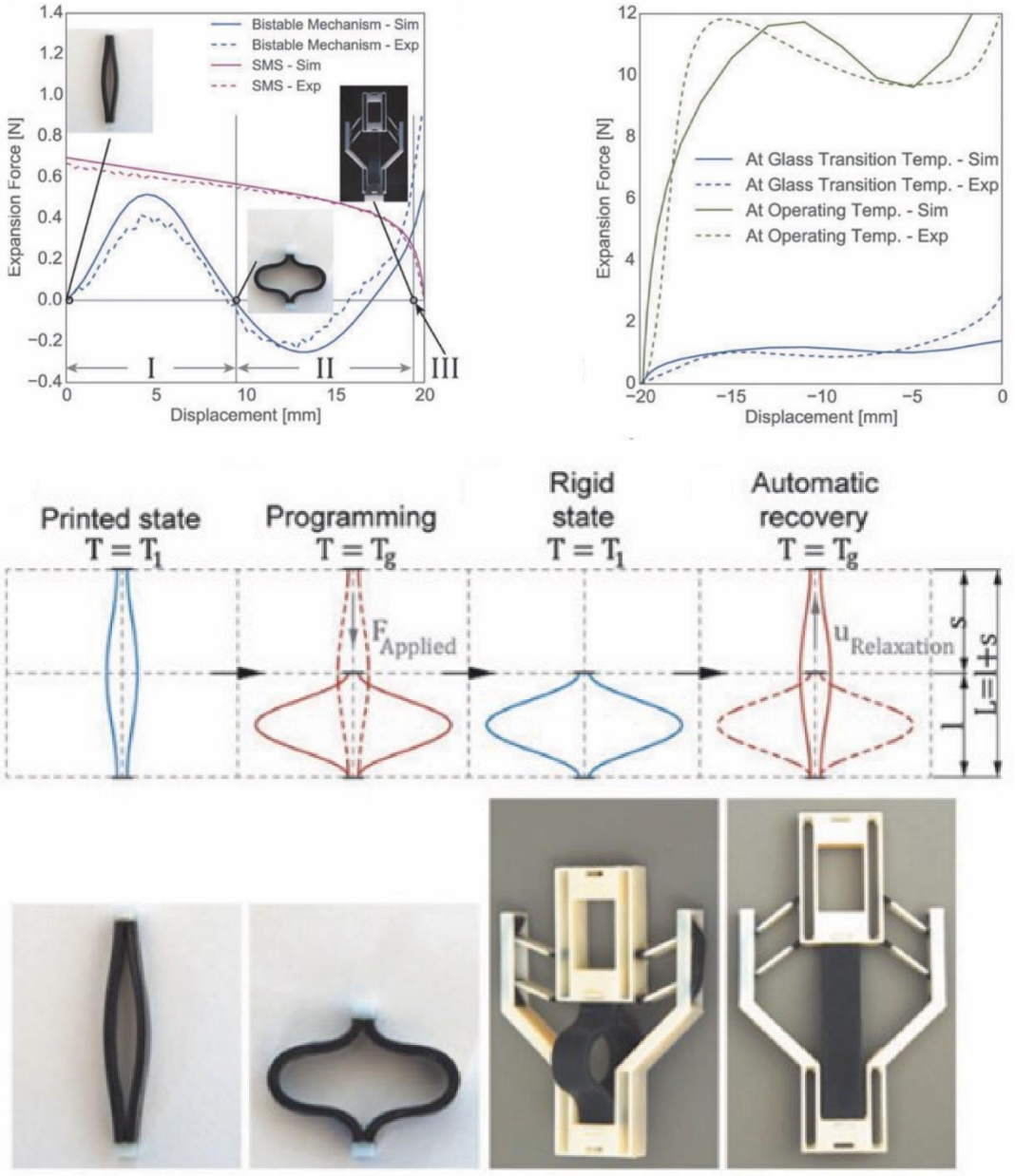

Figure 2.11. Expansion Force (N) / Displacement (mm) diagram of SMP actuated bistable structure (top-left), Expansion Force (N) / Displacement (mm) diagram of SMP at Tg and operating temperature (top-right), programming and recovery of SMP and integration to bistable structure (bottom) (T. Chen & Shea, 2018)

SMP strip is attached to a bistable unit (Figure 2.11) and referred to as SMS (shape memory strip). The strip is designed according to the bistable unit since the actuation force of SMS needs to be above of bistable unit's activation force. Starting from this, the thickness of SMS is decided to tune the actuation force. When heated to Tg and passing the energy barrier, the actuation force of SMS is amplified by bistability.

After the activation of the unit, when cooled down belove Tg, the unit demonstrated load-bearing capacity not only by bistability but also by SMS, which acts as a rigid, static unit (Chen and Shea 2018).

Another research focusing on bistable structures used smart materials as tuning elements (Figure 2.12). The activation force of the twisting bistable structure can be controlled by changing the length of the rod between trusses. However, this requires 3D printing of a new structure with the desired length. To this end, the rigid rod was replaced with length adjustable SMP rod. When tuning of bistability is required, the SMP rod is heated above Tg, changed its length, and cooled down. Beloved Tg, SMP works as a rigid rod, achieving tuneable bistability (Jeong et al., 2019).

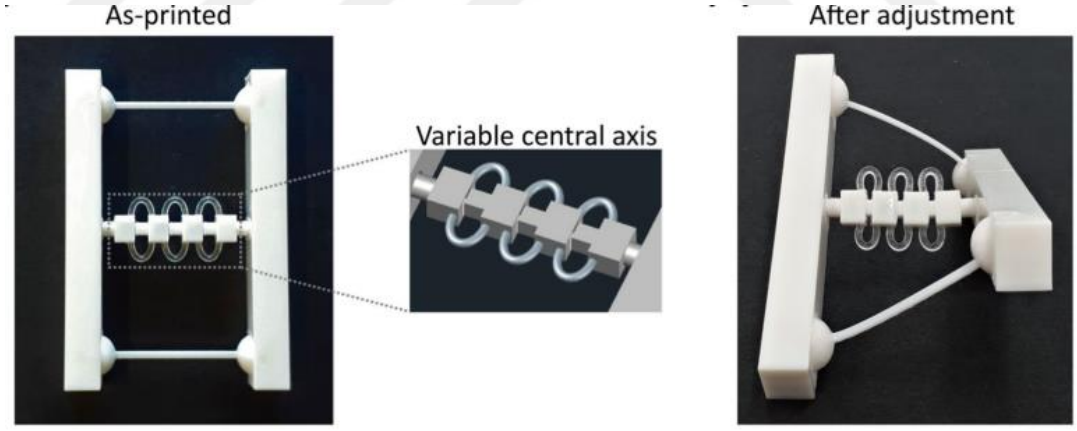

Figure 2.12. variable SMP in the central axis to tune the threshold energy of the twisting bistable structure (Jeong et al., 2019)

In addition to these methods, multistability can be directly encoded into smart materials. Hydrogels and LCEs are able to perform reversible actuation yet achieve

only two permanent states. Their expensive and difficult manufacturing is another drawback. The actuation of SMPs is not reversible, only the printed shape can be achieved when actuated, and programming is required for each actuation. However, it is possible to create SMP structures with encoded multi-stability by utilizing multiple-phase transition temperatures or multi-stage shape recovery (Riley et al., 2020).

The carefully designed micro-meso-macro structure hierarchy enables trapping elastic and is used for controllable actuation (Figure 2.13). Thanks to the rheological property of extrusion-based 3D printing, the microstructure of SMPs can be designed. SMP heated above Tg in the nozzle immediately cools down to belove Tg after deposition, which leaves the polymer chains in stretched, temporary position. Each infill line stores elastic energy dependent on the amount of pre-strain. When triggered by external stimuli, trapped energy transforms into mechanical energy, and the structure shrinks along the printing direction. Mesostructure can be controlled by the angle of infill lines, and the macrostructure of the object corresponds to the overall geometry and designed combination of pre-strain layers (Riley et al., 2020).

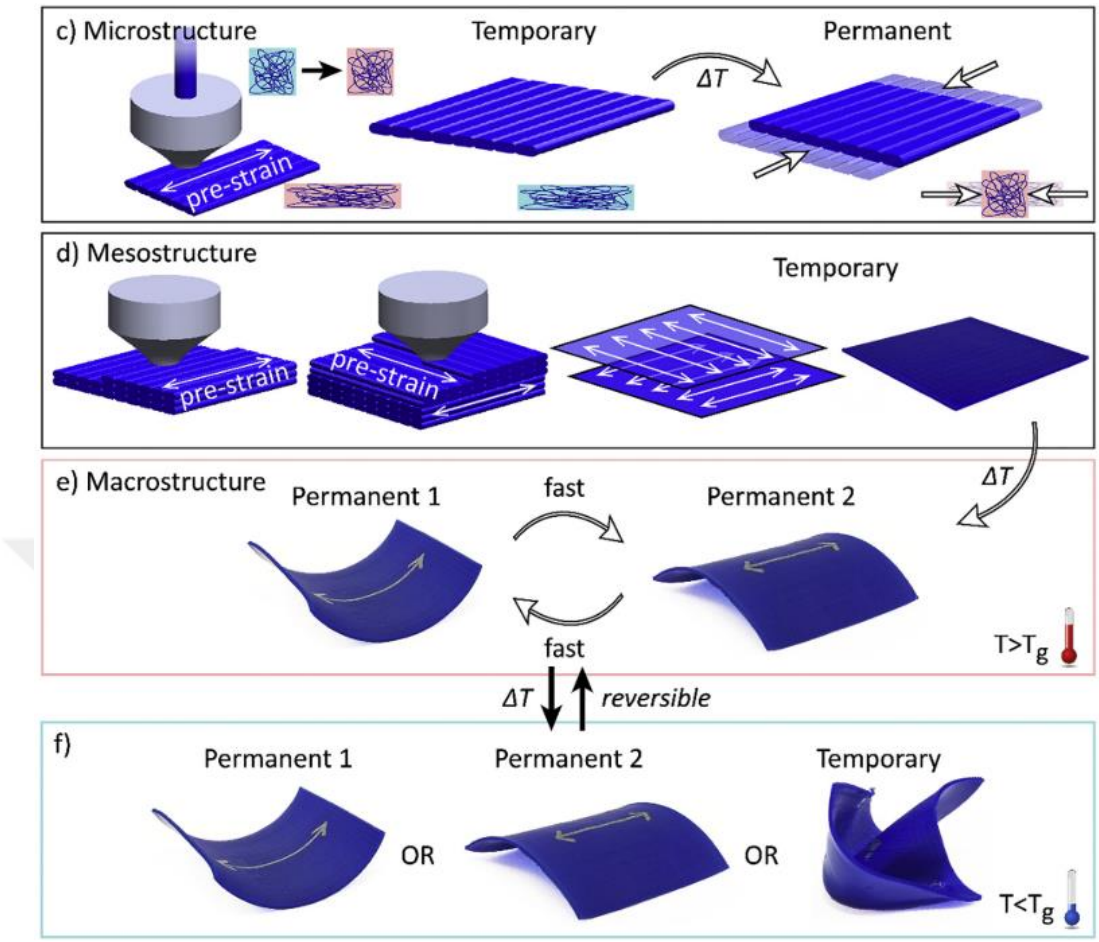

Figure 2.13. SMP with encoded multiple stable states by the design at both micro, meso and macroscale (Riley et al., 2020)

Authors report that the SMP object created with this method has multiple stable states, and transition between states is possible when the object is heated above Tg. However, belove the Tg, structure is static in one permanent shape. As a result, the multistability of the structure can be activated and deactivated by changing the temperature (Riley et al., 2020).

2.3.3 Active Origami

Origami is a Japanese art of folding paper in which “ori” means folding, and “kami” means “paper”. Origami-based designs display remarkable properties; thus, application fields are exponentially growing. Complex 3D forms can be achieved by sequential folds applied to a simple flat sheet. This enables simple construction, thus saving fabrication time and material costs. Structures designed with origami are usually lightweight and scaleable from nano-scale to meter-scale, facilitating a wide range of applications (Meloni et al., 2021).

Origami structures can reduce and enlarge their shape, providing deployability and ease of transportation. Some insects in nature have deployable wings thanks to their origami-based structure. Industries such as aerospace and biomedical also utilize origami for deployability purposes.

Origami-based designs allow both static structures with load-bearing capacity and dynamic structures with multiple functions. Plant leaves and flowers are examples of multi-functional origami, which can be opened and closed in response to light.

Such structures are called self-folding, which are able to fold without external forces. When smart materials are employed in self-folding structures to be able to respond to external stimuli, active origami structures are achieved (Peraza Hernandez et al., 2019).

Many methods have been developed to construct active origami structures. One research reported the design self-folding hinge (Figure 2.14), which can be used in active origami structures in complex forms such as Miura-ori and waterbomb origami fold patterns. Hydrogel material (Hydrophilic TPU) is used for actuation in between elastomer (Hydrophobic TPU) layers. The elastomer skin of constructed trilayer structure is removed in a certain size, and skin gaps are created. When submerged in water, hydrogel absorbs the water and swells through the skin gap, which triggers the folding. Both valley and mountain folds can be created depending on the removed elastomer layer. Moreover, the thickness of layers and the length of

the skin gap are parameterized to tune the folding angle. The authors report a direct correlation between skin gap and folding angle. Experiments also demonstrated that the highest folding angle is achieved when elastomer layers are thicker than the hydrogel layer. To summarize, a hydrogel-based, water-responsive, reversible hinge with a tuneable folding angle and consistent actuation behavior is manufactured in a low-cost, extrusion-based 3D printer. However, due to the hydrogel-based actuation, it takes so much time to achieve the targeted folding angle (Baker et al., 2019).

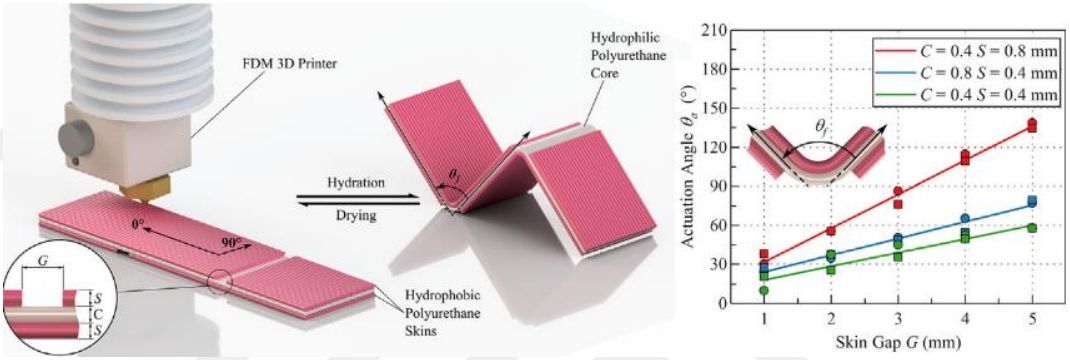

Figure 2.14. Hygroscopic actuation of hydrogel-based trilayer folding mechanism (Baker et al., 2019)

Another hybrid hinge structure (Figure 2.15) is reported in the literature in which the smart material actuation is only used for deployment after the printing and not for reversible shape change. The trilayer hinge structure consists of two layers of stiff material on the shell and an elastomer (TPU) layer in the core. Similar to the previous article, a skin gap was created to achieve folding. SMP material (PLA) in one side of the core decides the folding direction, and the pre-strain mesostructure induces only the initial folding for deployment purposes. After the deployment, the hybrid hinge structure is tested durable for more than 500 cycles of folding belove the Tg of SMP thanks to the single elastomer layer in creases. The Miura-ori folding pattern is constructed to display the potential of hinge structure for the deployment of complex shapes (Yamamura & Iwase, 2021).

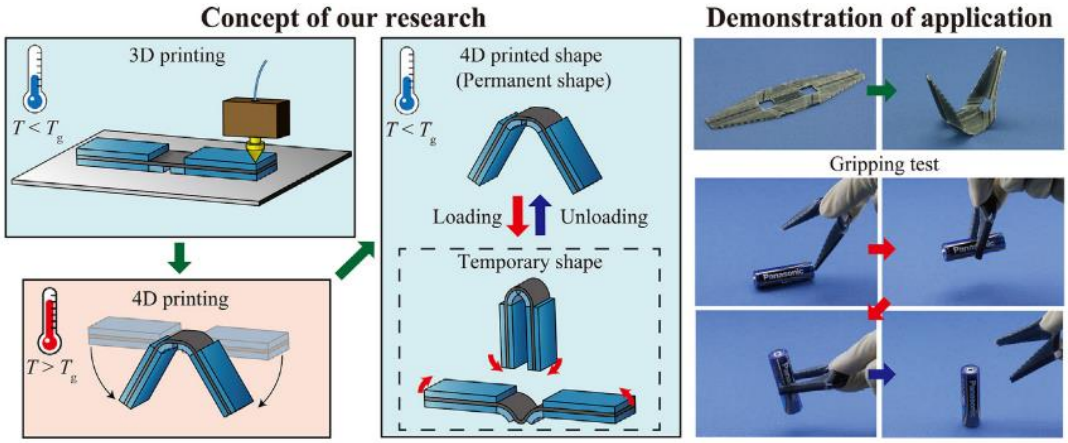

Figure 2.15. 4D printing of hybrid hinge for deployment (Yamamura & Iwase, 2021)

As can be seen in Figure 2.16, a different approach was developed by (Minori et al., 2020a), in which the activation of a thick origami structure is made by LCE material. Origami-based composite sarrus linkage module takes the linear motion by LCE contraction and converts it to circular motion. Since used LCE needs to perform only in one direction, the mechanical alignment method is selected for ease of manufacturing. Heaters are embedded in LCE to trigger the actuation, which is fast and reversible, thanks to LCE. However, to maintain the LCE in the contracted state, heaters must be kept open. In short, this tendon-driven approach exhibits the activation of origami with the actuation of smart material. This approach offers great potential where the material of origami structure requires better properties than the smart material. For example, LCE would not be the optimal material for this origami structure because it lacks the required stiffness. Another advantage of this approach is relatively low-cost fabrication since smart materials are usually more expensive than conventional materials; therefore, using smart materials only for actuation is a better solution. (Minori et al., 2020).

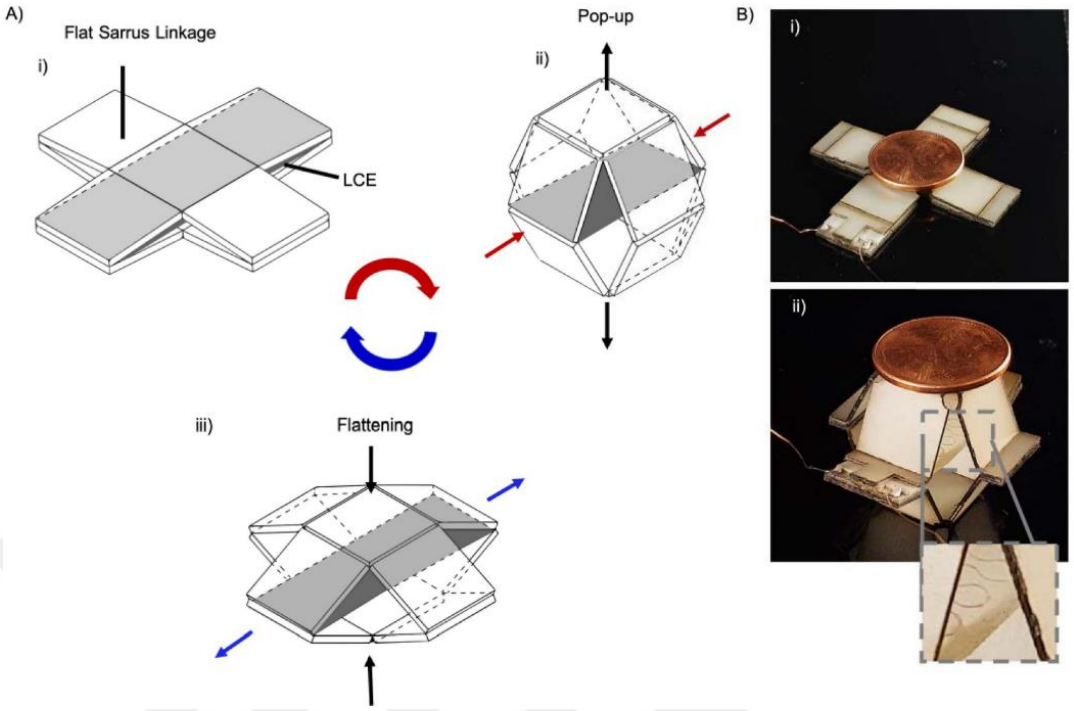

Figure 2.16. Reversible folding of LCE actuated folding mechanism and the demonstration of load-bearing capacity (Minori et al., 2020)

The manufacturing of origami structures is generally simple because they are initially flat sheets. However, the assembly of origami structures can be very complex, especially for curved-crease origami, where the folding sequence is mostly simultaneous. To this end, a computational design workflow is developed to manufacture curved-crease active origami structures (Tahouni et al., 2020).

In straight-crease origami, motion takes place only in creases, while in curved-crease origami, faces also transform or bend. According to the article, the simultaneous motion of both faces and creases is achieved by designing the mesostructure of the active origami structures. In order to distribute the actuation to the faces, a computational tool is developed which generates the g-code with the required 3D printing toolpath. The tool weaves the creases and enables print-in-place active

origami structures. In the end, an origami structure with predictable response behavior (Figure 2.17) is created thanks to the computational design workflow, which integrates design and fabrication (Tahouni et al., 2020).

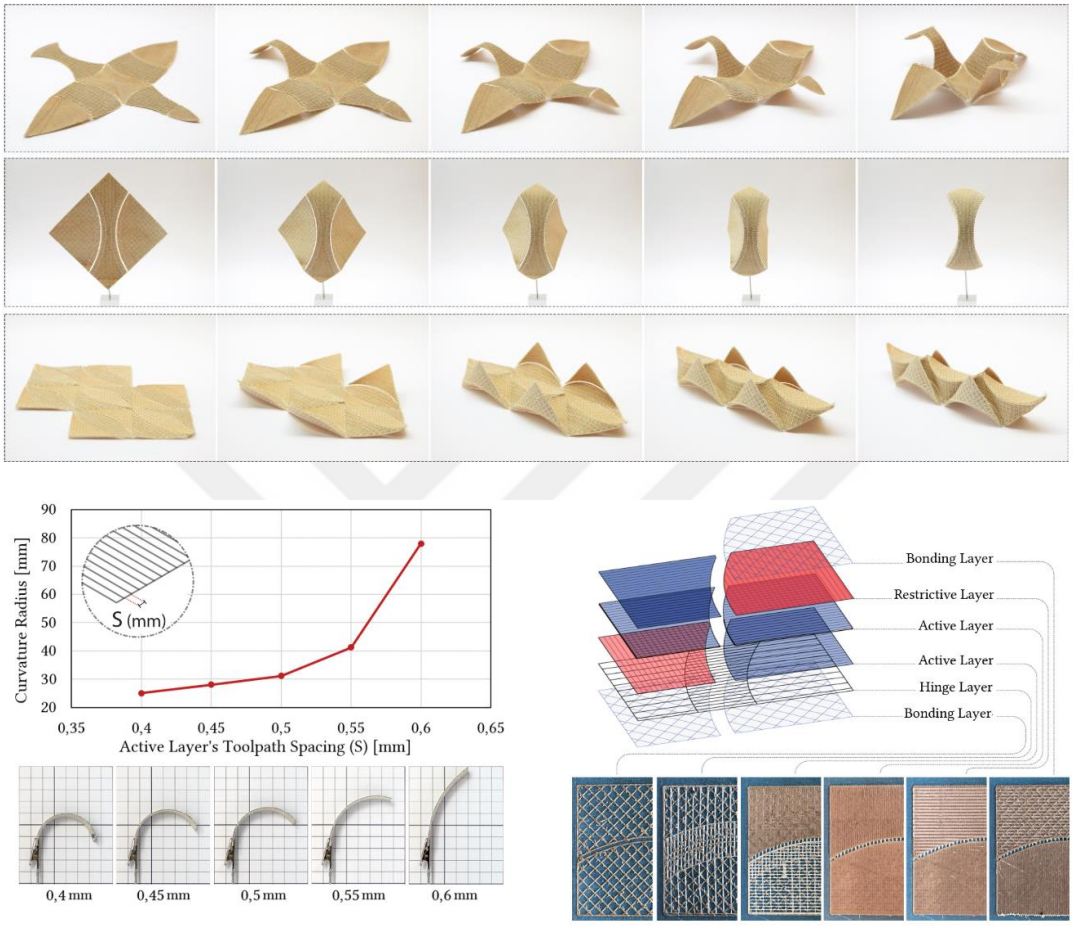

Figure 2.17. Demonstration of hygroscopically actuated wood-based curved folding mechanism (top), the diagram of printing path gap to curvature radius (bottom-left), demonstration of different layers for the motion mechanism (bottom-right) (Tahouni et al., 2020)

Increasing attention to origami engineering and complex design requirements emerged in the need for theoretical and computational approaches. Mathematical models and software are developed to understand the constraints and simulate the

origami structures (Peraza Hernandez et al., 2019). However, in nature, there are examples of origami that still can not be described by current origami models. Wings of earwigs are origami-based structures that self-lock during flight and display bistability. The bistability arises from the angle difference in the creases, called missing angles, and is incompatible with traditional folding patterns. Authors inspired by this natural phenomenon designed and 3D printed bistable origami (Figure 2.18). They printed the faces with rigid materials (ABS or PLA) and used TPU as an elastic membrane that allows folding in creases. Experiments with different missing angles demonstrated that when a certain threshold angle passed, monostable origami became bistable. The missing angle threshold is also related to the stiffness of membrane material, and stiffer materials decrease the missing angle threshold (Faber et al., 2018).

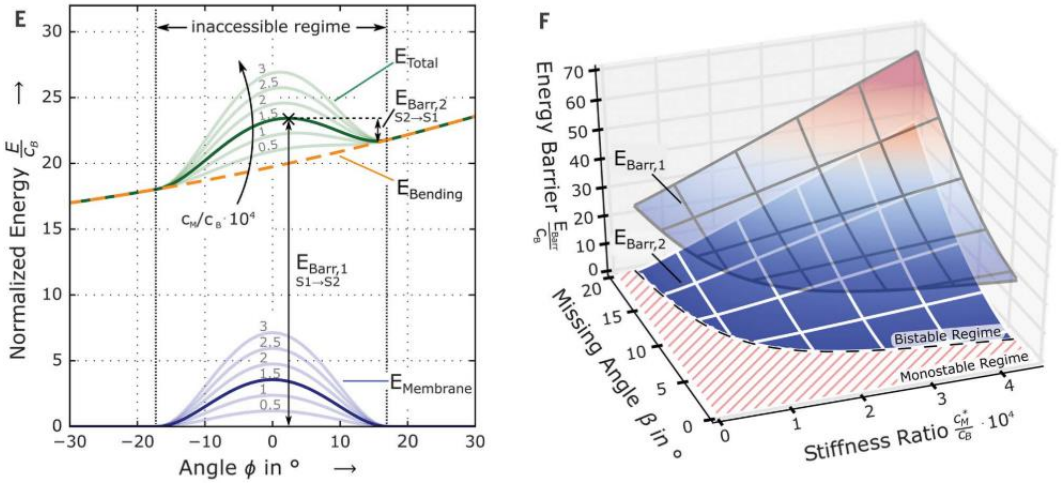

Figure 2.18. Diagrams showing the effect of missing angle on the threshold level of bistability and the stiffness ratio (Faber et al., 2018)

In bistable origami, a further increase in missing angles results in a higher energy barrier. However, after some degree, the origami structure stops working. Potential energy diagrams show that self-locking origami performs asymmetrical bistability, which means a self-locked state entraps the potential energy and releases it when a relatively lower force is applied. The released high-potential energy transforms into mechanical energy and causes a high-speed transition (Faber et al., 2018).

The article answers the question of how origami structures can be transformed into bistable structures. Moreover, high customization skills and available wide range of materials for 3D printing enable to manufacture of complex origami structures with tuneable bistability.

2.4 Evaluation and Summary of the Literature

The aim of this literature study is to define the background for the research problem, identify the requirements for climate responsive skins, and review the studies in the field to assess the feasibility of developing a reversible, precise, architectural-scale, and responsive shading device. When considering various shape-changing materials, wood emerges as a preferable choice due to its distinct properties. Other materials, such as Shape Memory Polymers, Shape Memory Alloys, Liquid Crystal Elastomers, and hydrogels have several limitations, including non-reversibility, the need for programming, the requirement of additional energy for actuation, high cost, manufacturing challenges, low actuation force and lack of sustainability. Wood-based materials, on the other hand, have significant advantages for the application of climate responsive skins. It displays reversible actuation and is triggered by the daily variation of humidity, which is closely related to sunlight. Additionally, wood is a bio-based, biodegradable, and recyclable material that is scalable and low-cost.

Considering the applications that utilize wood as a skin material present limitations in terms of durability, replaceability, and difficulty in manufacturing large surface areas, it is found more promising to use wood as an actuator. When wood is

incorporated with textile elements as the skin, only the wooden actuators need to be replaced, resulting in a cost-effective and lightweight solution with no significant additional load on buildings.

Moreover, extrusion-based 3D printing technology enables to manipulate fiber orientation during the printing process through shear stress on the build plate. This allows for precise control of the material's properties and offers great design space.

To overcome the challenges related to motion control and response speed of hygroscopic wood-based actuators, bistable structures are studied and found promising for integration into wood-based actuators. Bistable structures have well-defined states, which prevent collisions in arrayed systems. Moreover, they demonstrate stability and durability against outdoor conditions.

CHAPTER 3

RESEARCH DESIGN

This chapter presents the methodology employed in this research. The initial step involved conducting a literature survey on the topic of 4D printing of hygroscopic wood-based actuators for responsive skin. The literature review revealed that previous studies have successfully utilized the swelling and shrinkage response of wood-based materials to humidity for the development of responsive façade shading systems. However, challenges related to precise control of motion, slow actuation speed, and scalability of these systems persist. In light of these identified gaps, the subsequent experiments were designed to address these challenges by leveraging the insights gained from the literature.

The experiments developed in three consecutive categories (Table 3.1), which are sequential steps in terms of their scale. The first stage involved a systematic set of experiments designed to observe the relationship between key parameters that affect the response time and shape change. Key parameters are identified based on previous studies in the field. Observations of the literature were verified with the collected data from the experiments and used to construct a model. This model served as a basis for the next set of experiments.

In the second stage, multiple implementations of the model are developed to determine the configuration that best meets the requirements of a climate-responsive skin. Among the tested implementations, two configurations were selected based on the constraints related to motion control, response speed, robustness, and overall efficiency of the system. The first configuration utilized coupled actuators, while the second configuration employed pre-stressed bistability to achieve amplified response speed and motion control.

Moving to the third stage, 1-to-1 scale experiments were developed based on the two selected configurations in the previous stage. The aim of these experiments was to demonstrate that achieved amplified and controlled motion, facilitated by these configurations, could be successfully implemented at various scales and remained reliable when applied on a larger scale.

Table 3.1 Workflow

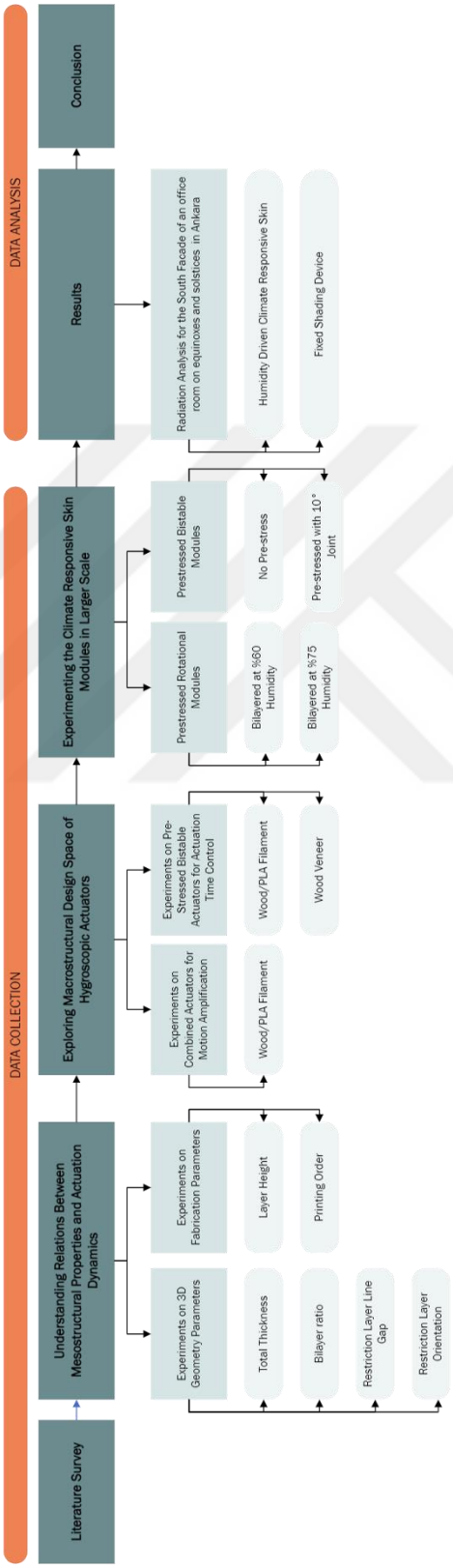

3.1 Observing the Actuation Dynamics

The purpose of the experiments is to observe the actuation characteristic of HWAs and determine the design and fabrication parameters that are most suitable for the climate responsive building skins. Initially, the requirements for a responsive skin need to be defined. For example, a responsive sun-shading device should be able to open and close in the time range of the day, covering the openings of a given building. The goals of this device can be defined as high response speed to sunlight, high open/close ratio, collision-free precise motion, and low-cost maintenance.

Therefore, In order to understand the actuation behavior of HWAs, firstly, variables that affect the morphing behavior of samples are identified based on the literature survey. Among these variables, five are design parameters, and two are printing parameters related to the manufacturing process. The design variables include total thickness, Bilayer numbers, Bilayer ratio, restriction layer line gap, and restriction layer rotation. On the other hand, layer height is considered a printing variable since it affects the alignment of the wood fibers, according to the literature. The second printing parameter is the printing priority of active and passive layers, as it is believed that printing on the porous layer enhances the bonding of bilayers.

Printing paths of the samples are designed using Rhino and custom Grasshopper script, then transformed to a g-code by Grasshopper plug-in named ‘Droid’. Printing parameters such as printing temperature (220), heated-bed temperature (75), printing speed (45), and flow rate (100%) were kept constant for all created g-codes.

A simple, gantry-based desktop 3D printer is used for the 3D printing process. Since it is a single-material printer, the 3D printer is paused, and the filament is changed when needed. Three samples were 3D printed for each design, and the most faultless print was selected for the experiments.

The weight of the selected samples is measured in a dry (30-40%) environment and recorded. They are fixed from the end points with a metal clamp and placed on a magnetic sheet. A gridal background is attached to facilitate motion tracking. An

aquarium is used to control the humidity of the environment during the experiment. A humidifier connected to the aquarium via a hose is used to increase the humidity of the environment during the experiment. The humidity and temperature are tracked with a hygrometer during the experiments. Photographs are taken before the experiment in a dry environment and then during the experiment in a humid environment in 0, 10, 20, 30, 40, 50, 60, 120, 180, and 360th minutes. Since this experiment focuses on the potential use of adaptive sun-shading, a maximum of 6 hours of motion is tracked with a focus on the short term. At the end of the experiments, an image analysis software called ImageJ is used to calculate the bending angle of each sample based on the photos. Angles are measured by drawing lines from the end points to the middle point and calculating the intersection of these two lines, as shown in Figure 3.2a and Figure 3.2b. Subsequently, a circumcircle based on the curvature of the sample is drawn, and the radius is calculated.

The constant sample is designed with the aspect ratio of 20x100x0,9mm. The specimen consists of one restriction (PLA) and two active layers (WOOD/PLA). Each layer's height is the same and equal to 0,3mm. Since the nozzle width is 0,4mm, a layer printed with a 0,4mm line gap creates a solid layer, while a line gap of more than 0,4mm creates a porous layer. Firstly, a porous layer with a line gap of 1,00mm is printed, and two active solid layers are printed on top of it. Selected parameters for the constant sample are shown in Table 3.2. For each experiment, these parameters are kept constant, and only selected variables are altered. Tracked angles of different specimens are shown in the charts.

In the first group of the experiment, total thickness is the independent variable, and measured angles are the dependent variables. Samples with 0.45mm, 0.90mm, and 1.80mm are tested. As can be seen from the chart, the thinnest specimen (0.45mm) displayed 13° of deflection at the end of 6 hours, the highest figure in the experiment (Table 3.4). On the other hand, the thickest specimen (1,80mm) displayed less than 1°, the least deflection in 3 specimens.

The results are parallel with the literature, proving that as the thickness of HWA increases, the time range of the actuation also increases. Based on this experiment, it can be stated that 1.8mm or thicker HWA actuators with these parameters would fail to generate the motion required for climate responsive skin. However, thinner samples show the potential to respond to sun movement in the required time range.

The next two experiments are designed to understand how the active layer to passive layer ratio affects the HWAs' motion. In the first experiment, the layer height of the samples was kept constant at 0.30mm, and the number of active layers changed to alter the ratio. On top of the one passive layer, 1, 2, 3, and four active layers are printed. Therefore, four different samples with four different thicknesses are manufactured. Overall, the bilayer ratio and the deflection figures displayed a significant correlation. However, results show that the sample with a 1 to 1 ratio displayed great motion and was clearly separated from other samples.

Table 3.2 Constant sample values and illustration of parameters, altered parameters and experiment results

Total Thickness (mm)	Active/Passive Layer Ratio	Restriction Layer Line Gap (mm)	Restriction Layer Rotation	Layer Height (mm)	3D Printing Priority (mm)
0.45	1/1	0.40	0	0.10	Restriction Layer First
0.90	2/1	0.50	45	0.15	
1.50	3/1	0.60	60	0.18	Active Layer First
1.80	4/1	0.80	90	0.225	
		1.00		0.30	
		1.50			

Total Thickness (mm)	Active/Passive Layer Ratio	Restriction Layer Line Gap (mm)	Restriction Layer Rotation	Layer Height (mm)	3D Printing Priority (mm)
0.45	2/1	1.00	0	0.30	Restriction Layer First
0.90					
1.80					

Total Thickness (mm)	Active/Passive Layer Ratio	Restriction Layer Line Gap (mm)	Restriction Layer Rotation	Layer Height (mm)	3D Printing Priority (mm)
0.60	1/1	1.00	0	0.30	Restriction Layer First
0.90	2/1				
1.20	3/1				
1.50	4/1				

Total Thickness (mm)	Active/Passive Layer Ratio	Restriction Layer Line Gap (mm)	Restriction Layer Rotation	Layer Height (mm)	3D Printing Priority (mm)
0.90	1/1	1.00	0	0.15	Restriction Layer First
	2/1			0.18	
	3/1			0.225	
	4/1				

Since total thickness clearly affects the deflection figures, in the second bilayer ratio experiment, the total thickness of the samples was kept constant at 0.90mm. To create 4 samples with 4 different bilayer ratios, layer height had to be altered. In the

1/1 sample, 3 passive and 3 active layers with 0.15mm layer height,

1/2 sample, 2 passive and 4 active layers with 0.15mm layer height,

1/3 sample, 1 passive and 3 active layers with 0.225mm layer height,

1/4 sample, 1 passive and 4 active layers with 0.18mm layer height

are printed. This time, no direct correlation can be seen from the results. However, similar to the first bilayer ratio test, the sample with a 1 to 1 ratio outnumbered the other three samples' deflection figures. At the end of the six hours, 1/2 and 1/4 bilayer ratio samples deflected nearly the same and higher than 1/3 bilayer ratio samples. However, all three samples are faraway from having a potential for climate responsive skin.

Another experiment conducted is related to the porosity of the HWAs. Six samples are manufactured with a restriction layer's line gap of 0.4mm, 0.5mm, 0.6mm, 0.8mm, 1.0mm, and 1.5mm. Results show that, from the solid restriction layer (0.4mm) to the more porous restriction layer, deflection figures increase until the sample with 0.8mm. However, as the gap increases, deflection increase stop at the sample with a 1.0mm line gap and suddenly drops at the sample with a 1.5mm line gap.

While the parameter of the restriction layer's line gap alters the porosity of the samples, it is believed that it also affects the bonding between the bilayers. Since the restriction layer is printed first with certain gaps between the lines, the active layer printed on top of this layer flows to these gaps. As a result, bonding between active and restriction layers increases. Conversely, when the porous restriction layer is printed last, the bonding of bilayers decreases. To demonstrate that, another experiment was conducted with reverse printing order of bilayers.

Table 3.3 The altered parameters and experiment results

Total Thickness (mm)	Active/Passive Layer Ratio	Restriction Layer Line Gap (mm)	Restriction Layer Rotation	Layer Height (mm)	3D Printing Priority (mm)
0.90	2/1	0.40	0	0.30	Restriction Layer First
		0.50			
		0.60			
		0.80			
		1.00			
		1.50			

Total Thickness (mm)	Active/Passive Layer Ratio	Restriction Layer Line Gap (mm)	Restriction Layer Rotation	Layer Height (mm)	3D Printing Priority (mm)
0.90	2/1	0.40	0	0.30	Active Layer First
		0.50			
		0.60			
		0.80			
		1.00			
		1.50			

Total Thickness (mm)	Active/Passive Layer Ratio	Restriction Layer Line Gap (mm)	Restriction Layer Rotation	Layer Height (mm)	3D Printing Priority (mm)
0.90	2/1	1.00	0	0.30	Restriction Layer First
			45		
			60		
			90		

Total Thickness (mm)	Active/Passive Layer Ratio	Restriction Layer Line Gap (mm)	Restriction Layer Rotation	Layer Height	3D Printing Priority (mm)
0.90	2/1	1.00	0	0.10	Restriction Layer First
				0.15	
				0.30	

In the second experiment on the altered restriction layer's line gap of HWAs (Table 3.3), the active layer is printed first to understand the relation between printing priority and line gaps. This time, the printed restriction layer (PLA) on top of the active layer created tension on AL and resulted in opposite curvature on samples. The deflection can be seen in the graph at the beginning of the experiment. Starting curvatures range between 180 and 182, and the highest starting deflection is on the sample with the most PLA (solid restriction layer, 0.4mm line gap). At the end of the 6 hours, when the overall deflection results are compared with the prior experiment, lower curvatures are observed. Results prove that printing the porous restriction layer first results in higher bonding, thus, higher curvatures.

Altering the restriction layer rotation resulted in the expected results. As stated in the literature, restriction layer print paths vertical to the active layer print paths generate the greatest shape change.

The layer height test is conducted based on studies that report the higher orientation of the fibers due to the shear-induced stress during printing (Compton & Lewis, 2014; Correa et al., 2015). In line with these reports, the sample printed with the thinnest layer height showed the greatest shape change.

Table 3.4 Example of collected data from the total thickness test experiment

Total Thickness	*0*	*10*	*20*	*30*	*40*	*50*	*60*	*120*	*180*	*360*
1.8 mm	180,2	180,19	179,95	179,92	180	179,98	179,94	179,75	179,72	179,38
0.9 mm	179,46	179,23	178,99	178,77	178,47	178,34	178,11	177,29	176,74	175,28
0.45 mm	179,94	177,37	176,34	175,42	174,65	174,13	173,5	170,94	169,26	166,85
RH	46	87	87	88	89	90	90	93	94	96
T	25,8	25,8	25,8	25,6	25,7	25,6	25,7	25,5	25,3	25

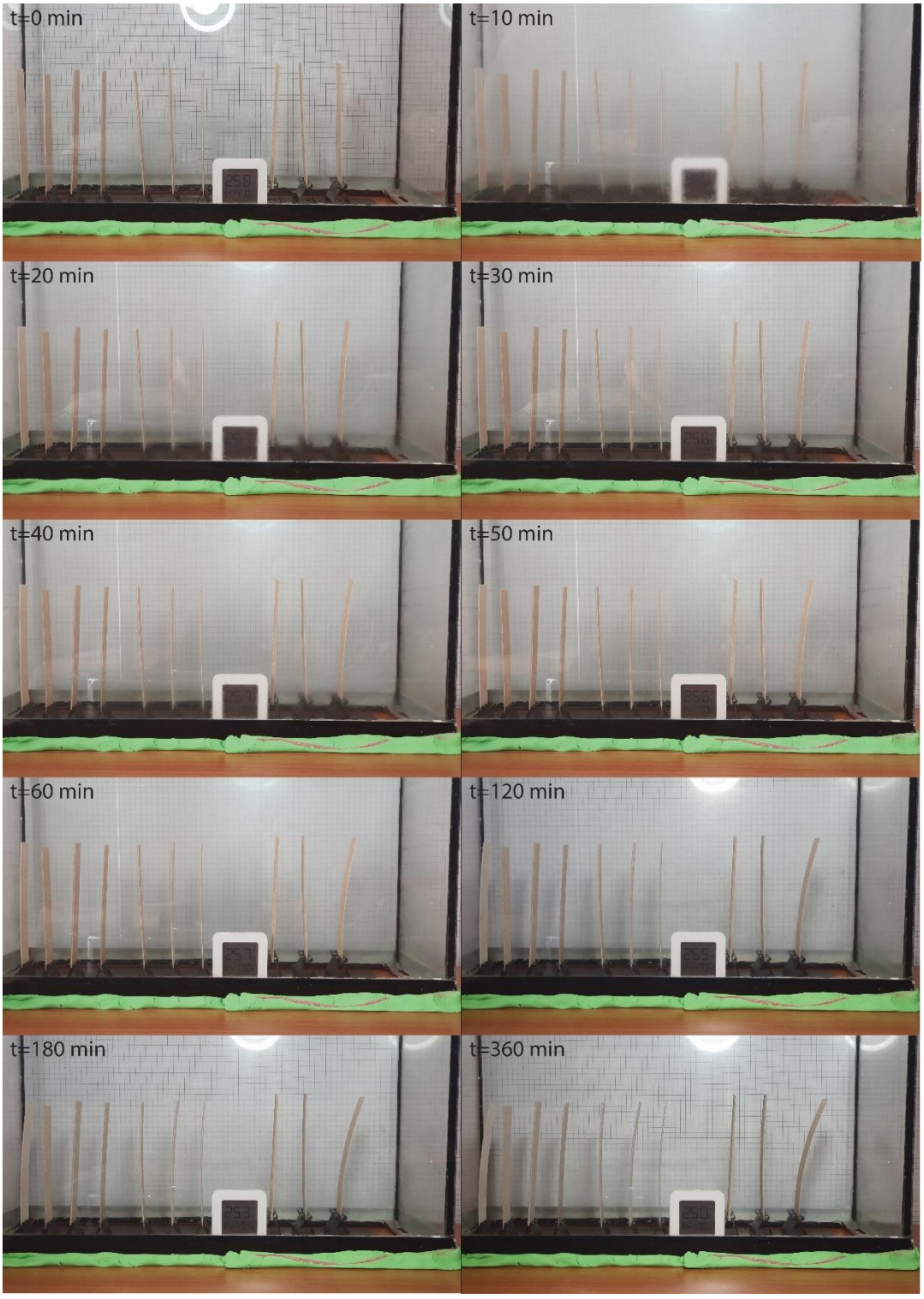

Figure 3.1. Photographs taken during the total thickness and bilayer ratio test

3.2 Implementations of the Model

Collected data demonstrated the effect of each parameter on bending angle, thus, allowing the construction of a reliable model to predict hygroscopic actuators' actuation. Values that displayed the greatest shape change can be seen in Table 3.5. This table enabled the selection of the best configuration of actuators in terms of response speed and shape change. A sample with a 20x100x0.9mm aspect ratio having these configurations is tested. At the end of 6 hours, the resulting angle of 170° and the circumcircle with a radius of r=286.48mm (Figure 3.2 c) of this sample is used as predicted curvatures of HWA's while designing the possible implementations.

However, results also showed that displacement speed is not enough to meet the requirements of climate-responsive skin. Therefore, in the next stages of this research, parameters of the sample that result in the highest response speed are used, and strategies for further amplification of the response speed are investigated.

Table 3.5 Parameter values that displayed the greatest shape change in the experiments

Parameter	*Found Value*
Total Thickness (mm)	0.45
Active/Passive Layer Ratio	1/1
Restriction Layer Line Gap (mm)	0.8
Restriction Layer Rotation	0°
Layer Height (mm)	0.1
3D Printing Priority	RL

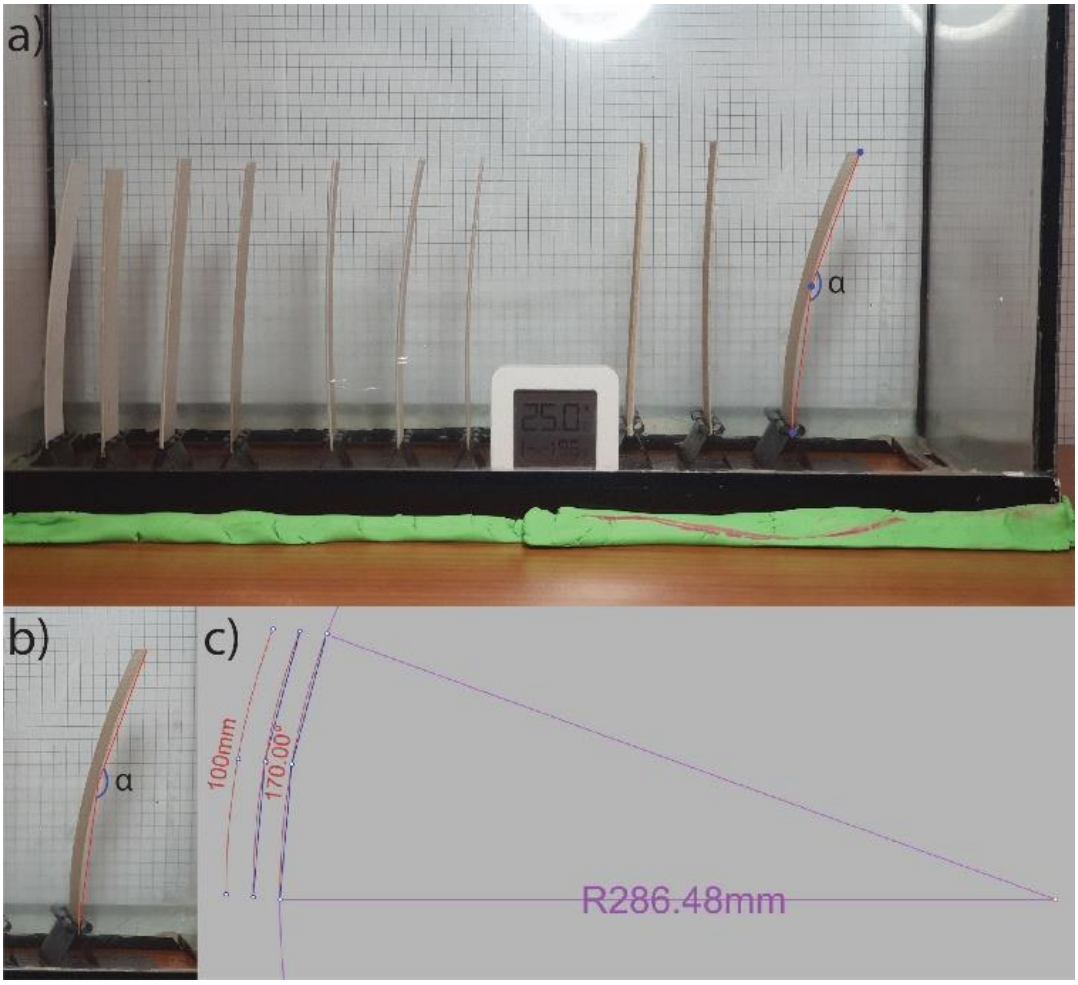

Figure 3.2. Measurement method of bending angle and radius of resulted circumcircle

3.2.1 Parametric Design Process of the Modules

The form of shading devices in relation to actuation material and available fabrication technology has been extensively studied. As discussed in the literature review, wood outperforms other responsive materials for climate-responsive skin applications in terms of the required stimuli, scalability, generated actuation force, and sustainability. With 4D printing of wood, actuation can be controlled by

designated print paths, offering a vast design space and the opportunity for actuator form optimization.

The primary objectives of passive, climate responsive skin design are high response speed and covering surface area with minimum material as well as ensuring robustness in outdoor conditions. However, the responsiveness of 4D-printed wood-based actuators to relative humidity is limited due to material technology constraints. The low response speed and shape change have pushed the researchers to leverage the design space and overcome associated challenges. Several methods are employed in literature, such as biomimicry and origami. In this study, prominent design examples will be evaluated alongside possible alternatives. Table X provides an evaluation of wood-based smart structures employing various motion mechanisms. Note that examples not specifically designed for climate-responsive skin are also included for potential application scenarios. Evaluation of the designs made on the formal features, including response speed, movement type, strategy for employing responsive material, material efficiency, and resilience to distortions.

Response speed varies significantly depending on the material properties and number of actuators that contributes to a single motion. This evaluation focuses on formal aspects. Therefore, only the number of joined actuators is considered. Different types of movement generated by actuators, such as translation, rotation, or a combination of both, are also studied.

A detailed study on design strategies for shape-changing, climate-responsive skins has been conducted (Vazquez, Randall, et al., 2019). The study reports the distinction between the use of smart materials as an actuator, skin, amplifier, structure, or combination with non-responsive material. However, in this study, only wood-based mechanisms are included. The most convenient application scenario is selected for mechanisms not originally designed for responsive skin. The material efficiency of the designs is evaluated based on the ratio of covering surface area (cm^2) to total weight (grams). Lastly, the functional robustness of the designs is categorized as low, medium, and high based on the length of the longest arm from fixed to unfixed

point. When specific dimensions, area, and weight information are not available, they are estimated from the pictures.

closed state	open state	number of joined actuators	movement Types	responsive material as	material efficiency	functional robustness
	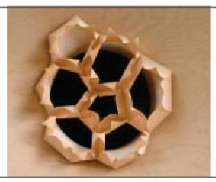	one	translation	skin	low	medium
		(Menges & Reichert, 2015)				
		one	translation	skin	low	medium
		(Holstov et al., 2017)				
		two	translation + translation	skin	low	high
		(Tahouni et al., 2020)				
		two	translation + translation	actuator	high	high
		(Sharp et al., 2021).				
		one	rotation	actuator	high	medium
		(Kam et al., 2022)				

Figure 3.3. Wood-based motion mechanisms in literature (part 1)

One of the earliest projects that utilize hygroscopic properties of wood for climate responsive skin is Hygroskin. The radial array of triangular actuators is used as a skin in a hexagonal template. One edge of the triangular is fixed to the template. From unfixed point to fixed edge, the low height of the triangles provides resilience to distortions. However, the translation movement of the triangle is actuated by a

single actuator (the triangle itself); therefore, it would result in a slow response speed (Menges & Reichert, 2015). Even though the employed materials and their appearances are different, the work by Holstov et al. (2017) is categorized under the same category because the motion mechanisms are identical.

The study by Tahouni et al. (2020) is an exceptional example of motion mechanisms. The mechanism utilizes curved folding origami for enhanced motion. Authors state that curved folding amplifies the response speed since the folding motion is generated not at creases but along the surfaces. Both of the surfaces neighboring the crease contribute to the motion, which increases the active area that provides functional motion.

Plant movement principles inspired many studies in the field thanks to their high efficiency and stability. Biomechanic principles derived from Water Lily (Nymphaea) and Purple Shamrock (Oxalis triangularis) are utilized for 4D printed wood-based actuators and coupled to increase the response speed and stability. The bio-inspired shading facade system employs two joined actuators to move leaf-like elements. Actuators that contribute to the folding in different directions provide enhanced speed and robustness (Sharp et al., 2021).

The research on wood-warping composites by Kam et al. (2022) focuses on wood-based material. However, rotational implementation of the work is included in this study for its possible application as an actuator for climate responsive skin.

closed state	open state	number of joined actuators	movement Types	responsive material as	material efficiency	functional robustness
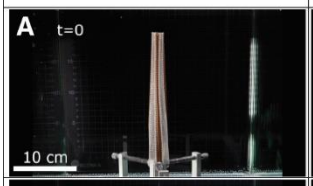	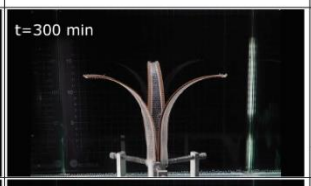	one	translation	actuator	high	low
		(Poppinga et al., 2020)				
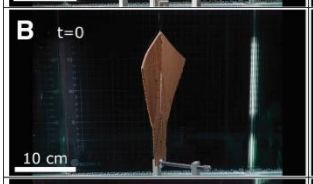	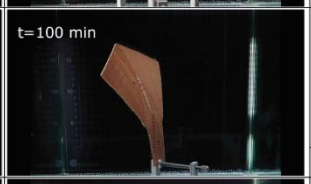	two	translation + translation	skin	low	high
		(Poppinga et al., 2020)				
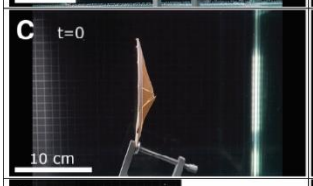		one	translation	skin	low	low
		(Poppinga et al., 2020)				
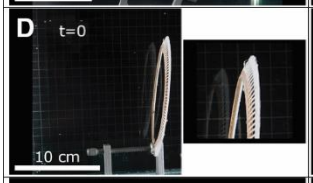	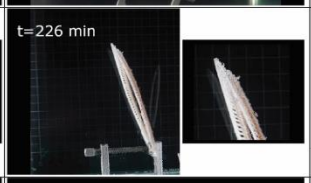	one	translation	actuator	high	high
		(Poppinga et al., 2020)				
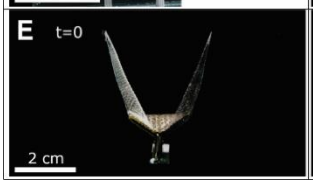	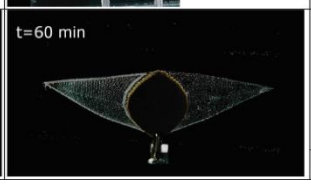	one	translation	actuator	high	medium
		(Poppinga et al., 2020)				

Figure 3.4. Wood-based motion mechanisms in literature (part 2)

Another research inspired by plant movement principles demonstrates five biomimetic compliant mechanisms for hygroscopic actuation of 4D printed wood-based actuators. The authors aimed to create a catalog of mechanisms that varies in response speed, efficiency, and robustness (Poppinga et al., 2020).

The first mechanism (A) uses the biomechanism of a lily flower. The active material is used only on the edges and is responsible for the actuation of thinner elements. This resulted in a lightweight structure with efficient use of material. Although only one actuator contributes to the translation, great shape change is achieved thanks to

the long arms of the mechanism. On the other hand, the longevity of these arms may create difficulties in outside applications.

The second mechanism (B), inspired by pinecone seed, consists of two actuators that contribute to the same motion in vertical directions. Wood-based material used as a skin and the folding motion provide promising robustness for environmental conditions.

Derived from the teeth of the peristome, the third mechanism (C) consist of many actuators on a small scale. Apart from the scale, this mechanism is similar to the Hygroskin in terms of generated motion and employs only one actuator for the same motion, which results in a slow response speed.

The mechanism inspired by the Venus fly-trap (D) displays enhanced speed of shape change and robustness thanks to the bistability. Moreover, wood-based material is used efficiently and acts as an actuator for the non-responsive material on the outer edge.

The final mechanism employs curved folding for amplified motion. One surface in the middle act as an actuator of two surfaces connected to it by curved creases. Moreover, the curved structure of the surfaces in the closed state provides significant robustness to the mechanism (Poppinga et al., 2020).

closed state	open state	number of joined actuators	movement Types	responsive material as	covering surface area (cm2)	total weight (g)	material efficiency (cm2/g)	functional robustness
		one	translation	actuator	38.26	6	6.38	low
	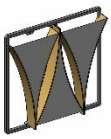	one	translation	actuator	35.25	6	5.88	low
		one	translation	actuator	4.79	3	1.6	high
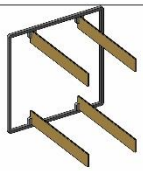	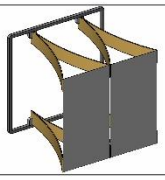	one	translation	actuator	110	12	9.16	low
		one	translation	actuator	55	8	6.88	medium
		two	translation + rotation	actuator	32.69	3.78	8.65	high
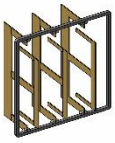	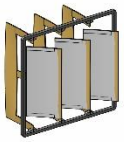	five	translation (x3) + rotation (x2)	actuator	40.96	5.89	6.95	low

Figure 3.5. The parametric design process of the modules

Results of the experiments in the section ‘Observing the Actuation Dynamics’ showed that hygroscopic actuators that are printed in the best configuration with available wood-based material display curvature with a radius of 286.48mm. Using this value, a parametric design process is developed to see possible alternatives and to select the most material-efficient, robust design that displays the highest response speed.

As can be seen in the evaluated designs in the literature, employing active materials as actuator is a more efficient method than using them as skin. Therefore all the alternatives are designed with wood-based material as an actuator of the lightweight elements. In this study, textile is used as the actuated element for its simplicity and lightweight. The same template of 15x15cm is used for all the designs actuators are fixed to this template.

Evaluated designs in the literature showed that the coupling of actuators significantly increases the response speed. Therefore two designs with different numbers of joined actuators are designed.

The length and scale of the actuators significantly affect the response speed as well as the material efficiency and robustness. Therefore actuators with various scales are designed to understand this relation.

The designed alternatives for this study were evaluated based on the single units in the template and not all the repetitions. The weight of these units is calculated based on the volume of the actuators multiplied by the density of 0.011 g/mm2. The density value is gathered from the first phase of the experiments.

According to the calculated values of material efficiency and robustness, it can be stated that the long arms of the actuators enhance the material efficiency while resulting in lower resilience. Designs with coupled actuators increase the arm length, therefore, may result in lower robustness. To mitigate this challenge, coupled actuators are designed with two fixed ends. This is achieved thanks to the vertical

elements printed in 45-degree print paths that show rotational movement. An illustration of the print-paths can be seen in Figure 3.9 a.

The coupled designs are found promising and selected for experimentation. Both of the designs are fabricated without textiles to observe their performance in terms of response speed and robustness.

Even though the design with joined five actuators showed remarkable response speed, the distortions at the end of the experiment are concerning. The design failed even in indoor conditions. Therefore, it is not found promising to continue with to larger scale (Figure 3.6).

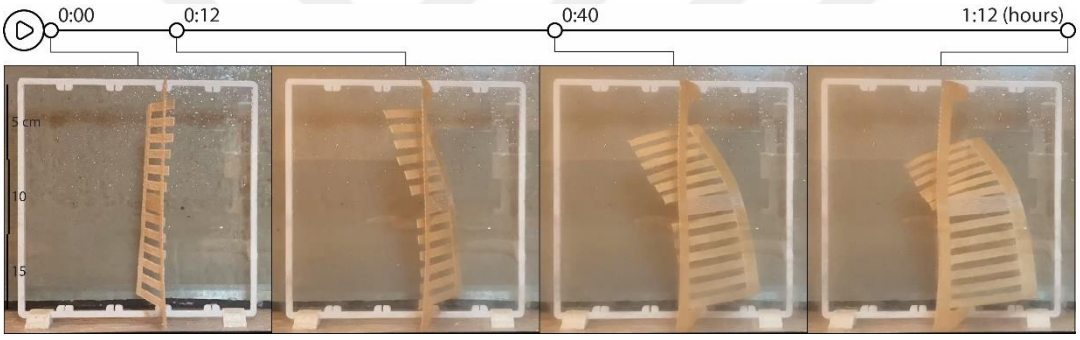

Figure 3.6. Experiment photographs of the module with five joined actuators in a humid environment

The more simple design with two joined actuators displayed great robustness. Moreover, Results showed that vertical elements significantly contributed to the rotation motion, and response speed is enhanced by the coupling of actuators (Figure 3.7 and Figure 3.8).

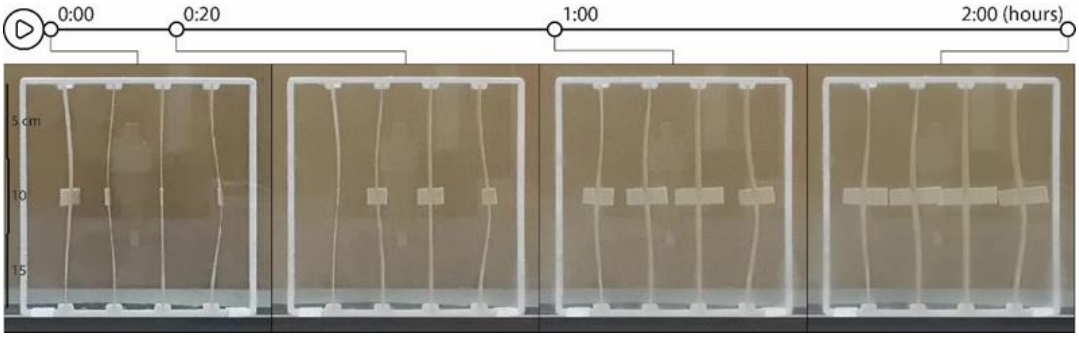

Figure 3.7. Experiment photographs of the module with two joined actuators in a humid environment

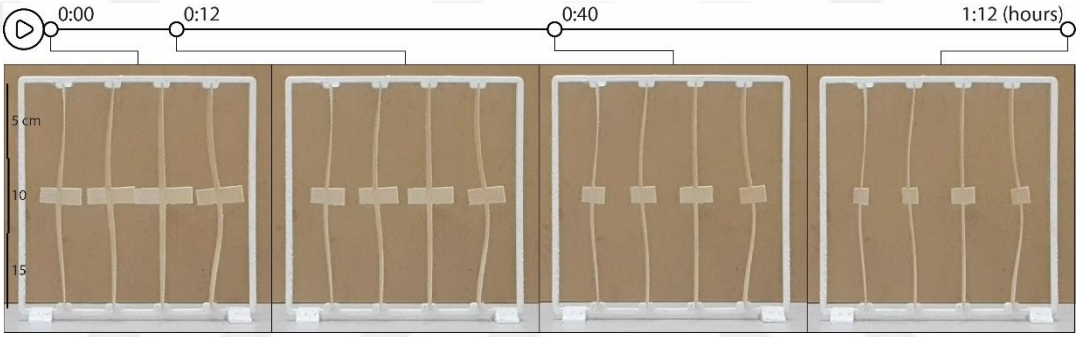

Figure 3.8. Experiment photographs of the module with two joined actuators in a dry environment

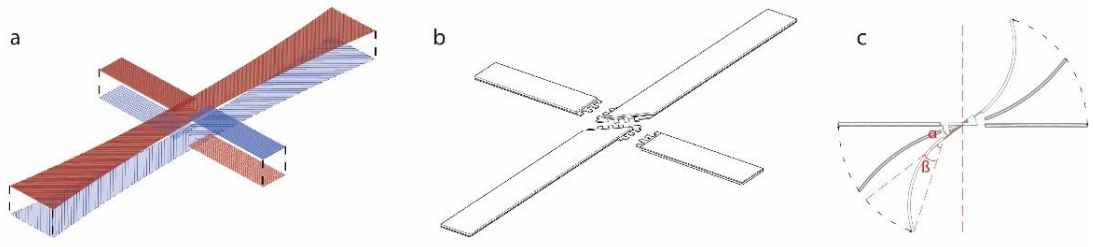

Figure 3.9. a) Print-paths of coupled, rotational design (blue: PLA, red: PLA-Wood) b)Upscaled design with dovetail joints c)Top view of rotational movement of vertical (α) and horizontal (β) element

3.2.2 Pre-stressed Bistability Module

Bistable structures are defined as having two mechanically stable shapes separated by a critical potential energy level (Cao et al., 2021). When an impact surpasses this energy level, it triggers a snap-through action. This leads to amplified input energy, resulting in significant movement characterized by precision and reliability (Cao et al., 2021).

The integration of hygroscopic actuators as activation sources for bistable structures holds particular promise (Chen et al., 2022). Moisture transfer between the environment and wood-based actuators follows an exponential time-dependent pattern (Time, 1998). Consequently, the speed of both displacement and kinetic energy decrease continuously. This means that the first half of the actuation occurs at a higher speed than the second half. Therefore, a bistable structure that is triggered by the first half of the actuator's total displacement could amplify the response speed. Because the rest of the displacement will be realized by the triggered bistable structure.

Energy needed for shape-shifts in bistable structures can be asymmetrically controlled (Faber et al., 2018), allowing for tailored energy thresholds in different directions (Jeong et al., 2019). Introducing pre-stress involves a trade-off: raising the threshold for one shift while reducing it for the reverse shift. This tunable motion asymmetry proves valuable for climate-responsive applications, enabling trade-offs in shape-shift timeframes. For instance, slowing actuation speed at night in favor of faster daytime actuation. Tuning humidity triggers for diverse climates or seasons is crucial for maintaining optimal skin performance.

This experiment is designed and conducted to demonstrate these disccussed foreseen merits of pre-stressed bistability integration to hygroscopic actuators. There are many ways to employ pre-stress to bistable structures. Utilizing gravity to create asymmetric motion behavior is one of the simplest alternatives. Another method is to integrate pre-stressed textile elements into hygroscopic actuators in order to create

tension in one direction. Both of these methods can be employed to create pre-stressed mechanisms. However, it is very challenging to adjust the pre-stress levels with these strategies. Therefore, 3D-printed angled joints are chosen to create tuneable pre-stress levels.

To demonstrate adjustable pre-stress in bistable structures, firstly, hygroscopic actuators are fabricated. Two porous restriction layers (PLA) are 3D printed at once with a flexible layer (TPU Shore A 95) in between for required elasticity during shape-shifts. Maple wood veneer is used as an active material for a larger actuation force. The wood veneers equalized at 65% humidity are glued on the restriction layers.

A simple square template is designed with joints for bistable samples. Following a series of experiments, three different joints with rotation of 15, 10, and 5 degrees have been found promising to demonstrate sequential activation. The joints are 3D printed along with a control joint without rotation.

Fabricated samples are attached to joints and placed in a humid environment (90%) for twenty minutes. Shape-shifts are triggered in the order of no pre-stress to highest pre-stress so that no inference to each other's motion is observed. Then, samples are placed in a relatively dry environment (45%) for twenty minutes. The order of the shape-shifts is reversed, and the last sample that triggered is the one with no pre-stress (Figure 3.10).

The results of these two experiments proved that the response speed of snap-through actuation can be reduced for the sake of increasing the speed in the reverse direction. Tuning the response speed also means adjusting the threshold humidity level, thus, allowing adaptivity to various climatic conditions.

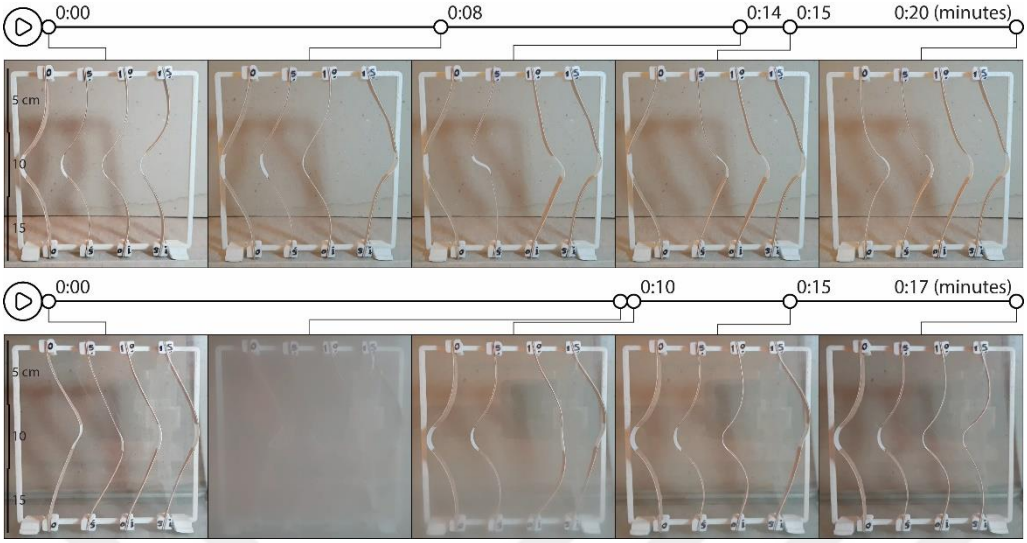

Figure 3.10. Sequential actuation of bistable samples with different pre-stress levels in dry and humid environments

3.3 One-to-one Scale Experiment

To demonstrate the scaleability of the controlled actuation of the designs, large-scale experiments are conducted. These experiments included two promising designs from the previous experiments. Both designs are fabricated in two different versions to demonstrate adaptability to various climatic conditions.

The first one is the rotational module that is 4D printed with wood-based filament. In the larger scale version of this design, dovetail joints are used for the connection of actuators (Figure 3.9 b) due to the print bed's size limitations. Both joints and restriction layers are printed at once with PLA, but the wood veneer is used as an active material instead of PLA Wood filament because of the limited wood content and actuation. Vood veneer sheet was placed in a laser cut machine in a determined direction, as seen in Figure 3.11, so that the orientation of the fibers aligned according to the design. For the vertical elements with 45° print-paths, actuators are

45° rotated and laser cut in a rotated shape. The laser-cut actuators are then humidified for 3 hours and equalized at different humidity levels (60% and 75%) to create two versions of this design. The humidified actuators are glued with printed restriction layers and placed in a dry environment. All the separate actuators are sorted according to their bending angle. The actuators that bent too much or too low are classified as outliers and removed from the experiment. The other actuators were then glued with each other from the dove joints and glued to complete the designed rotational unit. Vertical and horizontal elements' contribution to the rotational motion can be seen in Figure 3.9 c.

The second implementation is the pre-stressed bistability module. The previous experiment on a small scale demonstrated the achieved sequential motion with angled joints of 0°, 5°, 10°, and 15°. For the large-scale projection, only 0° and 10° angled joints are fabricated to create two versions. A similar process to the first design is followed for the fabrication of actuators. However, all the actuators are equalized at the same humidity level (60%) for pre-stressed modules.

Figure 3.11. The fabrication process of wood-based hygroscopic actuators

To deploy all the fabricated modules, a quadrangular and hexagonal template is designed. Linear wooden elements connected to each other by 3D-printed joints are used to create modular structures for the large-scale experiment. On the left top rotational modules equalized to 75% humidity, and on the left bottom rotational modules equalized to 60% humidity are placed. Textile elements are attached to these joints from the end points to demonstrate the surface coverage of actuators.

On the right top, pre-stressed modules with 10° angled joints are placed, while on the right bottom bistable modules are placed with no pre-stress. The vertical folded textile elements attached to these modules demonstrate linear actuation generated by actuators.

Figure 3.12. The large-scale prototype of responsive skin: left: rotational modules equalized to 75% and 60% humidity, right: modules pre-stressed with 10° angled joints and no pre-stressed

Modules are placed in a dry environment (~30%) for two and a half hours and a humid environment (~90%) for five hours. Overall, the actuation behavior is very similar to the experiments on a small scale. All the modules generated the expected motion and demonstrated reversible open and closed states in a short period of time. Moreover, similar to the previous experiments, greater response speed is observed during the drying process (Figure 3.12).

Results of the experiment demonstrated that bilayering at different humidity levels causes a pre-stress in modules, and different open/close states can be achieved in the same environmental conditions (Figure 6). This can be clearly seen at the t=300 min. The two versions of rotational modules are at different states. The upper module is open, while the modules at the bottom are closed.

This distinction between the versions is not that clear in pre-stressed bistable modules. For example, during the drying process, all the upper pre-stressed modules should have opened before the bottom modules with no pre-stress. However, as can be seen from the t=30 min, One pre-stressed actuator remained closed while all the bistable actuators were opened. This is due to the distortions in the actuators at the end points. Angled joint to create pre-stress in hygroscopic actuators created distortion and removed the pre-stress.

CHAPTER 4

RESULTS AND DISCUSSION

4.1 Results

In this section, studies were conducted to explore the radiation impacts of tested hygroscopic wood-based actuators. The modeling and analysis of the rotational shading device (Figure 4.1a) were performed using the parametric design tool Grasshopper and the environmental plugin Ladybug.

The study area was set in 4x4 meters office room with 3 meters height in Ankara. The analyses were timed to coincide with the equinoxes and solstices, namely March 21, June 21, September 22, and December 21 (Figure 4.1c). These dates represent key points in the annual solar cycle, allowing for an assessment of performance across a range of solar conditions.

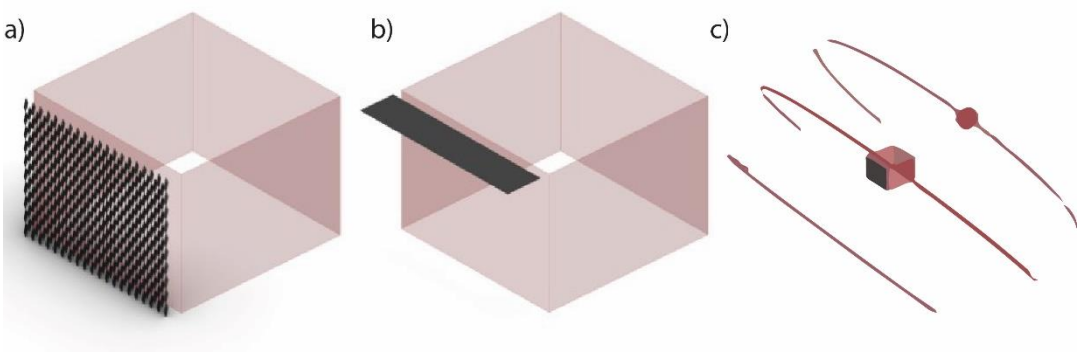

Figure 4.1. a) Responsive skin, b) Fixed shading device, c) Sun-paths during equinoxes and solstices

The radiation analysis was also conducted for a fixed shading device (Figure 4.1b). This fixed device, stationary by design, provided a control group against which the performance of the wood-based responsive skin could be evaluated. The horizontal

shading device's dimensions are determined by the formula 'P=H/tan(A)' (Kim et al., 2013), where P is the length of horizontal shading, H is the horizontal length to shade from the bottom of the window, and A is the summer meridian altitude (90-latitude + 23.5). The length of the fixed shading device is found 83,33 cm by this formula.

For the rotational module, Ankara's daily humidity data is derived from the website climate.onebuilding.org, Etimesgut location. The yearly humidity data is separated into branches of datasets for equinoxes and solstices. For example, the humidity data for 21 June can be seen in Figure (4.2). This data is used to rotate the rotational modules.

Since the experiments are conducted only in humid (90%) and dry (30%) environments, the exact state of the rotational module at certain humidity levels is unknown. In other words, the states of the rotational module in 30% and 90% humidity can be modeled, but the states in 50% or 70% can only be assumpted. Therefore, facade states in humid (90%) and dry (30%) environment is modeled based on the collected data, and the states in between are interpolated (Figure 4.2).

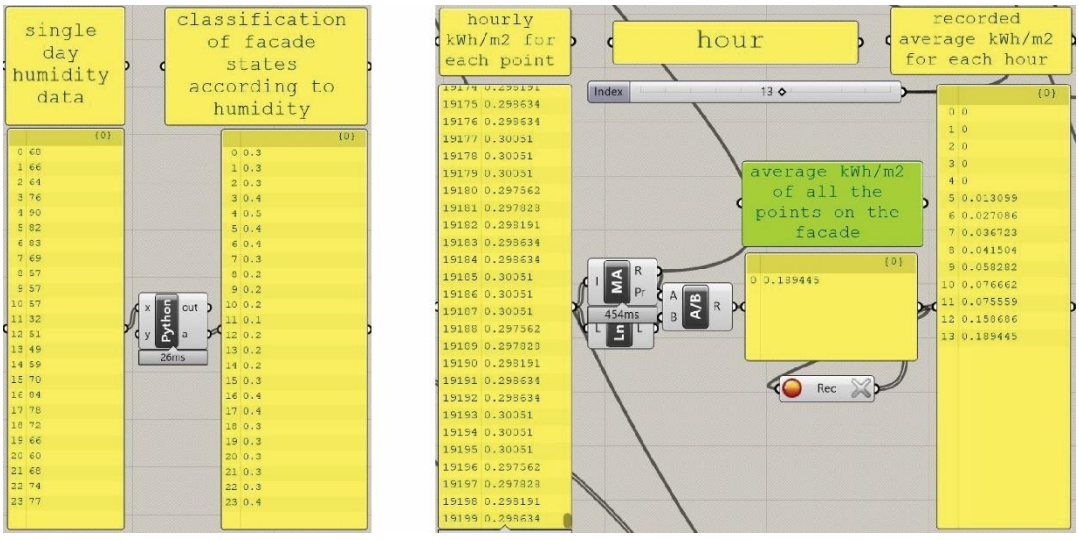

Figure 4.2. Ankara's daily humidity data drives the rotational motion (left), hourly kWh/m2 values for 19200 points on the facade, and calculated average (right)

The radiation simulation is conducted hour by hour. Each hour, the skin changed shape according to humidity, and radiation intensity per square meter was computed for every 19200 points on the facade. The average value of all the points is calculated, and the hourly average kWh/m2 is found. The screenshots from the simulation showing the states of the facade and analyzed radiation values on 21 June at 11-12 am and 4-5 pm can be seen in Figure 4.3.

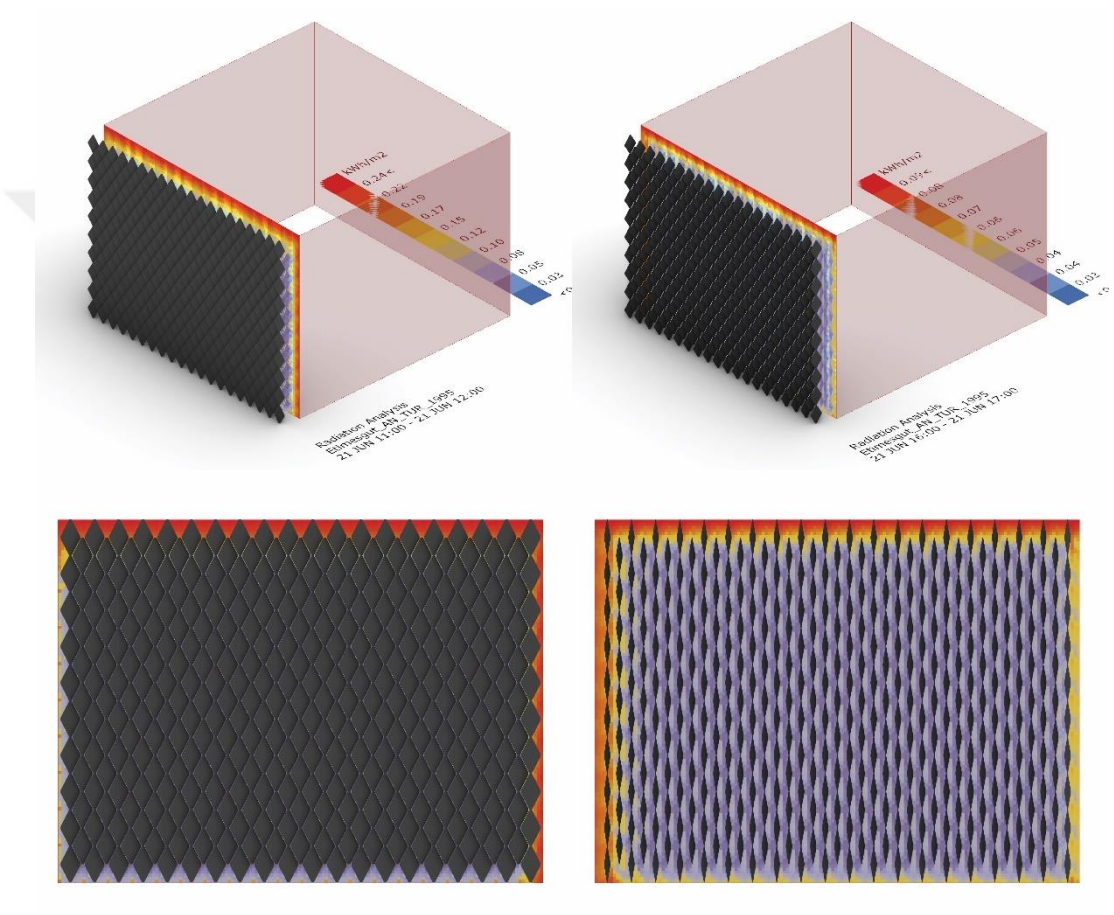

Figure 4.3. Perspective and elevation screenshots from the simulation showing the states of the climate responsive skin and analyzed radiation values on 21 June at 11-12 am (left) and 4-5 pm (right)

The relative humidity to temperature chart belove (Figure 4.4) demonstrates the behavior of responsive skin on 21 June. At 5 am, while the temperature is at 16 Celcius, relative humidity is reached 90%, and the responsive skin is all open. On the other hand, at 12 am, while the temperature is at 28 Celcius, RH is dropped to 32%, and the responsive skin is all closed. At 5 pm, responsive skin displays the semi-open state when the temperature is at 21 Celcius and the RH is at 84%.

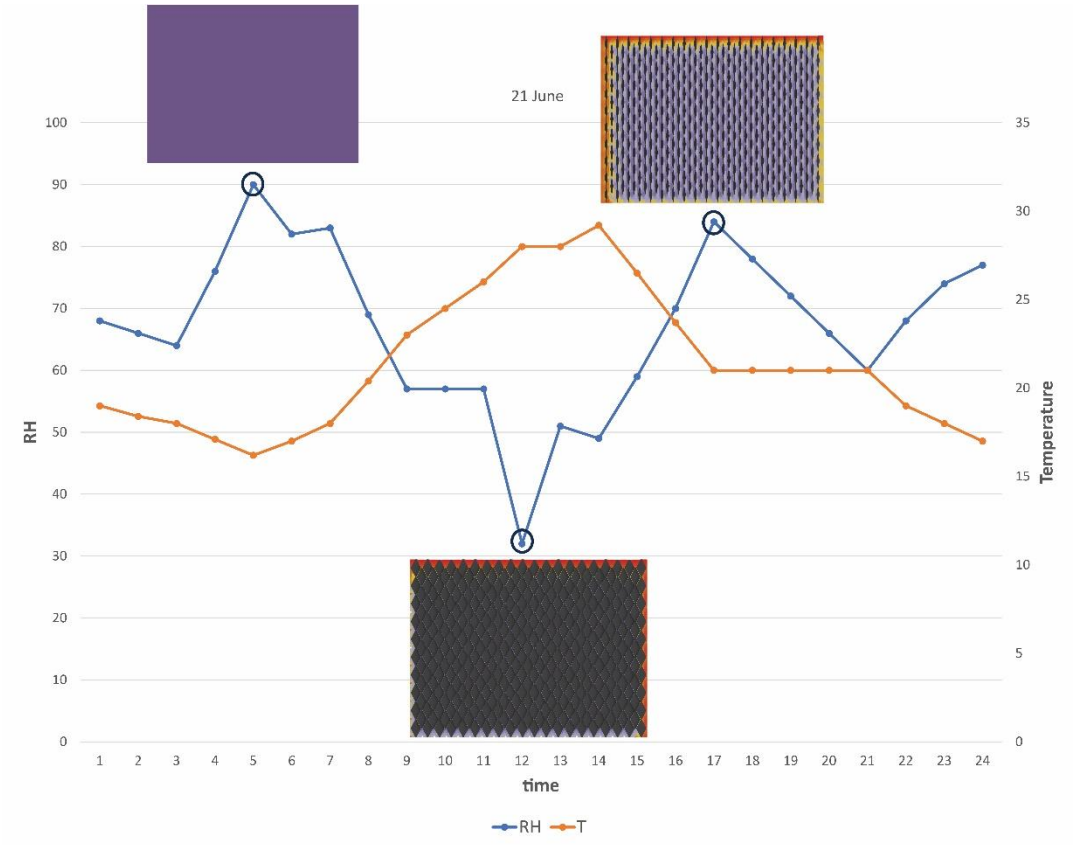

Figure 4.4. The relative humidity to temperature chart on 21 June in Ankara demonstrating the behavior of responsive skin

The results of the radiation simulation show that the responsive skin provided far more consistent performance throughout the year. The responsive skin's (bilayered at 95%) total daily kWh/m2 ranged from 0,76 kWh/m2 on June 21st to 1,26 kWh/m2 on December 21st. These values are much lower than those obtained for the fixed

shading device, emphasizing the skin's ability to adapt and respond to changing environmental conditions, reducing the amount of solar radiation entering the room. All versions of the responsive skin blocked more sunlight than the fixed shading device, preventing excessive radiation and overheating, resulting in decreased cooling energy. On the other hand, fixed shading device allow much greater radiation in winter than responsive skin, which is crucial for energy efficiency. This is due to the calibration of the responsive skin, and these values can be significantly improved. By changing the humidity level at the bilayering stage of wood-based actuators, the motion of the responsive skin can be calibrated to allow more sunlight into the room. These results demonstrated the significance of the pre-stress and calibration of the hygroscopic actuator on the energy efficiency of the buildings.

Figure 4.5. The hourly kWh/m2 data of fixed shading device and responsive skins bilayered at different humidity levels

4.2 Discussion

This research questioned the applicability of hygroscopic wood-based materials as a climate-responsive façade component. For this purpose, a series of experiments are conducted. The wood-based filament is used as an active material for small-scale experiments. Gained knowledge projected to large-scale experiments utilizing hygroscopicity of wood veneer. Similar actuation behavior was observed in both experiments, which proved the scalability of the designs. Then, collected experimental data is used to develop the imagined model in Grasshopper. The array of the components at the façade of a room can be seen in Figure 4.1. Tuned at different pre-stress levels, actuators are at various open and closed states in the same humidity level.

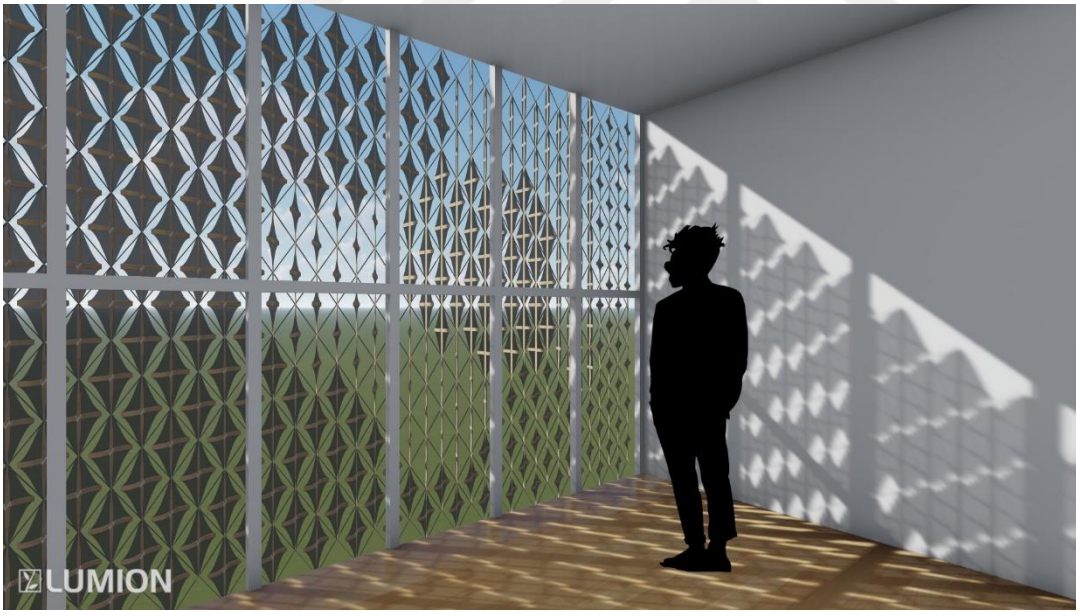

Figure 4.6. Imagined array of the components at the façade of a room

Configuration, scale, and pre-stress level of the components can be adjusted for various climatic conditions. Even each façade of a building can be designed before the installation to maximize energy efficiency and user comfort.

Responsive skins that utilize the passive actuation of wood bilayers offer distinct advantages over electric or motor-driven skins. These advantages include reduced installation and maintenance costs, simplicity, and a lower carbon footprint, making them highly promising for future applications. However, passive responsive skins currently lack adaptability to both climatic and seasonal changes, as well as occupant preferences.

One approach to address this limitation is by programming the triggering humidity level for shape change during the actuator's bilayering process. By adjusting the humidity of the active material, the triggering humidity level can be set. However, once programmed, the triggering humidity cannot be reprogrammed, limiting the adaptability of the skin to seasonal changes.

To overcome this challenge, external forces can be employed to pre-stress the actuators and tune the triggering humidity. This research has demonstrated that pre-stressed bistable design by angled joints allows significant control over the threshold levels. However, a strategy to dynamically tune the pre-stress on an architectural scale is currently unknown. Such a system that can be tuned by occupants would enable both the adaptability to climatic changes and user preferences.

CHAPTER 5

CONCLUSION

5.1 Summary

This study emerged to make a contribution to the literature on hygroscopic wood-based climate responsive skin applications for enhanced energy efficiency and occupant comfort. Comprehensive research on design and fabrication parameters, as well as pre-stress bistability integration, is investigated to overcome the challenges related to response speed, motion control, and scalability.

A literature review is conducted on building envelopes, which defines the basis of the problem statement. The review revealed that traditional adaptive envelopes are complex systems with a high maintenance cost, and they require additional energy input to operate, which compromises their effectiveness. Alternatively, responsive materials that shape change in response to environmental stimuli are promising since they do not require any additional energy to operate. Moreover, they are much more simple since the sensing, operation control, and actuation are all done by the material itself. The shape-changing materials are reviewed and evaluated based on their features for applicability to climate responsive skin applications. Among these materials, the evaluation revealed that wood has significant advantages over other shape-changing materials, including the reversibility of the motion, triggered stimuli (RH, which changes significantly throughout the day), high actuation force and design space, inexpensive and sustainable material. Then, fabrication methods for wood-based hygroscopic actuators are studied. Extrusion-based printing techniques (FDM and DIW) are found more promising over the bilayering wood layers since they allow the utilization of wood flour derived from wood waste. Moreover, printing paths dictate the fiber direction, which allows to control the shape change. Among FDM and DIW techniques, FDM is used in this study for material availability. In

the final part of the literature review, smart structures and motion mechanisms are reviewed to enhance the response speed and stability of wood-based actuators. Studies report that the coupling of multiple actuators increases the response speed. It is also found that the integration of pre-stress bistability into hygroscopic actuators is promising. While bistability allows for precise, controlled motion, stable and robust states, pre-stressed bistability allows trade-off between shape-shift times. In other words, it is possible to create structures with much quicker shape-shift in one direction while slower in the opposite direction.

Based on the evaluation of the literature, experiments are developed in three consecutive stages. In the first stage, actuation dynamics of the 4D printed hygroscopic wood-based actuators are observed. The wood-based filament is used as the active layer, and PLA is used as the restriction layer. Systematic experiments are conducted on identified design parameters (Porosity, Total Thickness, Bilayer Ratio, Layer Orientation) and fabrication parameters (Layer Height, Printing Priority). The effect of the parameters on bending angle is observed in a humid environment for six hours. Based on the collected data, a model is built to predict and control the shape change of actuators. The parameter values that resulted in the greatest shape change are identified. However, the response speed was not enough to fulfill the requirements of the climate responsive building skin.

In the second stage of the experiments, two implementations of the model are developed to enhance the response speed, shape change, and motion control. The first implementation employs coupled actuators for higher response speed. The vertical actuators with 45-degree print paths and linear actuators joined together for the same rotational motion. The design with custom print-paths is 3D printed and the experiment is conducted in a humid environment. Results demonstrated the enhanced response speed by the coupling of actuators. The second implementation explored the pre-stress bistability integration into hygroscopic wood-based actuators. The bistable module is developed with two actuators combined with a TPU layer in between. Actuators are placed in a rectangular template with angled joints to create pre-stress. The experiments in both humid and dry environments with angled (15,

10, 5, 0) joints demonstrated that response speed can be amplified by the pre-stress. The trade-off between triggering response time is achieved, which enables greater control of the actuation. The results are promising for the adaptivity of climate responsive skin in various climates and higher energy efficiency for the buildings.

In the third stage of the experiments, both implementations are tested at a higher scale and with wood veneer to demonstrate the material and scale independency of the modules. The print paths of 4D printed implementations transferred to wood veneers fiber orientation. The complex printing path patterns had to be fabricated separately and combined together by joints. To demonstrate the effect of pre-stress on the movement of actuators, both implementations are created with two versions with different pre-stress levels. The rotational modules are bilayered at 60% and 75% humidity, while bistable modules are pre-stressed with 10-degree angular joints and with no pre-stress. Experiments conducted in both dry and humid environments demonstrated that rotational modules with different pre-stress levels are at different states in the same environment. This can be utilized for adaptivity to different climatic conditions or seasonal changes. On the other hand, no clear difference is observed in bistable modules because the prestressed joints caused a deformation of the actuators.

The collected data from the experiments are used for radiation analysis. The climate responsive skin employing rotational modules with different pre-stress levels is compared with the basic fixed shading device. Grasshopper and LadyBug plug-ins are used to develop humidity data-driven responsive skin and for hourly radiation analysis. The simulation model is developed for the south facade of and office room in Ankara, and simulations are considered equinoxes and solstices. The results demonstrated that pre-stress levels significantly affect the energy efficiency of the buildings. Moreover, responsive skins outperformed the fixed shading device in summer and blocked excessive sunlight. This demonstrates that responsive skins can prevent the overheating of spaces, thus, decreasing the cooling energy. On the other hand, responsive skins block more sunlight also during winter, which can cause

higher heating energy during winter. Further research is required to develop responsive skins that enhance energy efficiency throughout the year.

5.2 Limitations

Several limitations are associated with the study due to the available equipment used for experimentation. These limitations have the potential to impact the precision and accuracy of the results obtained. Firstly, the 3D printer used in the experiment may have inherent limitations in terms of accuracy caused by the buildplate calibration. This can introduce variations in the thickness of the samples, which could potentially affect the reliability and consistency of the experimental outcomes.

The control of humidity in the experiment's environment is another aspect that presents limitations. The humidity levels are manually regulated using a humidifier, which can result in imprecise control and fluctuations in humidity. Moreover, the measurement of the bending angle of the samples during hygroscopic actuation is conducted manually using ImageJ software. This manual measurement process introduces the possibility of human error.

It should be noted that the prototypes developed in this study were not tested in outdoor conditions. The absence of outdoor testing limits the understanding of the effects of weathering and wind loads on the performance of the prototypes. Future research should consider conducting outdoor experiments to investigate these aspects more comprehensively.

Furthermore, the experiments in this study were conducted in specific humidity conditions, namely dry (30%) or humid (90%) environments, to observe the shape changes. However, no testing was performed at humidity levels in between. Consequently, the states of the hygroscopic actuators at different humidity levels remain unknown. Acquiring knowledge about the states of the actuators at various humidity levels would provide valuable insights for designing more effective and adaptable systems.

These limitations need to be addressed and taken into consideration in future studies to improve the precision, reliability, and overall understanding of the research findings in this field.

5.3 Future Work

Compared to traditional building materials, the biorenewability and biodegradability of wood are vital for the future of the construction industry. From forestry to commercial use, each process of wood produces wood waste. Utilization of wood waste through 4D printing for responsive skin would significantly help the circularity of construction. However, the maximum wood content of filaments for FDM printers is limited due to the risk of nozzle blockage. This has a detrimental effect on hygroscopic actuation, decreasing the response speed and displacement.

Alternatively, the direct ink writing (DIW) technique offers greater material customization (Deng & Lin, 2022), enabling mixtures with higher wood content and cost-efficient manufacturing (Rosenthal et al., 2018). Recent research has reported significant shape change of 4D printed wood using the DIW technique, which can be manipulated by adjusting the printing speed (Kam et al., 2022). The combination of the DIW technique and advanced material compositions shows promise for their enhanced responsiveness and needs to be investigated further for architectural implementations.

Leveraging these recent innovations in material science and the DIW technique, future studies will aim to further narrow the time range of targeted shape change for climate-responsive skins. In addition to responsiveness, challenges related to precise motion control and durability against outdoor conditions need to be addressed for successful architectural implementations. Introducing polymers in specific quantities can enhance the durability of wood-based ink while reducing its hygroscopic behavior (El-Haggar et al., 2011). Therefore, a comprehensive understanding of the material matrix and design parameters is crucial for developing both responsive and

durable hygroscopic actuators. Future work will focus on these aspects to overcome state-of-the-art challenges.

REFERENCES

Addington, Michelle., & Schodek, D. L. (2005). *Smart materials and new technologies : for the architecture and design professions*. Architectural. https://www.routledge.com/Smart-Materials-and-Technologies-For-the-Architecture-and-Design-Professions/Addington-As/p/book/9780750662253

Aelenei, D., Aelenei, L., & Vieira, C. P. (2016). Adaptive Façade: Concept, Applications, Research Questions. *Energy Procedia*, *91*, 269–275. https://doi.org/10.1016/j.egypro.2016.06.218

Ahmad, I. (1988). Smart structures and materials. *Proceeding of US Army Research Office Workshop of Smart Materials*, 13–16. https://doi.org/10.2749/kualalumpur.2018.0917

An, S. M., Ryu, J., Cho, M., & Cho, K. J. (2012). Engineering design framework for a shape memory alloy coil spring actuator using a static two-state model. *Smart Materials and Structures*, *21*(5). https://doi.org/10.1088/0964-1726/21/5/055009

Baker, A. B., Bates, S. R. G., Llewellyn-Jones, T. M., Valori, L. P. B., Dicker, M. P. M., & Trask, R. S. (2019). 4D printing with robust thermoplastic polyurethane hydrogel-elastomer trilayers. *Materials and Design*, *163*. https://doi.org/10.1016/j.matdes.2018.107544

Barozzi, M., Lienhard, J., Zanelli, A., & Monticelli, C. (2016). The Sustainability of Adaptive Envelopes: Developments of Kinetic Architecture. *Procedia Engineering*, *155*, 275–284. https://doi.org/10.1016/j.proeng.2016.08.029

Berköz, E., & Yílmaz, Z. (1987). Determination of the overall heat transfer coefficient of the building envelope from the bioclimatic comfort point of view. *Architectural Science Review*, *30*(4), 117–121. https://doi.org/10.1080/00038628.1987.9696613

Burgert, I., & Fratzl, P. (2009). Actuation systems in plants as prototypes for bioinspired devices. *Philosophical Transactions of the Royal Society A: Mathematical, Physical and Engineering Sciences*, *367*(1893), 1541–1557. https://doi.org/10.1098/RSTA.2009.0003

Cao, Y., Derakhshani, M., Fang, Y., Huang, G., Cao, C., Cao, Y., Derakhshani, M., Fang, Y., Cao, C., & Huang, G. (2021). *Bistable Structures for Advanced Functional Systems*. https://doi.org/10.1002/adfm.202106231

Chen, E., Lu, G., Barnik, L., & Correa, D. (2022). Fast and Reversible Bistable Hygroscopic Actuators for Architectural Applications based on Plant Movement Strategies. *Proceedings of the International Conference on Education and Research in Computer Aided Architectural Design in Europe*, *1*, 261–270. https://doi.org/10.52842/conf.ecaade.2022.1.261

Chen, T., Mueller, J., & Shea, K. (2017). Integrated Design and Simulation of Tunable, Multi-State Structures Fabricated Monolithically with Multi-Material 3D Printing. *Scientific Reports 2017 7:1*, *7*(1), 1–8. https://doi.org/10.1038/srep45671

Chen, T., & Shea, K. (2018). An Autonomous Programmable Actuator and Shape Reconfigurable Structures Using Bistability and Shape Memory Polymers. *3D Printing and Additive Manufacturing*, *5*(2), 91–101. https://doi.org/10.1089/3DP.2017.0118

Chen, T., & Shea, K. (2021). Computational design of multi-stable, reconfigurable surfaces. *Materials & Design*, *205*, 109688. https://doi.org/10.1016/J.MATDES.2021.109688

Cheng, T., Thielen, M., Poppinga, S., Tahouni, Y., Wood, D., Steinberg, T., Menges, A., & Speck, T. (2021). Bio-Inspired Motion Mechanisms: Computational Design and Material Programming of Self-Adjusting 4D-Printed Wearable Systems. *Advanced Science*, *8*(13), 2100411. https://doi.org/10.1002/advs.202100411

Cho, K. J., Koh, J. S., Kim, S., Chu, W. S., Hong, Y., & Ahn, S. H. (2009). Review of manufacturing processes for soft biomimetic robots. *International Journal of Precision Engineering and Manufacturing*, *10*(3), 171–181. https://doi.org/10.1007/S12541-009-0064-6/METRICS

Correa, D., Papadopoulou, A., Guberan, C., Jhaveri, N., Reichert, S., Menges, A., & Tibbits, S. (2015). 3D-Printed Wood: Programming Hygroscopic Material Transformations. *3D Printing and Additive Manufacturing*, *2*(3), 106–116. https://doi.org/10.1089/3dp.2015.0022

Correa, D., Poppinga, S., Mylo, M. D., Westermeier, A. S., Bruchmann, B., Menges, A., & Speck, T. (2020). 4D pine scale: biomimetic 4D printed autonomous scale and flap structures capable of multi-phase movement. *Philosophical Transactions of the Royal Society A*, *378*(2167). https://doi.org/10.1098/RSTA.2019.0445

D. I, A., P, C., R, A. K., & B, S. (2018). *Shape Memory Materials*. CRC Press. https://books.google.com/books/about/Shape_Memory_Materials.html?hl=tr&id=eJxYDwAAQBAJ

Dawson, C., Vincent, J. F. V., & Rocca, A. M. (1997). How pine cones open [4]. In *Nature* (Vol. 390, Issue 6661, p. 668). Nature Publishing Group. https://doi.org/10.1038/37745

Del Grosso, A. E., & Basso, P. (2010). Adaptive building skin structures. *Smart Materials and Structures*, *19*(12), 124011. https://doi.org/10.1088/0964-1726/19/12/124011

Dinwoodie, J. M. (2000). *Timber: Its nature and behavior*. CRC Press. https://www.routledge.com/Timber-Its-Nature-and-Behaviour/Dinwoodie/p/book/9780419235804

Elahinia, M. H. (2016). *Shape memory alloy actuators : design, fabrication, and experimental evaluation*. John Wiley & Sons.

https://books.google.com/books/about/Shape_Memory_Alloy_Actuators.html?hl=tr&id=hJAvCgAAQBAJ

El-Dabaa, R., Abdelmohsen, S., & Mansour, Y. (2020). Programmable passive actuation for adaptive building façade design using hygroscopic properties of wood. *Wood Material Science and Engineering*, *16*(4), 246–259. https://doi.org/10.1080/17480272.2020.1713885

Erb, R. M., Sander, J. S., Grisch, R., & Studart, A. R. (2013). Self-shaping composites with programmable bioinspired microstructures. *Nature Communications*, *4*(1), 1–8. https://doi.org/10.1038/ncomms2666

Faber, J. A., Arrieta, A. F., & Studart, A. R. (2018). Bioinspired spring origami. *Science*, *359*(6382), 1386–1391. https://doi.org/10.1126/SCIENCE.AAP7753/SUPPL_FILE/AAP7753S3.MOV

Fiorito, F., Sauchelli, M., Arroyo, D., Pesenti, M., Imperadori, M., Masera, G., & Ranzi, G. (2016). Shape morphing solar shadings: A review. In *Renewable and Sustainable Energy Reviews* (Vol. 55, pp. 863–884). Pergamon. https://doi.org/10.1016/j.rser.2015.10.086

Gauss, C., Pickering, K. L., & Muthe, L. P. (2021). The use of cellulose in bio-derived formulations for 3D/4D printing: A review. In *Composites Part C: Open Access* (Vol. 4, p. 100113). Elsevier. https://doi.org/10.1016/j.jcomc.2021.100113

González-Henríquez, C. M., Sarabia-Vallejos, M. A., & Rodriguez-Hernandez, J. (2019). Polymers for additive manufacturing and 4D-printing: Materials, methodologies, and biomedical applications. *Progress in Polymer Science*, *94*, 57–116. https://doi.org/10.1016/J.PROGPOLYMSCI.2019.03.001

Grönquist, P., Panchadcharam, P., Wood, D., Menges, A., Rüggeberg, M., & Wittel, F. K. (2020). Computational analysis of hygromorphic self-shaping

wood gridshell structures. *Royal Society Open Science*, *7*(7), 192210. https://doi.org/10.1098/rsos.192210

Grönquist, P., Wood, D., Hassani, M. M., Wittel, F. K., Menges, A., & Rüggeberg, M. (2019). Analysis of hygroscopic self-shaping wood at large scale for curved mass timber structures. *Science Advances*, *5*(9). https://doi.org/10.1126/sciadv.aax1311

Hartl, D. J., & Lagoudas, D. C. (2007). Aerospace applications of shape memory alloys. *Proceedings of the Institution of Mechanical Engineers, Part G: Journal of Aerospace Engineering*, *221*(4), 535–552. https://doi.org/10.1243/09544100JAERO211

Herbert, K. M., Fowler, H. E., McCracken, J. M., Schlafmann, K. R., Koch, J. A., & White, T. J. (2021). Synthesis and alignment of liquid crystalline elastomers. *Nature Reviews Materials 2021*, 1–16. https://doi.org/10.1038/s41578-021-00359-z

Hinton, T. J., Jallerat, Q., Palchesko, R. N., Park, J. H., Grodzicki, M. S., Shue, H. J., Ramadan, M. H., Hudson, A. R., & Feinberg, A. W. (2015). Three-dimensional printing of complex biological structures by freeform reversible embedding of suspended hydrogels. *Science Advances*, *1*(9). https://doi.org/10.1126/SCIADV.1500758/SUPPL_FILE/1500758_SM.PDF

Holstov, A., Bridgens, B., & Farmer, G. (2015). Hygromorphic materials for sustainable responsive architecture. *Construction and Building Materials*, *98*, 570–582. https://doi.org/10.1016/j.conbuildmat.2015.08.136

Holstov, A., Farmer, G., & Bridgens, B. (2017). Sustainable materialisation of responsive architecture. *Sustainability (Switzerland)*, *9*(3), 435. https://doi.org/10.3390/su9030435

Huang, W. M., Ding, Z., Wang, C. C., Wei, J., Zhao, Y., & Purnawali, H. (2010). Shape memory materials. *Materials Today*, *13*(7–8), 54–61. https://doi.org/10.1016/S1369-7021(10)70128-0

International Energy Agency. (2019). 2019 Global Status report for Buildings and Construction. In *Global Status Report*. https://www.unep.org/resources/publication/2019-global-status-report-buildings-and-construction-sector

IP/03/1278 Indoor air pollution: new EU research reveals higher risks than previously thought. (2003). https://ec.europa.eu/commission/presscorner/detail/en/IP_03_1278

Jakab, K., Norotte, C., Marga, F., Murphy, K., Vunjak-Novakovic, G., & Forgacs, G. (2010). Tissue engineering by self-assembly and bio-printing of living cells. *Biofabrication*, *2*(2), 022001. https://doi.org/10.1088/1758-5082/2/2/022001

Jeong, H. Y., An, S. C., Seo, I. C., Lee, E., Ha, S., Kim, N., & Jun, Y. C. (2019). 3D printing of twisting and rotational bistable structures with tuning elements. *Scientific Reports*, *9*(1), 1–9. https://doi.org/10.1038/s41598-018-36936-6

Jeong, H. Y., Woo, B. H., Kim, N., & Jun, Y. C. (2020). Multicolor 4D printing of shape-memory polymers for light-induced selective heating and remote actuation. *Scientific Reports*, *10*(1). https://doi.org/10.1038/s41598-020-63020-9

Kam, D., Layani, M., BarkaiMinerbi, S., Orbaum, D., Abrahami BenHarush, S., Shoseyov, O., & Magdassi, S. (2019). Additive Manufacturing of 3D Structures Composed of Wood Materials. *Advanced Materials Technologies*, *4*(9). https://doi.org/10.1002/admt.201900158

Kam, D., Levin, I., Kutner, Y., Lanciano, O., Sharon, E., Shoseyov, O., & Magdassi, S. (2022). Wood Warping Composite by 3D Printing. *Polymers*, *14*(4), 733. https://doi.org/10.3390/polym14040733

Kariz, M., Sernek, M., Obućina, M., & Kuzman, M. K. (2018). Effect of wood content in FDM filament on properties of 3D printed parts. *Materials Today*

Communications, *14*, 135–140. https://doi.org/10.1016/J.MTCOMM.2017.12.016

Krapež Tomec, D., Balzano, A., Žigon, J., Šernek, M., & Kariž, M. (2022). The Effect of Printing Parameters and Wood Surface Preparation on the Adhesion of Directly 3D-Printed PLA on Wood. *Journal of Renewable Materials*, *10*(7), 1787–1796. https://doi.org/10.32604/jrm.2022.019760

Krüger, F., Thierer, R., Tahouni, Y., Sachse, R., Wood, D., Menges, A., Bischoff, M., & Rühe, J. (2021). Development of a material design space for 4d-printed bio-inspired hygroscopically actuated bilayer structures with unequal effective layer widths. *Biomimetics*, *6*(4). https://doi.org/10.3390/biomimetics6040058

Kuang, X., Roach, D. J., Wu, J., Hamel, C. M., Ding, Z., Wang, T., Dunn, M. L., & Qi, H. J. (2019). Advances in 4D Printing: Materials and Applications. *Advanced Functional Materials*, *29*(2). https://doi.org/10.1002/ADFM.201805290

Kuru, A., Oldfield, P., Bonser, S., & Fiorito, F. (2019). Biomimetic adaptive building skins: Energy and environmental regulation in buildings. *Energy and Buildings*, *205*, 109544. https://doi.org/10.1016/j.enbuild.2019.109544

L. Novakova-Marcincinova and J. Novak-Marcincin. (2012). Testing of Materials for Rapid Prototyping Fused Deposition Modelling Technology. *International Journal of Mechanical, Aerospace, Industrial, Mechatronic and Manufacturing Engineering*, *6*(10), 2081–2085.

Le Duigou, A., Castro, M., Bevan, R., & Martin, N. (2016a). 3D printing of wood fibre biocomposites: From mechanical to actuation functionality. *Materials & Design*, *96*, 106–114. https://doi.org/10.1016/J.MATDES.2016.02.018

Le Duigou, A., Castro, M., Bevan, R., & Martin, N. (2016b). 3D printing of wood fibre biocomposites: From mechanical to actuation functionality. *Materials & Design*, *96*, 106–114. https://doi.org/10.1016/J.MATDES.2016.02.018

Le Duigou, A., Correa, D., Ueda, M., Matsuzaki, R., & Castro, M. (2020). A review of 3D and 4D printing of natural fibre biocomposites. In *Materials and Design* (Vol. 194, p. 108911). Elsevier. https://doi.org/10.1016/j.matdes.2020.108911

Lee, A. Y., An, J., & Chua, C. K. (2017). Two-Way 4D Printing: A Review on the Reversibility of 3D-Printed Shape Memory Materials. *Engineering*, *3*(5), 663–674. https://doi.org/10.1016/J.ENG.2017.05.014

Lee, J. H., Chung, Y. S., & Rodrigue, H. (2019). Long Shape Memory Alloy Tendon-based Soft Robotic Actuators and Implementation as a Soft Gripper. *Scientific Reports*, *9*(1), 11251. https://doi.org/10.1038/S41598-019-47794-1

Loonen, R. C. G. M., Trčka, M., Cóstola, D., & Hensen, J. L. M. (2013). Climate adaptive building shells: State-of-the-art and future challenges. *Renewable and Sustainable Energy Reviews*, *25*, 483–493. https://doi.org/10.1016/J.RSER.2013.04.016

López, M., Rubio, R., Martín, S., & Ben Croxford. (2017). How plants inspire façades. From plants to architecture: Biomimetic principles for the development of adaptive architectural envelopes. *Renewable and Sustainable Energy Reviews*, *67*, 692–703. https://doi.org/10.1016/J.RSER.2016.09.018

Mazzanti, V., Malagutti, L., & Mollica, F. (2019). FDM 3D printing of polymers containing natural fillers: A review of their mechanical properties. In *Polymers* (Vol. 11, Issue 7, p. 1094). Multidisciplinary Digital Publishing Institute. https://doi.org/10.3390/polym11071094

Mazzanti, V., Mollica, F., & El Kissi, N. (2016). Rheological and mechanical characterization of polypropylene-based wood plastic composites. *Polymer Composites*, *37*(12), 3460–3473. https://doi.org/10.1002/pc.23546

Mehrpouya, M., Vahabi, H., Janbaz, S., Darafsheh, A., Mazur, T. R., & Ramakrishna, S. (2021). 4D printing of shape memory polylactic acid (PLA). *Polymer*, *230*, 124080. https://doi.org/10.1016/J.POLYMER.2021.124080

Melly, S. K., Liu, L., Liu, Y., & Leng, J. (2020). On 4D printing as a revolutionary fabrication technique for smart structures. *Smart Materials and Structures*, *29*(8), 083001. https://doi.org/10.1088/1361-665X/AB9989

Meloni, M., Cai, J., Zhang, Q., Sang-Hoon Lee, D., Li, M., Ma, R., Emilov Parashkevov, T., Feng, J., Meloni, M., Cai, J., Zhang, Q., Ma, R., Feng, J., Sang-Hoon Lee, D., Li, M., & Parashkevov, T. E. (2021). Engineering Origami: A Comprehensive Review of Recent Applications, Design Methods, and Tools. *Advanced Science*, *8*(13), 2000636. https://doi.org/10.1002/ADVS.202000636

Memarian, F., Fereidoon, A., Khonakdar, H. A., Jafari, S. H., & Saeb, M. R. (2019). Thermo-mechanical and shape memory behavior of TPU/ABS/MWCNTs nanocomposites compatibilized with ABS-g-MAH. *Polymer Composites*, *40*(2), 789–800. https://doi.org/10.1002/PC.24738

Méndez Echenagucia, T., Capozzoli, A., Cascone, Y., & Sassone, M. (2015). The early design stage of a building envelope: Multi-objective search through heating, cooling and lighting energy performance analysis. *Applied Energy*, *154*, 577–591. https://doi.org/10.1016/j.apenergy.2015.04.090

Menges, A., & Reichert, S. (2012). Material Capacity: Embedded Responsiveness. *Architectural Design*, *82*(2), 52–59. https://doi.org/10.1002/AD.1379

Menges, A., & Reichert, S. (2015). Performative wood: Physically programming the responsive architecture of the HygroScope and HygroSkin projects. *Architectural Design*, *85*(5), 66–73. https://doi.org/10.1002/ad.1956

Minori, A. F., He, Q., Glick, P. E., Adibnazari, I., Stopol, A., Cai, S., & Tolley, M. T. (2020a). Reversible actuation for self-folding modular machines using liquid crystal elastomer. *Smart Materials and Structures*, *29*(10). https://doi.org/10.1088/1361-665X/AB9FD6

Minori, A. F., He, Q., Glick, P. E., Adibnazari, I., Stopol, A., Cai, S., & Tolley, M. T. (2020b). Reversible actuation for self-folding modular machines using

liquid crystal elastomer. *Smart Materials and Structures*, *29*(10). https://doi.org/10.1088/1361-665X/ab9fd6

Mohd Jani, J., Leary, M., Subic, A., & Gibson, M. A. (2014). A review of shape memory alloy research, applications and opportunities. *Materials & Design (1980-2015)*, *56*, 1078–1113. https://doi.org/10.1016/J.MATDES.2013.11.084

Momeni, F., M.Mehdi Hassani.N, S., Liu, X., & Ni, J. (2017). A review of 4D printing. *Materials & Design*, *122*, 42–79. https://doi.org/10.1016/J.MATDES.2017.02.068

Muehlenfeld, C., & Roberts, S. A. (2018). 3D/4D Printing in Additive Manufacturing: Process Engineering and Novel Excipients. *3D and 4D Printing in Biomedical Applications*, 1–23. https://doi.org/10.1002/9783527813704.CH1

Nan, M., Chen, Z., Liu, L., & Baharlou, E. (2020). *A full-scale meteorosensitive shading system based on wood ' s self-actuated* (Vol. 1, pp. 133–142).

Negroponte, N. (1973). The Architecture Machine: Toward a More Human Environment. *The Architecture Machine*. https://doi.org/10.7551/MITPRESS/8269.001.0001

Ngo, T. D., Kashani, A., Imbalzano, G., Nguyen, K. T. Q., & Hui, D. (2018). Additive manufacturing (3D printing): A review of materials, methods, applications and challenges. *Composites Part B: Engineering*, *143*, 172–196. https://doi.org/10.1016/J.COMPOSITESB.2018.02.012

Odent, J., Vanderstappen, S., Toncheva, A., Pichon, E., Wallin, T. J., Wang, K., Shepherd, R. F., Dubois, P., & Raquez, J. M. (2019). Hierarchical chemomechanical encoding of multi-responsive hydrogel actuators via 3D printing. *Journal of Materials Chemistry A*, *7*(25), 15395–15403. https://doi.org/10.1039/C9TA03547H

Ohm, C., Brehmer, M., & Zentel, R. (2012). Applications of Liquid Crystalline Elastomers. *Adv Polym Sci*, *250*, 49–93. https://doi.org/10.1007/12_2011_164

Oral, G. K., & Yilmaz, Z. (2003). Building form for cold climatic zones related to building envelope from heating energy conservation point of view. *Energy and Buildings*, *35*(4), 383–388. https://doi.org/10.1016/S0378-7788(02)00111-1

Pelliccia, G., Baldinelli, G., Bianconi, F., Filippucci, M., Fioravanti, M., Goli, G., Rotili, A., & Togni, M. (2020). Characterisation of wood hygromorphic panels for relative humidity passive control. *Journal of Building Engineering*, *32*. https://doi.org/10.1016/j.jobe.2020.101829

Peng, X., He, H., Jia, Y., Liu, H., Geng, Y., Huang, B., & Luo, C. (2019). Shape memory effect of three-dimensional printed products based on polypropylene/nylon 6 alloy. *Journal of Materials Science*, *54*(12), 9235–9246. https://doi.org/10.1007/S10853-019-03366-2/FIGURES/8

Peraza Hernandez, E. A., Hartl, D. J., & Lagoudas, D. C. (2019). Active Origami. In *Active Origami*. https://doi.org/10.1007/978-3-319-91866-2

Perino, M., & Serra, V. (2015). Switching from static to adaptable and dynamic building envelopes: A paradigm shift for the energy efficiency in buildings. *Journal of Facade Design and Engineering*, *3*(2), 143–163. https://doi.org/10.3233/fde-150039

Poppinga, S., Correa, D., Bruchmann, B., Menges, A., & Speck, T. (2020). Plant movements as concept generators for the development of biomimetic compliant mechanisms. *Integrative and Comparative Biology*, *60*(4), 886–895. https://doi.org/10.1093/icb/icaa028

Ramesh, T., Prakash, R., & Shukla, K. K. (2010). Life cycle energy analysis of buildings: An overview. *Energy and Buildings*, *42*(10), 1592–1600. https://doi.org/10.1016/J.ENBUILD.2010.05.007

Reichert, S., Menges, A., & Correa, D. (2015). Meteorosensitive architecture: Biomimetic building skins based on materially embedded and hygroscopically enabled responsiveness. *CAD Computer Aided Design*, *60*, 50–69. https://doi.org/10.1016/j.cad.2014.02.010

Riley, K. S., Ang, K. J., Martin, K. A., Chan, W. K., Faber, J. A., & Arrieta, A. F. (2020). Encoding multiple permanent shapes in 3D printed structures. *Materials & Design*, *194*, 108888. https://doi.org/10.1016/J.MATDES.2020.108888

Rüggeberg, M., & Burgert, I. (2015). Bio-Inspired wooden actuators for large scale applications. *PLoS ONE*, *10*(4), e0120718. https://doi.org/10.1371/journal.pone.0120718

Sadineni, S. B., Madala, S., & Boehm, R. F. (2011a). Passive building energy savings: A review of building envelope components. *Renewable and Sustainable Energy Reviews*, *15*(8), 3617–3631. https://doi.org/10.1016/J.RSER.2011.07.014

Sadineni, S. B., Madala, S., & Boehm, R. F. (2011b). Passive building energy savings: A review of building envelope components. *Renewable and Sustainable Energy Reviews*, *15*(8), 3617–3631. https://doi.org/10.1016/J.RSER.2011.07.014

Sartori, I., & Hestnes, A. G. (2007). Energy use in the life cycle of conventional and low-energy buildings: A review article. *Energy and Buildings*, *39*(3), 249–257. https://doi.org/10.1016/j.enbuild.2006.07.001

Sharp, A., Blay, G., Kholodova, J., & Correa, D. (2021). An Autonomous Bio-Inspired Shading Façade System based on Plant Movement Principles. *Proceedings of the International Conference on Education and Research in Computer Aided Architectural Design in Europe*, *2*, 463–472. https://doi.org/10.52842/conf.ecaade.2021.2.463

Skaar, C. (1988). *Wood-Water Relations*. Springer Berlin Heidelberg. https://doi.org/10.1007/978-3-642-73683-4

Stoychev, G., Zakharchenko, S., Turcaud, S., Dunlop, J. W. C., & Ionov, L. (2012). Shape-programmed folding of stimuli-responsive polymer bilayers. *ACS Nano*, *6*(5), 3925–3934. https://doi.org/10.1021/NN300079F/SUPPL_FILE/NN300079F_SI_002.AVI

Tahouni, Y., Cheng, T., Lajewski, S., Benz, J., Bonten, C., Wood, D., & Menges, A. (2022). Codesign of Biobased Cellulose-Filled Filaments and Mesostructures for 4D Printing Humidity Responsive Smart Structures. *3D Printing and Additive Manufacturing*. https://doi.org/10.1089/3dp.2022.0061

Tahouni, Y., Cheng, T., Wood, D., Sachse, R., Thierer, R., Bischoff, M., & Menges, A. (2020, November 5). Self-shaping Curved Folding:: A 4D-printing method for fabrication of self-folding curved crease structures. *Proceedings - SCF 2020: ACM Symposium on Computational Fabrication*. https://doi.org/10.1145/3424630.3425416

Tahouni, Y., Krüger, F., Poppinga, S., Wood, D., Pfaff, M., Rühe, J., Speck, T., & Menges, A. (2021). Programming sequential motion steps in 4D-printed hygromorphs by architected mesostructure and differential hygro-responsiveness. *Bioinspiration and Biomimetics*, *16*(5). https://doi.org/10.1088/1748-3190/ac0c8e

Tarkow, H., & Turner, D. (2005). Handbook of Wood Chemistry and Wood Composites. In *Handbook of Wood Chemistry and Wood Composites*. CRC Press. https://doi.org/10.1201/9780203492437

Tibbits, S. M. C. O. C. D. D. H. S. (2014). 4D Printing and Universal Transformation. *ACADIA 14: Design Agency [Proceedings of the 34th Annual Conference of the Association for Computer Aided Design in Architecture (ACADIA) ISBN 9781926724478]Los Angeles 23-25 October, 2014), Pp. 539-548*, 440.

Time, B. (1998). Hygroscopic moisture transport in wood. *Department of Building and Construction Engineering*, *PhD*(February), 1–232. http://www.ivt.ntnu.no/docs/bat/bm/phd/AvhandlingBeritTime.pdf

Timoshenko, S. (1925). Analysis of Bi-Metal Thermostats. *Journal of the Optical Society of America*, *11*(3), 233. https://doi.org/10.1364/josa.11.000233

Tomec, D. K., Straže, A., Haider, A., & Karič, M. (2021). Hygromorphic response dynamics of 3d-printedwood-PLA composite bilayer actuators. *Polymers*, *13*(19), 3209. https://doi.org/10.3390/polym13193209

Turrin, M., Von Buelow, P., Kilian, A., & Stouffs, R. (2012). Performative skins for passive climatic comfort: A parametric design process. *Automation in Construction*, *22*, 36–50. https://doi.org/10.1016/J.AUTCON.2011.08.001

Tzikopoulos, A. F., Karatza, M. C., & Paravantis, J. A. (2005). Modeling energy efficiency of bioclimatic buildings. *Energy and Buildings*, *37*(5), 529–544. https://doi.org/10.1016/J.ENBUILD.2004.09.002

Vailati, C., Bachtiar, E., Hass, P., Burgert, I., & Rüggeberg, M. (2018). An autonomous shading system based on coupled wood bilayer elements. *Energy and Buildings*, *158*, 1013–1022. https://doi.org/10.1016/j.enbuild.2017.10.042

Vailati, C., Hass, P., Burgert, I., & Rüggeberg, M. (2017). Upscaling of wood bilayers: design principles for controlling shape change and increasing moisture change rate. *Materials and Structures/Materiaux et Constructions*, *50*(6), 1–12. https://doi.org/10.1617/s11527-017-1117-4

Vazquez, E., & Gursoy, B. (2020). *3D Printed Responsive Wood Interfaces: Shape-Changing Origami-Inspired Prototypes* (pp. 600–607). https://doi.org/10.5151/sigradi2020-83

Vazquez, E., Gursoy, B., & Duarte, J. (2019). Designing for shape change: A Case study on 3D Printing Composite Materials for Responsive Architecture. In *Intelligent and Informed - Proceedings of the 24th International Conference*

on Computer-Aided Architectural Design Research in Asia, CAADRIA 2019 (Vol. 2).

Vazquez, E., Randall, C., & Duarte, J. P. (2019). Shape-changing Architectural Skins A Review on Materials, Design and Fabrication Strategies and Performance Analysis. In *Journal of Facade Design and Engineering* (Vol. 7, Issue 2, pp. 93–114). https://doi.org/10.7480/jfde.2019.2.3877

Velikov, K., & Thün, G. (2012). Responsive Building Envelopes: Characteristics and Evolving Paradigms. In *Design and Construction of High-Performance Homes* (pp. 78–95). Routledge. https://doi.org/10.4324/9780203721797-13

Wang, Z., Wang, Z., Zheng, Y., He, Q., Wang, Y., & Cai, S. (2020). Three-dimensional printing of functionally graded liquid crystal elastomer. *Science Advances*, *6*(39). https://doi.org/10.1126/sciadv.abc0034

Wei, H., Zhang, Q., Yao, Y., Liu, L., Liu, Y., & Leng, J. (2017). Direct-write fabrication of 4D active shape-changing structures based on a shape memory polymer and its nanocomposite. *ACS Applied Materials and Interfaces*, *9*(1), 876–883. https://doi.org/10.1021/ACSAMI.6B12824/SUPPL_FILE/AM6B12824_SI_004.MOV

Wood, D. M., Correa, D., Krieg, O. D., & Menges, A. (2016). Material computation-4D timber construction: Towards building-scale hygroscopic actuated, self-constructing timber surfaces. *International Journal of Architectural Computing*, *14*(1), 49–62. https://doi.org/10.1177/1478077115625522/ASSET/IMAGES/LARGE/10.1177_1478077115625522-FIG8.JPEG

Wood, D., Vailati, C., Menges, A., & Rüggeberg, M. (2018). Hygroscopically actuated wood elements for weather responsive and self-forming building parts – Facilitating upscaling and complex shape changes. *Construction and*

Building Materials, *165*, 782–791. https://doi.org/10.1016/J.CONBUILDMAT.2017.12.134

Xia, Y., He, Y., Zhang, F., Liu, Y., Leng, J., Xia, Y., He, Y., Zhang, F., Leng, J., & Liu, Y. (2021). A Review of Shape Memory Polymers and Composites: Mechanisms, Materials, and Applications. *Advanced Materials*, *33*(6), 2000713. https://doi.org/10.1002/ADMA.202000713

Yamamura, S., & Iwase, E. (2021). Hybrid hinge structure with elastic hinge on self-folding of 4D printing using a fused deposition modeling 3D printer. *Materials & Design*, *203*, 109605. https://doi.org/10.1016/J.MATDES.2021.109605

Yang, H., Leow, W. R., Wang, T., Wang, J., Yu, J., He, K., Qi, D., Wan, C., & Chen, X. (2017). 3D Printed Photoresponsive Devices Based on Shape Memory Composites. *Advanced Materials*, *29*(33), 1701627. https://doi.org/10.1002/ADMA.201701627

Yang, W. G., Lu, H., Huang, W. M., Qi, H. J., Wu, X. L., & Sun, K. Y. (2014). Advanced Shape Memory Technology to Reshape Product Design, Manufacturing and Recycling. *Polymers 2014, Vol. 6, Pages 2287-2308*, *6*(8), 2287–2308. https://doi.org/10.3390/POLYM6082287

Yi, H., & Kim, Y. (2021). Self-shaping building skin: Comparative environmental performance investigation of shape-memory-alloy (SMA) response and artificial-intelligence (AI) kinetic control. *Journal of Building Engineering*, *35*, 102113. https://doi.org/10.1016/j.jobe.2020.102113

Yu, K., Li, H., McClung, A. J. W., Tandon, G. P., Baur, J. W., & Qi, H. J. (2016). Cyclic behaviors of amorphous shape memory polymers. *Soft Matter*, *12*(13), 3234–3245. https://doi.org/10.1039/C5SM02781K

Zhang, Y. S., & Khademhosseini, A. (2017). Advances in engineering hydrogels. *Science*, *356*(6337).

https://doi.org/10.1126/SCIENCE.AAF3627/ASSET/DA9C967B-F098-46FD-8612-68D9054A7DF3/ASSETS/GRAPHIC/356_AAF3627_FA.JPEG

Zheng, C., Jin, F., Zhao, Y., Zheng, M., Liu, J., Dong, X., Xiong, Z., Xia, Y., & Duan, X. (2020). Light-driven micron-scale 3D hydrogel actuator produced by two-photon polymerization microfabrication. *Sensors and Actuators B: Chemical*, *304*, 127345. https://doi.org/10.1016/J.SNB.2019.127345

Zhou, J., & Sheiko, S. S. (2016). Reversible shape-shifting in polymeric materials. In *Journal of Polymer Science, Part B: Polymer Physics* (Vol. 54, Issue 14, pp. 1365–1380). John Wiley & Sons, Ltd. https://doi.org/10.1002/polb.24014

Zhou, Y., Huang, W. M., Kang, S. F., Wu, X. L., Lu, H. B., Fu, J., & Cui, H. (2015). From 3D to 4D printing: approaches and typical applications. *Journal of Mechanical Science and Technology 2015 29:10*, *29*(10), 4281–4288. https://doi.org/10.1007/S12206-015-0925-0

Zolfagharian, A., Kouzani, A. Z., Khoo, S. Y., Gibson, I., & Kaynak, A. (2017). 3D printed hydrogel soft actuators. *IEEE Region 10 Annual International Conference, Proceedings/TENCON*, 2272–2277. https://doi.org/10.1109/TENCON.2016.7848433

Zuluaga, D. C., & Menges, A. (2015). 3D printed hygroscopic programmable material systems. *Materials Research Society Symposium Proceedings*, *1800*(1), 24–31. https://doi.org/10.1557/opl.2015.644